Ionophore-based complexometric titration

Zhai, Jingying

UNIVERSITÉ DE GENÈVE
FACULTÉ DES SCIENCES

Section de chimie et biochimie
Professeur Eric Bakker

Département de chimie minérale et analytique

Ionophore-based Complexometric Titration

THÈSE

Présentée à la Faculté des Sciences de l'Université de Genève

Pour obtenir le grade de Docteur ès Sciences, mention Chimie

par

Jingying ZHAI

de Chine

Thèse N° 5084

GENÈVE

Migros Print-Shop Plainpalais

2017

UNIVERSITÉ
DE GENÈVE

FACULTÉ DES SCIENCES

DOCTORAT ÈS SCIENCES, MENTION CHIMIE

Thèse de Madame Jingying ZHAI

intitulée :

« Ionophore-based Complexometric Titration »

La Faculté des sciences, sur le préavis de

Monsieur E.BAKKER, professeur ordinaire et directeur de thèse
Département de chimie minérale et analytique

Monsieur T. BÜRGI, professeur ordinaire
Département de chimie physique

Monsieur D. CITTERIO, professeur
Department of Applied Chemistry, Keio University, Hiyoshi, Japan

autorise l'impression de la présente thèse, sans exprimer d'opinion sur les propositions qui y sont énoncées.

Genève, le 31 mai 2017

Thèse - 5084 -

Le Doyen

N.B. - La thèse doit porter la déclaration précédente et remplir les conditions énumérées dans les "Informations relatives aux thèses de doctorat à l'Université de Genève".

Table of Contents

Abstract

Complexometric titration is a highly precise method of quantitative chemical analysis widely used in various fields including environmental monitoring, food industry, medical field, bioanalytical chemistry and clinical analysis. Its importance in analytical chemistry has rendered complexometric titration an indispensable part in all analytical chemistry textbooks. As a titrimetric method, it is based on the formation of strong complexes between the analyte and the titrant, and hence the exhaustive consumption of the analyte and the determination of the analyte concentration. Chelators and end point indicators are the most important parts of complexometric titrations. Up to now, ethylenediamine tetraacetic acid (EDTA) and its derivatives are the most widely used universal chelators. However, the selectivity of EDTA is limited and EDTA based titrations often require the use of masking agents. The multiple pKa values of the chelators also necessitate a careful adjustment of pH during the titration.

For a specific real sample, it would be highly desirable to use pH independent, selective and sensitive chelators and indicators. This thesis is focused on the development of a new class of titration reagents based on highly selective ionophores and ion exchangers. The matrices of the titration reagents include dichloromethane and nanoemulsions.

This thesis is divided into six chapters. Chapter 1 serves as an introduction to provide an overview of the development of the complexometric titration reagents in recent decades. Chapter 2 describes for the first time the Pluronic F-127 chelating nanospheres, which contain ion exchangers and highly selective ionophores. The titration of Pb^{2+} and Ca^{2+} are successfully demonstrated. Chapter 3 is centred around nanospheres containing a chromoionophore, ion exchanger and an ionophore of choice as end point indicators. The influence of sample pH values on the accuracy of end point detection is discussed. Chapter 4 presents the titrations for anions using ion-selective nanospheres. A titration of nitrate ions in a spinach sample is demonstrated. Chapter 5 introduces solvatochromic dye doped nanospheres as end point indicator, which is able to overcome the pH dependence of the chromoionophore doped indicating nanospheres. Chapter 6 introduces solvent based titration reagents to overcome limitations of nanosphere based reagents. In view of practical applications, titrations were also demonstrated with an automatic setup

which contains a syringe pump to inject sample with accurate volumes and a vortex to sufficiently mix the two phases. In addition to the experimental titration results, we also provide in each chapter a theoretical model based on ion exchange process to support the experimental results.

In a nutshell, this thesis work is dedicated to improve, if not revolutionize, the methodology and characteristics of complexometric titration reagents. The nanosphere and solvent based reagents have moved conventional complexometric titration from a homogeneous phase to heterogeneous phases. A number of proof-of-concept results have been achieved, forming a solid foundation for future work and the possible commercialization of these new reagents.

Résumé

Le titrage complexométrique est une analyse chimique quantitative très précise largement utilisée dans divers domaines, tels que l'observation de l'environnement, l'industrie alimentaire, le domaine médical, les analyses biochimiques ou encore l'analyse clinique, à tel point que cette méthode est devenue incontournable dans les manuels de chimie analytique. Cette méthode titrimétrique repose sur la formation de complexes forts entre l'analyte et le titrant : l'analyte est alors intégralement consommé, et sa concentration peut être déterminée. Les chélateurs et les indicateurs de fin de titrage sont les éléments les plus importants des titrages complexométriques. Jusqu'à présent, l'éthylène diamine tétraacétate (EDTA) et ses dérivés ont été les chélateurs universels les plus utilisés. Cependant, la sélectivité de l'EDTA est limitée, ce qui nécessite souvent l'utilisation d'agents masquants. Les multiples valeurs de pKa des chélateurs nécessitent par ailleurs un ajustement minutieux du pH pendant le titrage. Pour un échantillon réel donné, il est beaucoup plus commode d'utiliser des chélateurs et des indicateurs qui soient à la fois indépendants du pH, sélectifs et sensibles. Cette thèse introduit le une nouvelle classe de réactifs de titrage basés sur des ionophores et des échangeurs d'ions hautement sélectifs. L'on y introduit en particulier des nanoémulsions et le dicholorométhane comme matrices novatrices pour les réactifs de titrage.

Cette thèse est divisée en six chapitres. Chapitre 1 propose, en guise d'introduction, un aperçu du développement des réactifs de titrage complexométriques durant les dernières décennies. Le chapitre 2 décrit pour la première fois des nanosphères chélatantes basées sur le Pluronic F-127, contenant des échangeurs d'ions et des ionophores hautement sélectifs. L'application au titrage de Pb^{2+} et de Ca^{2+} y est présentée. Le chapitre 3 est centré sur la détermination du point de virage à l'aide de nanosphères contenant un chromoionophore, un échangeur d'ions et un ionophore adapté au titrage. L'on y discute également l'influence du pH de l'échantillon sur la précision de la valeur obtenue. Le chapitre 4 présente des titrages pour anions mettant en jeu des nanosphères sélectives. Un titrage d'ions nitrate dans un échantillon réel d'épinards y est démontré. Le chapitre 5 propose des nanosphères dopées à l'aide d'un colorant solvatochromique comme de bons indicateurs fin de titrage, surmontant ainsi la dépendance au pH des nanosphères

contenant des chromoionophores. Le chapitre 6 discute de l'utilisation de réactifs de titrage basés sur des solvants pouvant surmonter les limites imposées par les réactifs à base de nanosphères. Afin d'anticiper de potentielles applications, cette méthode a été testée sur un dispositif autonome composé d'une pompe à seringue – pour contrôler précisément le volume versé – et d'un vortex, nécessaire pour assurer le mélange des deux phases. En plus des résultats expérimentaux, nous proposons en outre à chaque chapitre un modèle théorique basé sur un processus d'échange d'ions venant en soutien aux résultats expérimentaux.

Pour résumer, ce travail de thèse est consacré à l'amélioration – et peut-être même à la révolution – de la méthodologie et des caractéristiques des réactifs de titrage complexométriques. Avec les nanosphères et les réactifs basés sur des solvants, le titrage complexométrique n'est plus uniquement limité aux phases homogènes. Les nombreux résultats et avances de concepts présentés dans cette thèse posent ainsi les fondations non seulement pour de futurs travaux de recherche, mais également pour une possible commercialisation de nouveaux réactifs.

List of Publications

Review Article

1) Jingying Zhai and Eric Bakker*, "Complexometric Titrations: New Reagents and Concepts to Overcome Old Limitations", *Analyst*, **2016**, *141*, 4252-4261.

Research Articles

1) Jingying Zhai, Xiaojiang Xie, Thomas Cherubini and Eric Bakker*, "Ionophore-Based Titrimetric Detection of Alkali Metal Ions in Serum", *ACS Sens.*, **2017**, *2*, 606-612.
2) Jingying Zhai, Xiaojiang Xie and Eric Bakker*, "Solvatochromic Dyes as pH-Independent Indicators for Ionophore Nanosphere-Based Complexometric Titrations", *Anal. Chem.*, **2015**, *87*, 12318-12323.
3) Jingying Zhai, Xiaojiang Xie and Eric Bakker*, "Anion-Exchange Nanospheres as Titration Reagents for Anionic Analytes", *Anal. Chem.*, **2015**, *87*, 8347-8352.
4) Jingying Zhai, Xiaojiang Xie and Eric Bakker*, "Ion-Selective Optode Nanospheres as Heterogeneous Indicator Reagents in Complexometric Titrations", *Anal. Chem.*, **2015**, *87*, 2827-2831.
5) Jingying Zhai, Xiaojiang Xie and Eric Bakker*, "Advancing Schwarzenbach's Complexometry: Nano-scale Titration Reagents Based on Heterogeneous Reactions", *Chimia*, **2014**, *68*, 899-899.
6) Jingying Zhai, Xiaojiang Xie and Eric Bakker*, "Ionophore-Based Ion-Exchange Emulsions as Novel Class of Complexometric Titration Reagents", *Chem. Commun.*, **2014**, *50*, 12659-12661.
7) Xiaojiang Xie*, Jingying Zhai, Zdeňka Jarolímová and Eric Bakker*, "Determination of pKa Values of Hydrophobic Colorimetric pH Sensitive Probes in Nanospheres", *Anal. Chem.*, **2016**, *88*, 3015-3018.

8) Xiaojiang Xie, Jingying Zhai and Eric Bakker*, "Potentiometric Response from Ion-Selective Nanospheres with Voltage-Sensitive Dyes", *J. Am. Chem. Soc.*, **2014**, *136*, 16465-16468.

9) Xiaojiang Xie, Jingying Zhai, Gastón A. Crespo, and Eric Bakker*, "Ionophore-Based Ion-Selective Optical NanoSensors Operating in Exhaustive Sensing Mode", *Anal. Chem.*, **2014**, *86*, 8770-8775.

10) Xiaojiang Xie, Jingying Zhai and Eric Bakker*, "pH Independent Nano-Optode Sensors Based on Exhaustive Ion-Selective Nanospheres", *Anal. Chem.*, **2014**, *86*, 2853-2856.

11) Lu Wang, Xiaojiang Xie, Jingying Zhai and Eric Bakker*, "Reversible pH-Independent Optical Potassium Sensor with Lipophilic Solvatochromic Dye Transducer on Surface Modified Microporous Nylon", *Chem. Commun.*, **2016**, *52*, 14254-14257.

12) Xiaojiang Xie*, István Szilágyi, Jingying Zhai, Lu Wang and Eric Bakker*, "Ion-Selective Optical Nanosensors Based on Solvatochromic Dyes of Different Lipophilicity: From Bulk Partitioning to Interfacial Accumulation", *ACS Sens.*, **2016**, *1*, 516-520.

13) Xiaojiang Xie*, Gastón A. Crespo, Jingying Zhai, István Szilágyi and Eric Bakker*, "Potassium-Selective Optical Microsensors Based on Surface Modified Polystyrene Microspheres", *Chem. Commun.*, **2014**, *50*, 4592-4595.

Chapter 1. Complexometric Titrations: New Reagents and Concepts to Overcome Old Limitations

This work has been published in *Analyst*, **2016**, *141*, 4252-4261.

1. Introduction

Titrimetry is a general and powerful method which is used to quantify a wide range of analytes. The high accuracy of the results and maturity of the procedure have made it a routine method in various fields such as environmental monitoring, bioanalytical chemistry and clinic analysis. Compared with quantitative instrumental measurements that depend on a readout using methods as ion chromatography, ICP-MS or AAS, titrimetry is the most simple and accurate because it relies on an exhaustive consumption of the analyte at the end point. Today, titrimetry can be easily automated and commercially available standardized reagents provide more convenience to the end users. These key advantages have made titrimetric methods an indispensible part of analytical chemistry, even with the arrival and establishment of newer instrumental techniques.

Complexometric titration (complexometry or chelatometry) is one of the classical titrimetric methods developed for the rapid and quantitative chemical analysis of metal ions. The ions of interest are titrated with the chelator of choice through a coordination complexation reaction and rapidly form stable monodentate or multidentate complexes. The chelator is sometimes called the complexing reagent or more simply, titrant. The end point can be identified by a metallochromic indicating dye, which shows a colour change, or by other instrumental indicators, such as ion-selective electrodes.

The earliest example for this type of titration reactions is the determination of cyanide ion concentration by silver nitrate, proposed by the German chemist Justus Liebig in the 1850s.[1] In 1945, Schwarzenbach, who made a significant contribution to this field, formally introduced the complexometric titration method to quantify metal ions, mainly using EDTA as chelator.[2] The discovery of EDTA dramatically pushed the field forward. Since 1950, complexometric titration has spread all over the world, for example to measure water hardness.[3] A comprehensive theory of complexometry was put forward by

Schwarzenbach in his book, published 10 years after the introduction of the method.[4,5] Almost at the same time, various indicating dyes started to appear to visualize the end point by the naked eye or by spectrophotometric instrumentation. Murexide and Eriochrome Black T were established as indicators for water hardness.[6,7] A number of researchers including Reilley, Hildebrand, Patton, Reeder and Tsien contributed to the synthesis of new indicators to improve their selectivity.[8-11] Powerful instrumental analysis methods such as potentiometry, conductometry, thermometry, coulometry and chronopotentiometry were also developed to provide improved choices for quantitative analyses.[12-19] Although EDTA has always been the most widely recognized chelator in complexometric titration, good chelators and indicators as well as new concepts have been continuously emerging. In addition, various titration protocols have been developed.[20,21] This review summarizes the most recent developments in complexometric titration reagents and methods.

2. Chelators

2.1 The classical chelator EDTA

Chelators are today widely applied in chemical industry, therapy, agriculture, biochemistry and other fields. Most chelators contain N, O or S atoms in their molecular structure to provide lone-paired electrons available for coordination.[4,22,23] Functional groups such as carboxylates, amines, hydroxyls and sulfhydryls are very commonly found. One of the structurally simple monodentate ligands is ammonia. It is able to strongly coordinate with metals including Cu^{2+}, Ni^{2+}, Co^{3+}, Ag^{+} and is useful to extract or dissolve metals.[23,24] However, it is not suited as a chelator in complexometric titrations because ammonia only exhibits one bond that can be used to coordinate the analyte. The resulting stepwise formation of metal complexes makes it difficult to observe the end point. Cyanide suffers from the same drawback.[23,24]

It has therefore been proposed early on that for a reagent to act as a chelator in complexometric titrations, (i) the reaction should be kinetically fast, (ii) it should proceed stoichiometrically; (iii) the change in free energy must be sufficiently large.

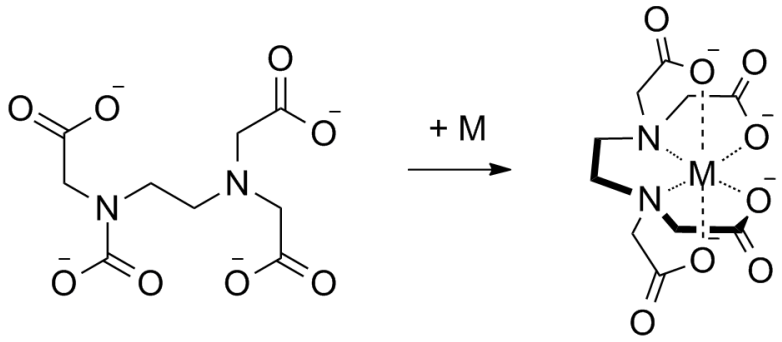

Figure 1. Chemical structure of fully deprotonated EDTA and its complexation with a metal ion M in 1:1 stoichiometry.

The introduction of EDTA was a revolution in the field of complexometric titrations because it fulfills the above-mentioned conditions. As shown in Figure 1, EDTA exhibits multiple coordinating groups and forms 1:1 metal-chelator complexes. EDTA is able to form complexes with various metal ions. Since its introduction, a large number of elements have been measured with this method. Early pioneering works have been done by Schwarzenbach and co-workers.[4,25-28] EDTA has been used to analyze almost half of the elements in the periodic table while its derivatives such as diethylene triamine pentaacetic acid (DTPA) and ethylene glycol tetraacetic acid (EGTA) provide similar usage.[4,29-37] EDTA and its derivatives belong to the aminopolycarboxylic acid family. It is able to dissociate into several protonation states. The effective formation constant of the metal-EDTA complexes therefore depends on pH, which makes titrations with EDTA pH dependent. Because EDTA and its derivatives and the above-mentioned pharmaceutical chelators exhibit high binding constants to many metals ions, they lack tunable selectivity and often require the use of masking reagents.[4,23]

The total amount of Ca^{2+} and Mg^{2+} is normally titrated with EDTA at pH 10 while Ca^{2+} alone is titrated at pH 13 upon masking the Mg^{2+} ions with OH^-.[38-41] Recently, EDTA titration was demonstrated by Kaneta and co-workers in microfluidic paper-based analytical devices.[42] This paper-based device contained various amounts of known EDTA and a small amount of indicator. The device is able to rapidly and quantitatively determine the Ca^{2+} and Mg^{2+} in mineral water, river water and seawater samples.

As an effective chelator, EDTA can also be used to remove the toxic transitional metals such as Pb^{2+}, Ni^{2+}, Hg^{2+}, Cd^{2+} and As^{3+} from wastewater, contaminated soil and lake water.[43-45]

Unfortunately, many chelaters are not biodegradable and will be persistent in the environment.[46,47] Therefore, recyclable/separable EDTA-functionalized compounds or materials have also been reported for these applications, such as EDTA bonded polymers, particles or natural materials.[43,48]

Stark and co-workers reported that EDTA-like chelator modified nanomagnets can remove Cd^{2+}, Pb^{2+} and Cu^{2+} from contaminated water.[43] In a very short time, the concentrations of transition metal ions may decrease to the ug/L range, which is often acceptable. The nanomagnets must be separated from the treated water.

Until today, 95% of the publications in the complexometric titration area are still based on EDTA and its derivatives. EDTA as an important conventional chelator has also been used medicinally for the treatment of human intoxication with heavy metals. For this type of medical treatment, three commonly other commonly used chelators also exist, including British Anti-Lewisite (BAL), dimercaptosuccinic acid (DMSA) and dimercaptopropane sulfonate (DMPS).[49] These pharmaceutical chelators can in principle equally be used in titrations.

2.2 Extractant based on diglycoamides

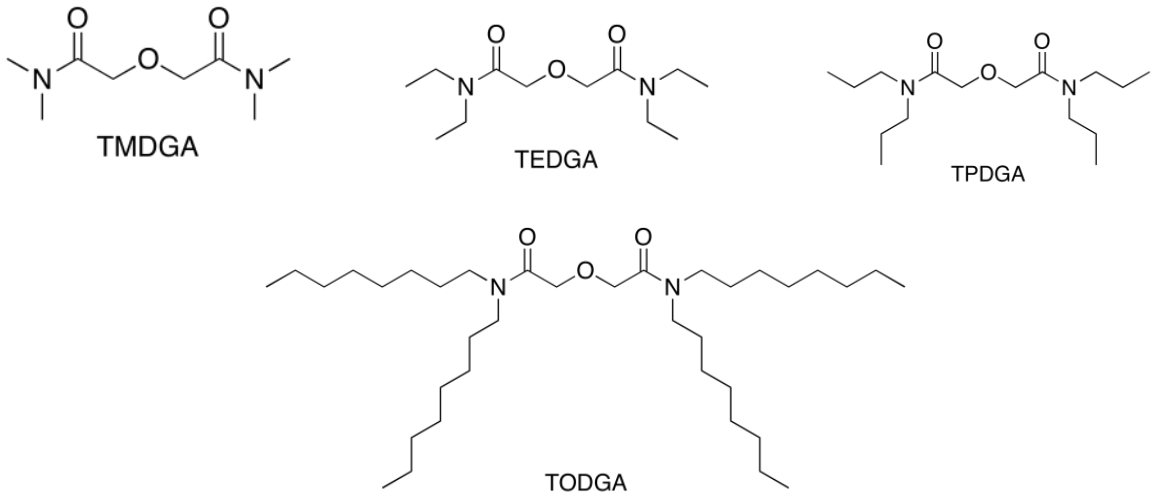

Figure 2. Structural formulates of the diglycolamide based ligands for actinide and lanthanide ions extraction.

Diglycolamides as a new class of extractants for actinide and lanthanides ions have been extensively studied during the past decades.[50] Separation, recycling and storage of these long-lived radioactive elements from high level waste generated from nuclear fuel are very important for the environment and human health. Diglycolamides and its analogs (see Figure 2) are found to be very effective and selective for the extraction of trivalent actinides compared with other extractants such as malomide and octyl-(phenyl)-N, N-diisobutyl carbamoyl methyl phosphine oxide (CMPO) based extractants.[51,52]

The lipophilicity of diglycolamide compounds can be tuned with different alkyl chains on N atoms. Sasaki and co-workers reported that water soluble diglycolamines, N, N, N', N'-tetramethyldiglycolamide (TMDGA), N,N,N,N'-tetraethyldiglycolamide (TEDGA), N,N,N',N'-tetrapropyldiglycolamide (TPDGA) can be used as complexing agents for Pu(IV) and Am(III).[53] As neutral complexing reagents, these diglycolamines display high affinity to Pu(IV) and Am(III) and form more stable complexes with Pu(IV) and Am(III) than EDTA in highly concentrated HNO_3 solution.

Water insoluble diglycolamides with long alkyl chains can be dissolved in solvents to perform liquid-liquid extraction of actinides and lanthanides.[50,54] Many groups have studied the synthesis and the characteristics of different diglycolamides extractants. Among these extractants, N,N,N',N'-tetraoctyl diglycolamide (TODGA) was found to be a promising extractant for trivalent actinides.[55,56] The metal ions will be extracted into the solvent together with a counteranion (NO_3^-) in high concentrated HNO_3 solution or its salt. If the concentration of the counter anion (NO_3^-) is not sufficiently high, the extractants could not function properly. The extraction process can also be based on ion exchange. Naganawa and co-workers reported on the role of the hydrophobic counteranions ($TFPB^-$) in the extraction of lanthanides(III) with TODGA.[57] The metal ions may be exchanged into the solvent by the counter ion of $TFPB^-$. The introduction of ion exchanger is greatly helpful to improve the extraction ability and selectivity with low background of ionic strength. On the other hand, without addition of hydrophobic cationic exchanger, dissolving the extractant into the ionic liquid can also result in a high extraction efficiency for lanthanides, still based on the cation-exchange mechanism.[58,59] Diglycolamide-functionalized task specific ionic liquids with functional groups attached to the cationic part of the ionic liquid showed high extraction efficiency to actinides and

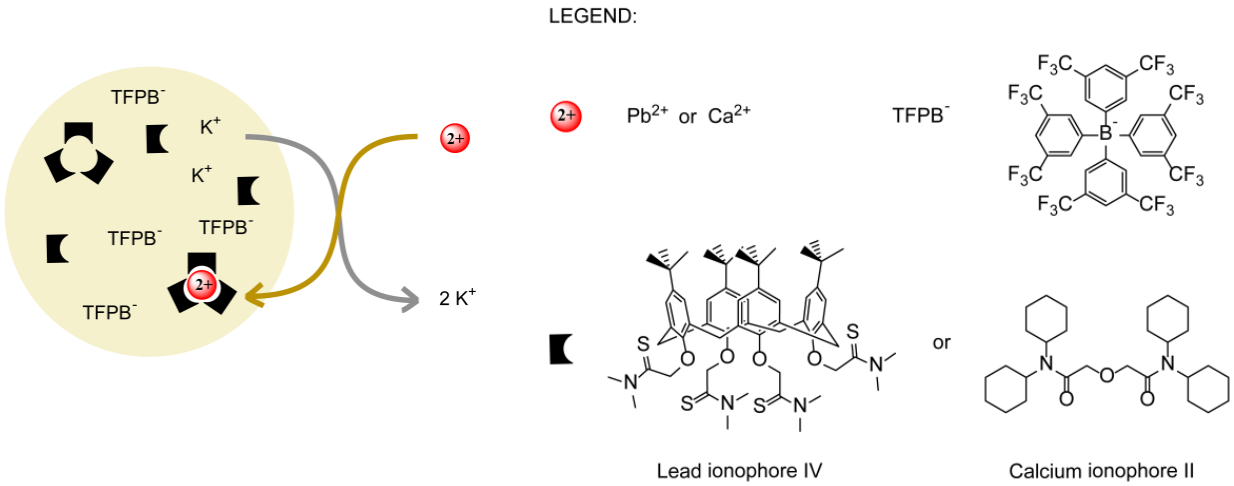

Figure 3. Ion-selective emulsions containing nanospheres as complexing agent and structures of the compounds used to form nanospheres. The nanosphere core is made of dodecyl 2-nitrophenyl ether (D-NPOE) and the hydophobic sub-structure of Pluronic F-127. The complexation reaction comprises (1) ion exchange between target ion (Ca^{2+} or Pb^{2+}) in aqueous phase and the counter ion of R^- (K^+) in the organic phase and (2) the complexation reaction between target ion and the receptor, which lowers the solvation energy for the target ion and provide the driving force for its uptake into the nanospheres.

lanthanides.[59-61] Verboom and co-workers also reported on a series of new ligands based on diglycolamides that have three functional groups at C-pivot and trialkylphenyl platforms.[62] These ligands also showed high affinity for Am (III) and Eu (III) with a 1:1 metal to ligand stoichiometry. In general, ligands based on diglycoamide with various platforms have demonstrated satisfactory extraction performance.

The water soluble diglycoamides based compounds are promising chelators for the titration and extraction of actinides and lanthanides in homogenous titrations. However, for the use of hydrophobic titrants/extractants, the extraction system should best contain an ion exchanger, which is further explained below with the nanospheres.

2.3 Ion selective nanospheres as a new generation of chelators

Conventional titration reactions occur directly in the aqueous sample. Recently, Bakker and co-workers proposed ion selective nanospheres as a novel class of complexometric titration reagents, which moved the titration process from the homogeneous to the heterogeneous phase.[63-65] One key advantage of using this new toolbox is that the titration reagents no longer need to be water soluble. Other lipophilic chelators with high

selectivity and high affinity to the analyte can be used, such as ionophores for Pb^{2+}, Ca^{2+}, Cu^{2+}, Na^{+}, K^{+} and Cl^{-}.[66-68] These classical ionophores have originally been introduced as active reagents in ion selective electrode membranes for many decades. As shown in Figure 3, the chelating nanospheres for calcium titration contain a lipophilic calcium ionophore II and cation exchanger in the core of emulsified organic nanodroplets, which is made of surfactant Pluronic F-127 and plasticizer.[63] Based on the principle of ion exchange, the analyte calcium readily exchanges into the nanospheres for the original counter ions (K^{+} or Na^{+}, which would only interference at extremely high concentration) of the ion exchanger. Every Ca^{2+} exchanges with two monovalent counter ion so that the core of the nanospheres remains neutral. In the chelating nanospheres the ionophore is chosen at molar compared to the ion exchanger. It is therefore the ion-exchanger that defines the extraction capacity, not the ionophore, and various ion–ionophore stoichiometries can be tolerated.

Figure 4 shows a comparison between titrations effected with calcium selective nanospheres and the chelator EDTA.[63] Because the calcium ionophore exhibits no protonatable groups, it was not necessary to control the sample pH during the titration:

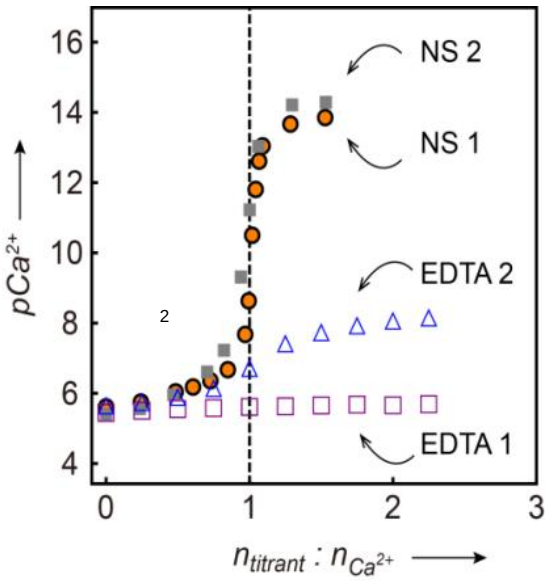

Figure 4. Comparing calcium selective emulsion with EDTA as complexing agents for the potentiometric titrations of 4 µM calcium. NS 1: titration in non-buffered water by calcium selective emulsion; NS 2: titration in 1mM pH 7.0 Tris-HCl by emulsion; EDTA 1: titration in non-buffered water by EDTA; EDTA 2: titration in 1 mM pH 7.0 Tris-HCl by EDTA. The dashed vertical line marks the end point.

titrations with the calcium selective nanospheres showed an almost indistinguishable behavior in pH 7.0 buffered solution than in unbuffered water. The titration curves were nearly identical, with sharp transitions at the endpoint. Titrations with EDTA did not show a visible endpoint in unbuffered water and the transition was not easily observable in samples buffered at pH 7.0. As established, EDTA titrations of calcium must be performed above pH 10.

The chelating nanospheres exhibit attractive versatility. By simply replacing the ionophore in the nanospheres, it is possible to create a palette of reagents of different selectivity. A potential limitation is that the nanospheres tend to coagulate at high concentration, resulting in undesirable light scattering if the end point is observed by optical methods. This method is still young and emulsion based titrations for monovalent metal ions such as Na^+ and K^+ still wait to be demonstrated.

3. Coulometric titration

Coulometry conversion has also been considered to directly generate titrants for the purpose of effecting titrations. This principle works on the basis of Faraday's law, which defines a direct relationship between the charge passing through the electrode and the molar amount of analyte that has reacted. A quantitative release of titrant can be achieved through precise manipulation of current and duration, if there are no cross-reactions.

Reilley and Porterfield reported earlier on a general method for the coulometric generation of EDTA, where EDTA was indirectly released upon the reduction of mercuric-EDTA. This method has been successfully demonstrated to measure calcium, copper, zinc and lead ions.[12] By applying an appropriate potential or current, the direct release of non-redox active ions was demonstrated. The released ions served directly as the titrant and were also used determine the end point of the titration. Compared with traditional volumetric titrations, this method is able to accurately release the titrant without requiring standardized stock solution. In addition, the sample is not diluted during the titration and the sample volume can remain quite limited. However, the lack of selectivity and limited options of reagents are still to be improved, and the use of mercury is today often no longer acceptable today.

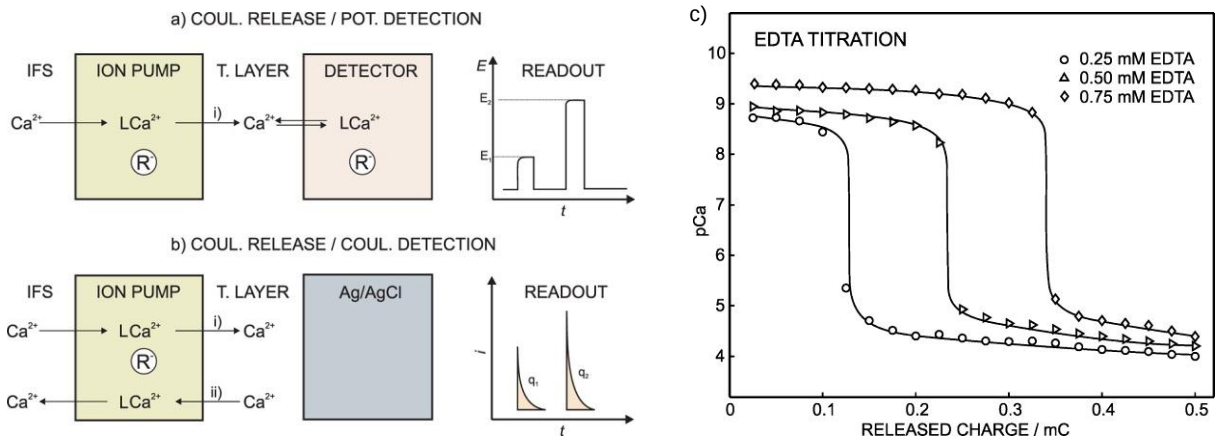

Figure 5. Illustration of coulometric release concept (labeled as ion pump) into a thin layer sample. (a) Flat sheet configuration with potentiometric readout (detector). E_1 and E_2 correspond to two different signals as a consequence of different excitation times. (b) Tubular configuration with a coulometric readout. The Ag/AgCl served as working electrode. The integrated charge, q_1 and q_2 correspond to two different signals obtained at two excitation times. IFS, internal filling solution; R^-, cation exchanger; L, ionophore.
(c) Complexometric titration by using the calcium pump plus potentiometric detection for three EDTA concentrations (0.25, 0.50, and 0.75 mM). Solid lines correspond to the calculated concentrations from equilibrium theory.
Flat sheet configuration indicates that the membrane of working electrode (calcium pump) use a flat porous polypropylene sheet. Tubular configuration means that the working electrode is a silver/silver chloride wire placed inside a hollow fiber doped with the lipophilic cocktail.

More recently, the introduction by our group of ion selective membranes to achieve coulometric titration has aimed to overcome the above mentioned limitations.[69] Calcium and barium ions (titrant ions) were chosen as initial examples. When a constant current and duration was applied across the ion selective membrane, Ca^{2+} or Ba^{2+} was released from the membrane to the sample solution with high selectivity and accuracy. A second ion selective electrode was used as end point indicator. As above, the amount of released titrant ions could be accurately calculated using Faraday's law.

Bakker and co-workers subsequently introduced the concept of thin layer coulometric titration (Figure 5).[70] By applying a constant potential, Ca^{2+} was electrochemically injected into a thin sample layer through transport across a calcium selective membrane (calcium pump). The free calcium ion activity in the thin layer was measured by another set of potentiometric ion-selective electrodes placed opposite the pumping electrode, only spaced by the thin layer gap. Calcium EDTA titration was demonstrated in the range of

0.25-0.75 mM with a precision of 3%, whereas the coulometric readout gave a range of 0.02-0.12 mM and a precision of 2%. This method requires only a very small amount of sample and is suitable for in-situ measurements. Moreover, it is potentially calibration free owing to the coulometric mode. For the latter to be true, the selectivity of the ionophore has to be high (which it normally is) and any non-Faradaic processes during the coulometric release must be negligible.

4. Indicators

4.1 Metallochromic dye based indicators

An end point detection by the naked eye is sometimes thought to be the most convenient way to visualize the titration end point, and metallochromic indicators can be applied for this purpose. As an indicator, it should also fulfill key criteria that include a high sensitivity to exhibit a drastic change at the end point, a high selectivity to obtain accurate results, and a sufficiently stable complex with the metal of interest. In the early days, Murexide and Eriochrome Black T were the classical dye indicators for Ca^{2+}, Mg^{2+} as well as other metal ions.[4,6,7] However, these dyes are not very selective and can only be used in a narrow window of pH.

The development of colorimetric/fluorescent metal sensors has gradually drawn people's attention to their wider applications in biochemical and environmental sciences. With the pursuit of high selective and sensitive metal ion sensors, a great number of specially

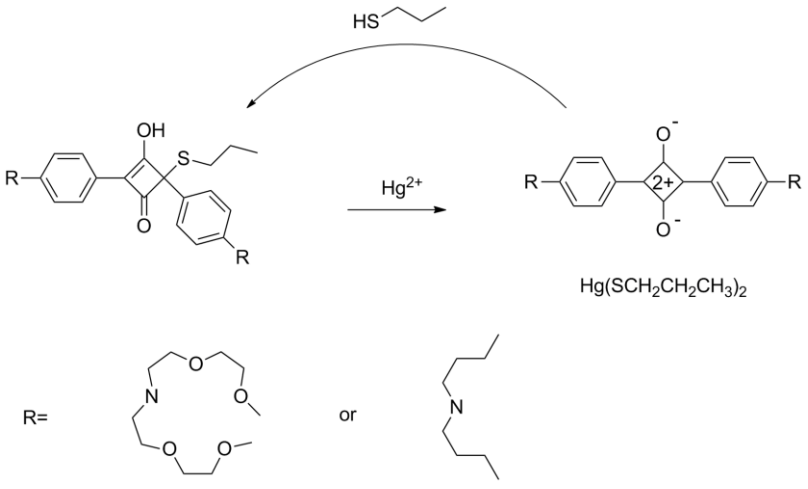

Figure 6. The analytical reverse reaction between squaraine derivatives and Hg^{2+}.

designed molecules have emerged where many proved to be good candidates as indicators for complexometric titration. The fluorophore/chromophore was usually modified with metal chelating groups and the metal binding would induce a change of the optical signal. Rhodamine, porphyrin, BODIPY , fluorescein, spiropyran, coumarin, dansyl derivatives and many others have been used as the fluorophore/chromophore[71-76] and dipicolylamine, glucosamine, Gly-His as receptor.[74,77,78] pH response sometimes accompanies the metal response because of protonatable groups on the fluorophore/chromophore and also on the metal chelating groups.

Martínez-Máñez, Rurack and co-workers designed a series of metal triggered dyes formation system for the highly selective determination of Hg^{2+}.[79] The squaraine derivatives were passivated first by a chemical addition reaction with thiols (spectroscopic inhibitor) that switch off the colorimetric and fluorescence properties of the indicator. When the target ions are present, they react with the thiols and release the indicator to induce the optical signal recovery shown in Figure 6. From the passivated state (colourless) to activated state (blue), the indicators generated dramatic changes in the optical signals, thereby improving sensitivity. The colour change was observed within a few seconds, making the compounds potential indicators for the titration of mercury ions. Fluorescent titration demonstrated that the indicator may detect less than 2 ppb of Hg^{2+} in solution. The indicator with a hydrophobic side chain was adsorbed onto powered silica and subsequently coated onto a polyethyleneterephthalate film. This film served to analyze Hg^{2+} and could easily be reused after washing with the thiol inhibitor.

Reymond and co-workers reported new types of fluorescent sensors for Cu^{2+} which are pH independent and exhibit a high selectivity.[80] These sensors were quinacridone (fluorophore) derivatives functionalized with a ethylenediamine group (binding site). The ethylenediamines were attached to each nitrogen atom of the symmetrical quinacridone via a linker. The presence of Cu^{2+} induced the quenching of the fluorescence by formation of the macrocyclic metal-chelator complex, which brought the complex and fluorophore closer to each other. To overcome the pH dependence, the authors modified the chemical structures of the indicator. By making the linker sufficiently long, the protonation/deprotonation of the chelating groups was found to no longer influence the fluorescence of the fluorophore. At the same time, the long linker did not affect the

ability for the metal to coordinate with the two ethylenediamines groups and to cause fluorescence quenching. The sensors showed good selectivity to copper and were independent of pH in the range from 2 to 10. The fluorescent titration showed a 1 to 1 stoichiometry of the complex.

Recently, our group has introduced emulsion based ion exchange nanospheres (discussed above) to serve also as optical indicators for complexometric titrations.[65] The indicating nanospheres contained a lipophilic pH sensitive dye (chromoionophore), an ion exchanger and an ionophore. For cationic analytes, the working principle of the indicating nanospheres is the exchange between the analyte and the H^+ released from the chromoionophore. The colour of the indicating nanospheres changes because the chromoionophore transitions from the protonated state to its deprotonated state. To serve as an indicator, the metal indicator complex should generally be 10 to 100 times less stable than the metal chelator complex so that the chelator can effectively displace the metal ion from the indicator complex. This is effectively achieved here with the same chelator/ionophore, since the effective affinity between metal and receptor is dictated by ion-exchange, which is weakened by the presence of the lipophilic pH indicator. The

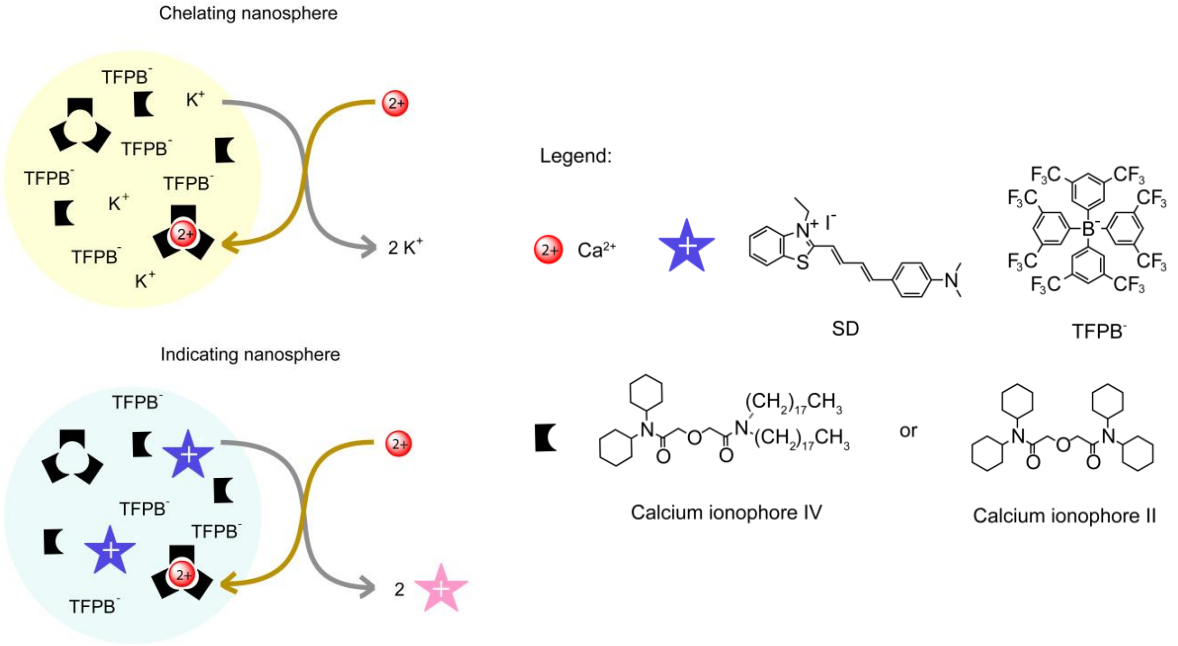

Figure 7. Schematic illustration of ion selective nanospheres as chelators and indicators in the complexometric titration of calcium. Chelating nanospheres contain calcium ionophore II and cation exchanger. Indicating nanosphere contain calcium ionophore IV, cation exchanger and solvatochromic dye SD.

chromoionophore-based indicating nanospheres may work in a wide pH range and even at very acidic pH. Unfortunately, however, the transitions become rather difficult to identify with increasing pH because the chromoionophore becomes more easily deprotonated at high pH.

To overcome this pH dependence, cationic solvatochromic dye based indicating nanospheres were recently introduced. The solvatochromic dye is not sensitive to pH and changes colour with the solvent environment.[64] In the emulsion based titration, a large amount of the chelating nanospheres and a much smaller amount of indicating nanospheres are mixed together, and the sample solution was gradually added. Here, the indicating nanospheres only function as indicator to show the colour change at the endpoint. Only when the chelating nanospheres become saturated at the endpoint, the cationic solvatochromic dye in the indicating nanopheres will be exchanged from the nanosphere core to the outside solution by the analyte (Figure 7). Owing to the different polarity between nanosphere core and aqueous solution, the colour of the solution will change. Essentially the same sharp titration curves were obtained at pH 5.5 and pH 9, which suggest that this concept can efficiently overcome the challenge of pH dependence

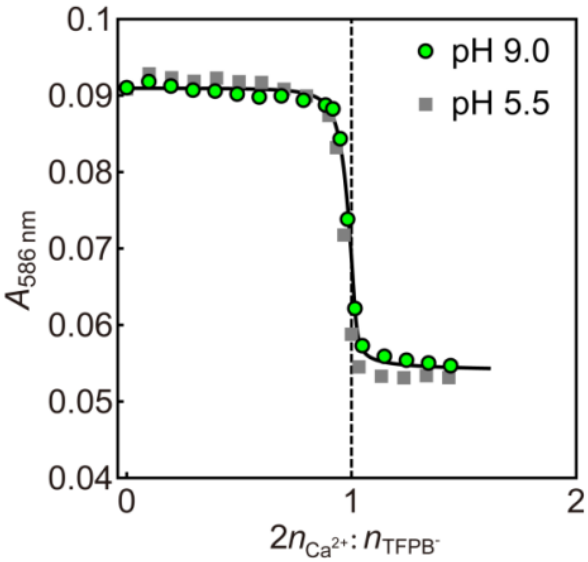

Figure 8. Optical reverse titration curves for calcium using solvatochromic dye SD based optical nanospheres as indicator at the indicated pH values. End point indicator: SD-based and Ca^{2+}-selective; pH 9.0: 10^{-3} M tris-H_2SO_4; pH 5.5: 10^{-3}M MES-NaOH; The dashed vertical line indicates the expected end point. Fitting parameters: V_T = 2 ml, $[TFPB^-]^{is}$ = $3.29\times10^{-6.15}$ M, V_{is} = 1.5 µL, $[TFPB^-]^{cs}$ =2.35×10^{-5} M, V_{cs} = 8 µL, $[Ca^{2+}]^{titrant}$ = 10^{-3} M, $K^{cs}_{Ca^{2+},J^+}[J^+]^{aq}$ =10^{-7} M, $K^{is}_{Ca^{2+},SD^+}[SD^+]^{aq}$ =$10^{-5.5}$ M.

in such titrations (Figure 8).

4.2 Instrument-based indicators

While the metallochromic indicators discussed above can directly visualize the end point by a colour change, sometimes appropriate indicating dyes are not easily found and instrumental methods are needed to identify the end point.

Potentiometry by ion selective electrodes is likely the most widely applied electrochemical indicator. An ion selective electrode can not only measure the activity of the ions but also act as end point indicator to visualize the so-called free activity of the analyte. In potentiometry, the observed signal, the electromotive force, is related to the analyte activity according to the Nernst equation. With the appropriate selectivity, a large change in the signal is usually observed at the end point.

Pretsch and co-workers suggested ways to improve the detection limits and sensitivity of potentiometric titrations, with lead(II) as example.[81] By changing the sensing components of the membrane and adjusting the flux of the primary ion, the detection limit of the titration could be improved by several orders of magnitude, and lower concentrations of lead could be titrated. To obtain lower detection limits of the lead selective electrode, a metal chelator, nitrilotriacetic acid (NTA) or EDTA, acting as a metal buffer at low concentrations was added to the inner solution of the ion selective electrode to keep the concentration of lead low and stable. In this particular case, the net Pb^{2+} flux was directed from the sample to the inner solution. With a significant inward flux, the ion selective electrode may show a super-Nernstian response slope to the analyte, thereby improving the sensitivity of the titration quite dramatically.

Daniele and co-workers used amperometry to detect the endpoint of Ca^{2+} and Mg^{2+} titrations with EDTA.[82] A platinum disc microelectrode was used to reduce the H^+ to H_2 in nonbuffered sample solutions. A second wave in the linear scan voltammogram was observed after the end point due to excess EDTA. The precision of the method was found to be satisfactory, the relative standard deviation being not larger than 2% for at least three replicates. Besides electrochemical methods, thermometric titration has been found to be an attractive universal method that measures the change of temperature with the added volume of titrant during a volumetric titration.[83] Since heat change is one of the

general characteristic of most reactions, a thermometric titration is suited for a wide range of reactions such as acid/base, precipitation, coordination and redox titrations.[83-87] Some factors such as light scattering, absorption inducing surface blocking, colour change or overlay, will influence the optical or potentiometric signal but have no significant influence on a thermometric titration. Thermometric titration has been successfully applied to monitor sulfate, total alkalinity, chlorinity in seawater,[85] and a wide range of metal ions such Ca^{2+}, Mg^{2+}, Fe^{2+}, Pb^{2+}.[83,84,87] The first thermometric titration research work was on acid and base neutralization and reported by Bell and Cowell in 1913.[88] Jordan successfully applied thermometric titration to estimate the heat produced by the complex formed between divalent metal ions and EDTA.[89] For example, both Ca^{2+} and Mg^{2+} could be determined by thermometric titration even if the formation constants differ by less than 2 orders of magnitude.[84,87] By comparison, the metallochromic indicator Eriochrome Black T is not sufficiently selective to separate Ca^{2+} and Mg^{2+} at the same time and require masking reagents or pH control.[4,6] In addition, different dynamic characteristics may also help separate the analytes by monitoring their release of heat in order to obtain a higher selectivity. A key disadvantage of this method is the relatively high detection limit compared with other instrumental indicators. The reason is that one requires a sufficiently large quantity of reaction substrate to observe a detectable temperature variance. The development of dedicated instruments encouraged the widespread use of this method. Recently, Barin and co-workers introduced a very simple and inexpensive setup for simultaneous enthalpimetric analysis by using an infrared camera as detector to monitor the temperature and disposable microplates to process the enthalpimetric analysis.[90] The noncontact and nondestructive infrared thermal imaging technique provided rapid signal acquisition with very good quantitative results. Even if some limitations for this new method remain, such as not being suitable for low reaction rate reactions, it still shows potential to be applied in a range of important applications.

5. Conclusion

The introduction of EDTA has made complexometric titrations a well known analytical technique. However, the drawbacks of EDTA have until recently not been overcome. As

summarized in this work, the advent of new titration reagents and end point indicators have injected new vitality into the field and also raised more issues to be resolved in further work.

Recent new concepts for chelators and indicators based on heterogeneous reactions involving emulsion based reagents show very promising characteristics for complexometric titration. Here, ion selective nanospheres really are multicomponent nanoscale solvent reactors that act in analogy to traditional chelators and indicators and extend the usage of lipophilic ionophores and other non-water-soluble compounds. This approach exhibits a high selectivity and sensitivity to a range of analytes, does not have to limit itself to a unique 1:1 complex stoichiometry, and is largely pH independent. Simply changing one or more of the components in the droplets, the nanospheres can be extended to other ions. This concept is highly suitable for titrating low concentrations of analyte. High analyte concentrations are more problematic, since nanosphere coagulation normally results in light scattering that interferes with an optical endpoint detection.

Thin layer coulometric titrations based on ion selective membranes consume only very small amount of sample. With a highly selective release of the titrant, only the analyte of interest is consumed or converted, which is very attractive for in situ analysis. Direct probes that give the same result as volumetric titrations, but without the hassle of sampling, splitting into aliquots, standardization of reagents, and volumetric delivery are potentially very attractive for a range of applications.

A number of the receptors or ionophores have been published and applied in different fields. However, there are not sufficient receptors of quality for anions, and highly selective and pH independent receptors are still very much needed.

Universal methods are also very popular, such as thermometric titrations, which measure the temperature change to indicate the end point. It is suitable to almost all reactions and not limited to complexation, but to obtain observable measurable temperature changes, it requires relatively large amount of substrates.

References

(1) Liebig, J. Justus Liebigs Ann. Chem. 1851, 77, 102.

(2) Schwarzenbach, G.; Kampitsch, E.; Steiner, R. *Helv. Chim. Acta.* **1945**, *28*, 1133.

(3) Yappert, M. C.; DuPré, D. B. *J. Chem. Educ.* **1997**, *74*, 1422.

(4) Schwarzenbach, G.; Flaschka, H. *Complexometric titrations* London, 1969.

(5) Ackermann, H.; Prue, J. E.; Schwarzenbach, G. *Nature* **1949**, *163*, 723.

(6) Gitelman, H. J.; Hurt, C.; Lutwak, L. *Anal. Biochem.* **1966**, *14*, 106.

(7) Lima, R. A. C.; Santos, S. R. B.; Costa, R. S.; Marcone, G. P. S.; Honorato, R. S.; Nascimento, V. B.; Araujo, M. C. U. *Anal. Chim. Acta* **2004**, *518*, 25.

(8) Patton, J.; Reeder, W. *Anal. Chem.* **1956**, *28*, 1026.

(9) Hildebrand, G. P.; Reilley, C. N. *Anal. Chem.* **1957**, *29*, 258.

(10) Tsien, R. Y. *Biochemistry* **1980**, *19*, 2396.

(11) Grynkiewicz, G.; Poenie, M.; Tsien, R. Y. *J. Biol. Chem.* **1985**, *260*, 3440.

(12) Reilley, C. N.; Porterfield, W. W. *Anal. Chem.* **1956**, *28*, 443.

(13) Reilley, C. N.; Schmid, R. W. *Anal. Chem.* **1958**, *30*, 947.

(14) Stock, J. T. *Anal. Chem.* **1976**, *48*, 1R.

(15) Reilley, C. N. *Anal. Chem.* **1960**, *32*, 185.

(16) Williams, K. R.; Young, V. Y.; Killian, B. J. *J. Chem. Educ.* **2011**, *88*, 315.

(17) Granholm, K.; Sokalski, T.; Lewenstam, A.; Ivaska, A. *Anal. Chim. Acta* **2015**, *888*, 36.

(18) Ni, Y.; Wu, Y. *Anal. Chim. Acta* **1997**, *354*, 233.

(19) Wilson, D.; Alegret, S.; Valle, M. d. *Electroanal.* **2015**, *27*, 336.

(20) DeGrandpre, M. D.; Martz, T. R.; Hart, R. D.; Elison, D. M.; Zhang, A.; Bahnson, A. G. *Anal. Chem.* **2011**, *83*, 9217.

(21) Maccà, C.; Soldà, L.; Zancato, M. *Anal. Chim. Acta* **2002**, *470*, 277.

(22) Reilley, C. N.; Vavoulis, A. *Anal. Chem.* **1959**, *31*, 243.

(23) Reilley, C. N.; Schmid, R. W.; Sadek, F. S. *J. Chem. Educ.* **1959**, *36*, 555.

(24) Martell, A. E.; Chaberek, S. *Anal. Chem.* **1954**, *26*, 1692.

(25) Wheelwright, E. J.; Spedding, F. H.; Schwarzenbach, G. *J. Am. Chem. Soc.* **1953**, *75*, 4196.

(26) Schwarzenbach, G.; Freitag, E. *Helv. Chim. Acta.* **1951**, *34*, 1503.

(27) Schwarzenbach, G.; Biedermann, W.; Bangerter, F. *Helv. Chim. Acta.* **1946**, *29*, 811.

(28) Schwarzenbach, G. *Helv. Chim. Acta.* **1946**, *29*, 1338.

(29) Ni, Y.; Peng, Z. *Anal. Chim. Acta* **1995**, *304*, 217.

(30) Maccà, C.; Soldà, L.; Favaro, G.; Pastore, P. *Talanta* **2007**, *72*, 655.

(31) Gao, J.; Guo, Y.; Wang, S.; Deng, T.; Chen, Y.-W.; Belzile, N. *J. Chem.* **2013**, *2013*, 1.

(32) Xian-ke, W. *Analyst* **1990**, *115*, 1611.

(33) Vlasák, M.; Luxemburková, Z.; Sychra, V.; Suchánek, M. *Accred. Qual. Assur.* **2013**, *18*, 491.

(34) Novick, S. G. *J. Chem. Educ.* **1997**, *74*, 1463.

(35) Yang, S.-P.; Tsai, R.-Y. *J. Chem. Educ.* **2006**, *83*, 906.

(36) Romero, M.; Guidi, V.; Ibarrolaza, A.; Castells, C. *J. Chem. Educ.* **2009**, *86*, 1091.

(37) Fabre, P.-L.; Reynes, O. *J. Chem. Educ.* **2010**, *87*, 836.

(38) Fritz, J. S.; Sickafoose, J. P.; Schmitt, M. A. *Anal. Chem.* **1969**, *41*, 1954.

(39) Yappert, M. C.; DuPré, D. B. *J. Chem. Educ.* **1997**, *74*, 1422.

(40) Malmstadt, H. V.; Hadjiioannou, T. P. *Anal. Chim. Acta* **1958**, *19*, 563.

(41) McCormick, P. G. *J. Chem. Educ.* **1973**, *50*, 136.

(42) Karita, S.; Kaneta, T. *Anal. Chim. Acta* **2016**, *924*, 60.

(43) Koehler, F. M.; Rossier, M.; Waelle, M.; Athanassiou, E. K.; Limbach, L. K.; Grass, R. N.; Günther, D.; Stark, W. J. *Chem. Commun.* **2009**, 4862.

(44) Vassileva, E.; Varimezova, B.; Hadjiivanov, K. *Anal. Chim. Acta* **1996**, *336*, 141.

(45) Chen, C.; Tian, T.; Wang, M. K.; Wang, G. *Geoderma* **2016**, *275*, 74.

(46) Bucheli-Witschel, M.; Egli, T. *FEMS Microbiol. Rev.* **2001**, *25*, 69.

(47) Nowack, B. *Environ. Sci. Technol.* **2002**, *36*, 4009.

(48) Rahman, M. A.; Won, M.-S.; Shim, Y.-B. *Anal. Chem.* **2003**, *75*, 1123.

(49) Sears, M. E. *Scientific World J.* **2013**, *2013*, 1.

(50) Ansari, S. A.; Pathak, P.; Mohapatra, P. K.; Manchanda, V. K. *Chem. Rev.* **2012**, *112*, 1751.

(51) Ansari, S. A.; Pathak, P.; Mohapatra, P. K.; Manchanda, V. K. *Sep. Purif. Rev.* **2011**, *40*, 43.

(52) Narita, H.; Yaita, T.; Tamura, K.; Tachimori, S. *J. Radioanal. Nucl. Chem.* **1999**, *239*, 381.

(53) Sasaki, Y.; Suzuki, H.; Sugo, Y.; Kimura, T.; Choppin, G. R. *Chem. Lett.* **2006**, *35*, 256.

(54) Sasaki, Y.; Sugo, Y.; Suzuki, S.; Tachimori, S. *Solvent Extr. Ion Exch.* **2001**, *19*, 91.

(55) Modolo, G.; Asp, H.; Schreinemachers, C.; Vijgen, H. *Solvent Extr. Ion Exch.* **2007**, *25*, 703.

(56) Ansari, S. A.; Pathak, P. N.; Manchanda, V. K.; Husain, M.; Prasad, A. K.; Parmar, V. S. *Solvent Extr. Ion Exch.* **2005**, *23*, 463.

(57) Suzuki, H.; Naganawa, H.; Tachimori, S. *Phys. Chem. Chem. Phys.* **2003**, *5*, 726.

(58) Shimojo, K.; Kurahashi, K.; Naganawa, H. *Dalton Trans.* **2008**, 5083.

(59) Mohapatra, P. K. *Chem. Prod. Process Model.* **2015**, *10*, 135.

(60) Mohapatra, P. K.; Sengupta, A.; Iqbal, M.; Huskens, J.; Verboom, W. *Chem. Eur. J.* **2013**, *19*, 3230.

(61) Sengupta, A.; Mohapatra, P. K.; Kadam, R. M.; Manna, D.; Ghanty, T. K.; Iqbal, M.; Huskens, J.; Verboom, W. *RSC Adv.* **2014**, *4*, 46613.

(62) Jańczewski, D.; Reinhoudt, D. N.; Verboom, W.; Hill, C.; Allignol, C.; Duchesne, M.-T. *New J. Chem.* **2008**, *32*, 490.

(63) Zhai, J.; Xie, X.; Bakker, E. *Chem. Commun.* **2014**, *50*, 12659.

(64) Zhai, J.; Xie, X.; Bakker, E. *Anal. Chem.* **2015**, *87*, 12318.

(65) Zhai, J.; Xie, X.; Bakker, E. *Anal. Chem.* **2015**, *87*, 2827.

(66) Rodriguez, J. D.; Vaden, T. D.; Lisy, J. M. *J. Am. Chem. Soc.* **2009**, *131*, 17277.

(67) Bakker, E.; Bühlmann, P.; Pretsch, E. *Chem. Rev.* **1997**, *97*, 3083.

(68) Bühlmann, P.; Pretsch, E.; Bakker, E. *Chem. Rev.* **1998**, *98*, 1593.

(69) Bhakthavatsalam, V.; Shvarev, A.; Bakker, E. *Analyst* **2006**, *131*, 895.

(70) Afshar, M. G.; Crespo, G. A.; Bakker, E. *Anal. Chem.* **2015**, *87*, 10125.

(71) Papkovsky, D. B.; Ponomarev, G. V.; Wolfbeis, O. S. *Spectrochim. Acta, Part A* **1996**, *52*, 1629.

(72) Sheng, R.; Wang, P.; Gao, Y.; Wu, Y.; Liu, W.; Ma, J.; Li, H.; Wu, S. *Org. Lett.* **2008**, *10*, 5015.

(73) Maity, S. B.; Banerjee, S.; Sunwoo, K.; Kim, J. S.; Bharadwaj, P. K. *Inorg. Chem.* **2015**, *54*, 3929.

(74) Zheng, Y.; Cao, X.; Orbulescu, J.; Konka, V.; Andreopoulos, F. M.; Pham, S. M.; Leblanc, R. M. *Anal. Chem.* **2003**, *75*, 1706.

(75) Hancock, R. D. *Chem. Soc. Rev.* **2013**, *42*, 1500.

(76) Winkler, J. D.; Deshayes, K.; Shao, B. *J. Am. Chem. Soc.* **1989**, *111*, 769.

(77) Hatai, J.; Bandyopadhyay, S. *Chem. Commun.* **2014**, *50*, 64.

(78) Mitra, A.; Mittal, A. K.; Rao, C. P. *Chem. Commun.* **2011**, *47*, 2565.

(79) Ros-Lis, J. V.; Marcos, M. D.; Martínez-Máñez, R.; Rurack, K.; Soto, J. *Angew. Chem. Int. Ed.* **2005**, *44*, 4405.

(80) Klein, G.; Kaufmann, D.; Schürch, S.; Reymond, J.-L. *Chem. Commun.* **2001**, 561.

(81) Peper, S.; Ceresa, A.; Bakker, E.; Pretsch, E. *Anal. Chem.* **2001**, *73*, 3768.

(82) Baldo, M. A.; Daniele, S.; Bragato, C.; Mazzocchin, G. A. *Analyst* **1999**, *124*, 1059.

(83) Zenchelsky, S. T. *Anal. Chem.* **1960**, *32*, 289.

(84) Callicott, R. H.; Carr, P. W. *Clin. Chem.* **1976**, *22*, 1084.

(85) Millero, F. J.; Schrager, S. R.; Hansen, L. D. *Limnol. Oceanogr.* **1974**, *19*, 711.

(86) Everson, W. L. *Anal. Chem.* **1971**, *43*, 201.

(87) Yoshida, H.; Hattori, T.; Arai, H.; Taga, M. *Anal. Chim. Acta* **1983**, *152*, 257.

(88) Bell, J. M.; Cowell, C. F. *J. Am. Chem. Soc.* **1913**, *35*, 49.

(89) Jordan, J.; Alleman, T. G. *Anal. Chem.* **1957**, *29*, 9.

(90) Barin, J. S.; Tischer, B.; Oliveira, A. S.; Wagner, R.; Costa, A. B.; Flores, E. M. M. *Anal. Chem.* **2015**, *87*, 12065.

Chapter 2. Ionophore-Based Ion-Exchange Emulsions as Novel Class of Complexometric Titration Reagents

This work has been published in *Chem. Commun.*, **2014**, *50*, 12659-12661

Abstract

Complexometric titrations rely on a drastic change of the pM value at the equivalence point with a water soluble chelator forming typically 1:1 complexes of high stability. The available chemical toolbox of suitable chelating compounds is unfortunately limited because many promising complexing agents are not water soluble. We introduce here a novel class of complexometric titration reagents, a suspension of polymeric nanospheres whose hydrophobic core is doped with lipophilic ion-exchanger and a selective complexing agent (ionophore). The emulsified nanospheres behave on the basis of heterogeneous ion exchange equilibria where the initial counter ion of the ion-exchanger is readily displaced from the emulsion for the target ion that forms a stable complex in the nanosphere core. Two different examples are shown with Ca^{2+} and Pb^{2+} as target ions. The lack of protonatable groups on the calcium receptor allows one to perform Ca^{2+} titration without pH control.

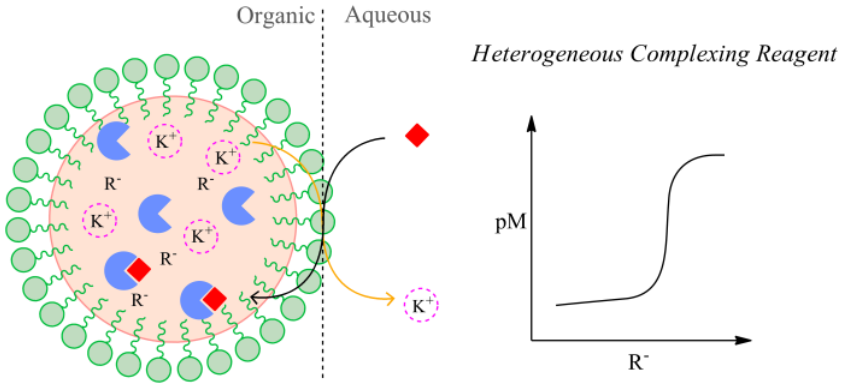

Introduction

Complexing agents for metal ions are today widely used in complexometric titrations, gravimetry, heavy metal detoxification, spectrophotometry, solvent extraction, and chromatography.[1-7] Complexometric titration (chelometry) is a well-established approach for the determination of metal ions where the complexing agent is used to drastically decrease the concentration of so-called free metal ion in solution at the equivalence point. This change is typically visualized electrochemically with ion-selective electrodes or optically with indicator dyes. [5,8]

As proposed by Schwarzenbach[9] , for a reagent to serve in a titration procedure, (i) the reaction must be rapid; (ii) it must proceed stoichiometrically; and (iii) the change in free energy must be sufficiently large.

Until today, complexometric titrations made use of chelators that undergo homogeneous complexation reactions. Water soluble polyaminocarboxylic acid chelators such as ethylenediaminetetraacetic acid (EDTA) and diethylenetriaminepentaacetic acid (DTPA) are the most widely used chelators, forming complexes of sufficient stability with nearly all polyvalent cations.[2,10,11] Because of this, their selectivity is not always satisfactory. To ensure adequate selectivity, additional masking agents are required and/or the pH of the solution needs be carefully controlled. For example, calcium titrations with EDTA must be performed above pH 10.[12] In addition, when chelators are used as antidotes for heavy metal intoxication, the potential toxicity of these compounds also requires attention.[2] For instance, the chelator 2,3-dimercaptopropanol (British Anti Lewisite, BAL), an early antidote for Hg^{2+}, was later found to be toxic because of its ability to accumulate organic and inorganic mercury in the brain.[13]

We propose here a new chemical principle for the design of complexometric titration reagents. Instead of relying on the complexation to occur in homogeneous phase, we make use of nanosphere containing emulsions doped with ion-exchanger and hydrophobic receptor. This makes it possible to move the complexation reaction from the aqueous phase to an organic environment, where many more receptor molecules with highly tunable binding selectivities are available. Moreover, such a design also allows further modification of the nanoparticle matrix material to reduce bio-toxicity.

Results and Discussion

The principle is shown in Scheme 1. The emulsion is doped with a lipophilic ion-exchanger whose counter ion is readily displaced by the ion of interest. While the relative preference of one (uncomplexed) ion over another is governed by the Hofmeister lipophilicity sequence, the hydrophobic receptor in the particle core forms additionally a stable and selective complex of defined complex stoichiometry with the target ion. While the receptor drives the selective uptake by the nanoscale reagent, the ion-exchanger defines the quantity of extractable ions.

Adequate lipophilic ion receptors, also known as ionophores, have been used in the design of highly selective optical and electrochemical ion sensors for some time with great success [14,15]. The complexation reaction between the ionophore and target ions is typically diffusion controlled. Together with a small size of less than 100 nm in diameter that ensures a rapid phase transfer process, the first requirement for the complexing agent is fulfilled. The stoichiometry is typically known, thus the second requirement is also fulfilled. Note that the complex stoichiometry is much less critical than with homogenous titrations since one quantifies the amount of extractable ions by the amount of the ion

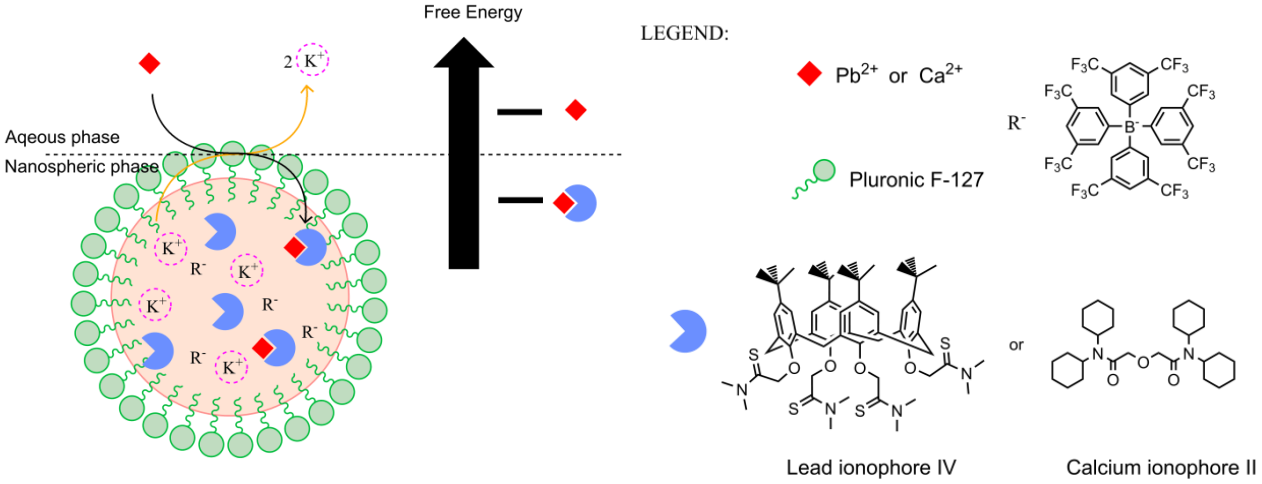

Scheme 1. Ion-selective emulsions containing nanospheres as complexing agent and structures of the compounds used in this work. The nanosphere core is made of dodecyl 2-nitrophenyl ether (D-NPOE) and the hydophobic sub-structure of Pluronic F-127. The complexation reaction comprises (1) ion exchange between target ion (Ca^{2+} or Pb^{2+}) in aqueous phase and the counter ion of R^- (K^+) in the organic phase and (2) the complexation reaction between target ion and the receptor, which lowers the solvation energy for the target ion and provide the driving force for its uptake into the nanospheres.

exchanger if the receptor is in sufficient molar excess. Such ionophores exhibit binding constants that are often very high, for divalent ions up to 25 orders of magnitude,[16] and thus fulfil the third requirement stated above for complexing agents.

The Ca^{2+} and Pb^{2+} selective emulsions were prepared by a precipitation method,[17-19] where a tetrahydrofuran (THF) solution containing calcium ionophore II (ETH 129) or lead ionophore IV, potassium tetrakis[3 ,5-bis(trifluoromethyl)phenyl]borate (KTFPB), dodecyl 2-nitrophenyl ether (D-NPOE) and surfactant Pluronic F-127 was injected into vortexing water to form a self-assembled nanosphere suspension. The ion-selective emulsions were obtained after removal of THF. The resulting emulsion exhibits monodipersity and is stable for at least four weeks.

In the complexometric titration of Ca^{2+} and Pb^{2+}, the calcium or lead ion-selective emulsions were used as complexing agents and potentiometric ion-selective electrodes were employed as endpoint detectors. Three different concentrations of lead and calcium were explored for the titration experiment shown in Figure 1. Accurate titration curves were obtained with relative errors of less than 3%. The results showed satisfactory agreement with theoretically expected equivalence points as indicated by the vertical

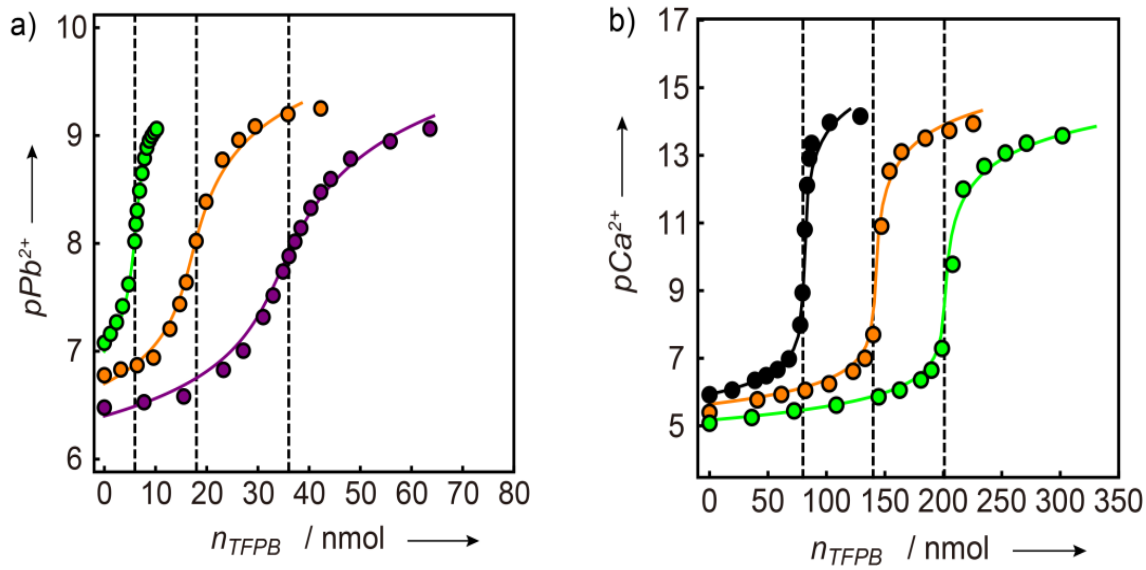

Figure 1. (a) Potentiometric titration curves for 10^{-7} M (green), 3×10^{-7} M (orange), 6×10^{-7} M (purple) Pb^{2+} in unbuffered solutions (amounts of Pb^{2+} in solution: 3 nmol, 9 nmol, and 18 nmol). (b) Potentiometric titration curves for 4×10^{-6} M (black), 7×10^{-6} M (orange), 10^{-5} M (green) of Ca^{2+} in unbuffered water, corresponding to total amounts of 40 nmol, 70 nmol, and 100 nmol. The dashed vertical lines show the expected endpoints.

dotted lines, which were calculated on the basis of number of moles of added ion-exchanger, which defines the amount of extractable ions from the sample. The response time is less than 1 min before the endpoint as shown in Figure S1, which is essentially given by the time response of the potentiometric detector. The emulsion containing only TFPB was confirmed to not function properly for Ca^{2+} or Pb^{2+} titration because it lacks selectivity.

As an early stage application, the calcium level in the river Arve (Geneva, Switzerland) was determined as 1.40 mM ± 0.06 mM SD using a calcium selective emulsion as complexing agent for Ca^{2+}. This titration compares favorably with an EDTA titration at pH 10 using EBT as endpoint indicator (1.37 mM ± 0.01 mM SD). The results also indicate that the selectivity of the nanospheres is sufficient for this application.

As mentioned above, most available chelators for complexometric titrations require careful pH control or the use of additional masking agents. For the emulsion based calcium chelator, this is generally not necessary because the interference by H^+ is very small, owing to the lack of protonatable groups on the calcium receptor. Figure 2 shows a comparison of titration curves between calcium selective emulsions and conventional

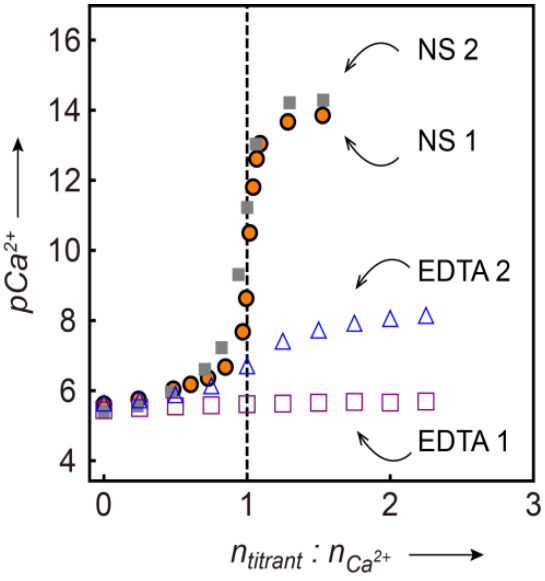

Figure 2. Comparing calcium selective emulsion with EDTA as complexing agents for the potentiometric titrations of 4 µM calcium. NS 1: titration in non-buffered water by calcium selective emulsion; NS 2: titration in 1mM pH 7.0 Tris-HCl by emulsion; EDTA 1: titration in non-buffered water by EDTA; EDTA 2: titration in 1 mM pH 7.0 Tris-HCl by EDTA. The dashed vertical line marks the endpoint.

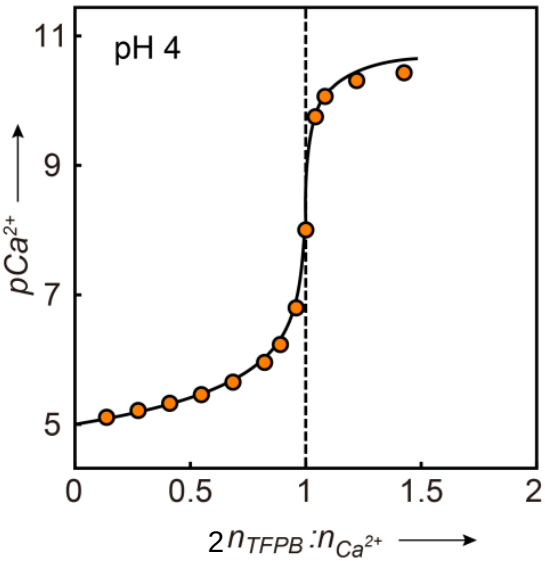

Figure 3. Potentiometric titration curve for 10^{-5} M $CaCl_2$ in pH 4 HCl solution with calcium selective emulsion as titration reagent. Dashed vertical line marks the expected endpoint.

calcium chelator EDTA. As established for EDTA, the lack of a pH buffer results in the disappearance of the endpoint with EDTA. On the other hand, the emulsion-based titrant gives essentially the same endpoint transitions for an unbuffered sample and one buffered at pH 7.0. Figure 3 even demonstrates the successful titration of calcium under acidic conditions (pH 4). At pH 7.0, the titration curves using the emulsions are much sharper than EDTA owing to the stronger Ca^{2+} binding affinity of calcium ionophore II.

In summary, we propose here ion-selective nanosphere containing emulsions as a new family of complexing reagents. The nanospheres work on the basis of heterogeneous ion exchange equilibria. Ca^{2+} and Pb^{2+} selective emulsions were shown here as initial examples for complexometric titrations. The ion-selective nanospheres can quantitatively bind calcium or lead ions, even without pH control. Chelators such as EDTA have been widely applied for chelometry but the selectivity and working pH range has not really evolved in the past 60 years. This work opens up new chemical avenues to attain binding affinities and selectivities that have so far not been achievable with homogeneous binding approaches.

Supporting Information

Experimental Section

Reagents:

Pluronic F-127 (F127), bis(2-ethylhexyl)sebacate (DOS), 2-nitrophenyl octyl ether (o-NPOE), dodecyl 2-nitrophenyl ether (D-NPOE), tetradodecylammonium tetrakis(4-chlorophenyl)borate (ETH 500), tetrahydrofuran (THF), sodium tetrakis-[3,5-bis(trifluoromethyl)phenyl]borate (NaTFPB), potassium tetrakis[3,5-bis(trifluoromethyl)phenyl]borate (KTFPB), calcium ionophore II (ETH 129), calcium ionophore IV, lead ionophore IV, poly(vinyl chloride) (PVC), $CaCl_2$, $Pb(NO_3)_2$, ethylenediaminetetraacetic acid disodium salt dehydrate (Na_2EDTA), 2-amino-2-hydroxymethyl-propane-1,3-diol (Tris) , hydrochloric acid (HCl) and Eriochrome Black T (EBT) were obtained from Sigma-Aldrich. Super pure nitric acid (65% w/w) was obtained from MERCK. Methyl methacrylate-decyl methacrylate copolymer (MMA-DMA) was synthetized in our group[20]. Arve River sample was obtained from Geneva, Switzerland.

Preparation of Ca^{2+}-selective and Pb^{2+}-selective emulsion:

For Ca^{2+}-selective emulsion, 2.24 mg of calcium ionophore II, 1.24 mg of KTFPB, 8.0 mg of D-NPOE and 3.0 mg of F127 were dissolved in 2.0 mL of THF to form a homogeneous solution. 0.5 mL of this THF solution was pipetted and injected into 3 mL of deionized water vortexing at 1000 rpm. Compressed air was blown on the surface for 30 min to remove THF.

For Pb^{2+}-selective emulsion, 1.83 mg of lead ionophore IV, 0.63 mg of KTFPB, 6.08 mg of D-NPOE, and 2.48 mg of F127 were dissolved in 2.0 mL of THF, followed by the procedure above.

Membranes and electrodes:

The Ca^{2+}-selective membrane was prepared by dissolving the mixture composed of 16.5 mmol/kg of calcium ionophore IV, 6.9 mmol/kg NaTFPB, 63.1 wt% o-NPOE, and 33.5

wt% PVC in 1.5 mL THF. For Pb^{2+}-selective membranes, the membranes optimized for low detection limits contained 0.74 mmol/ kg lead ionophore IV, 0.34 mmol/kg NaTFPB, 10.98 mmol/kg ETH 500, 33.00 wt% MMA-DMA, 22.80 wt% DOS, 42.83 wt% PVC, and 0.17 mmol/kg $Pb(NO_3)_2$. The cocktail solution was then poured into a glass ring (22 mm in diameter) placed on a glass slide and dried overnight at room temperature under a dust-free environment. Small disks were punched from the cast films and conditioned for 2 days in 5×10^{-9} M $Pb(NO_3)_2$ (diluted by 10^{-4} M HNO_3) for Pb^{2+}-selective membranes, and corresponding Ca^{2+}-selective membranes in 5×10^{-9} M $CaCl_2$. The conditioned membranes were mounted separately in Ostec electrode bodies (Ostec, Sargans, Switzerland). For the Ca^{2+} ISE, 10^{-2} M Na_2EDTA, 10^{-4} M $CaCl_2$, adjusted to pH 7.0 with NaOH, was used as inner filling solution. For the Pb^{2+} ISE with a low detection limit, 10^{-2} M Na_2EDTA, 10^{-4} M $Pb(NO_3)_2$, adjusted to pH 7.0 with NaOH, was used as inner filling solution.

Instrumentations and measurements:

Potentiometric titration signals were recorded on an EMF-16 precision electrochemistry

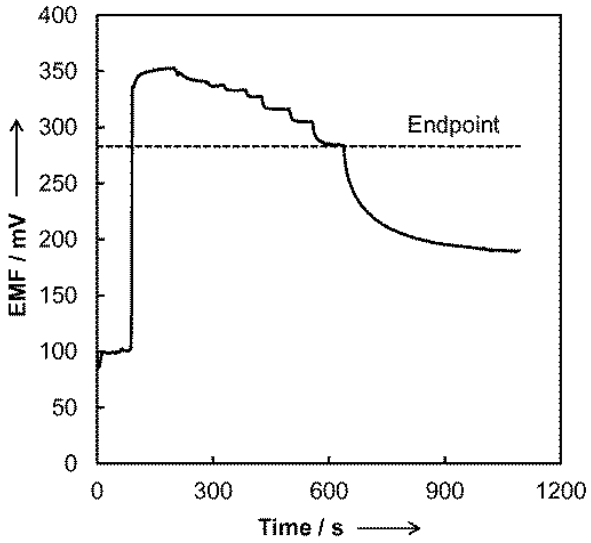

Figure S1. Potentiometric titration curve for 7×10^{-6} M of Ca^{2+} in 10 mL non-buffered water. The volumes of the added calcium selective emulsion were 200 µL, 4 × 100 µL, 50 µL, 2 × 34 µL respectively. The concentration of the ion exchanger KTFPB in the calcium selective emulsion stock solution was 2.05×10^{-4} M.The endpoint appeared at 684 µL. The amount of the KTFPB at the endpoint was 140 nano mole.The response time is less than 1 min before the endpoint, and mainly dictated by the response time of the ion-selective electrode used for the detection.

EMF interface from Lawson Laboratories, Inc. A double-junction Ag/AgCl was used as reference electrode (Mettler-Toledo AG, Schwerzenbach, Switzerland).

For potentiometric calcium titrations, samples were prepared by diluting 4 µL, 7 µL, 10 µL of 10^{-2} M of $CaCl_2$ to 10 mL by water to obtain the Ca^{2+} concentrations of 4×10^{-6} M, 7×10^{-6} M, and 10^{-5} M, respectively. Ca^{2+}-selective electrodes were used as endpoint detectors and Ca^{2+}-selective emulsion as titration reagent.

For potentiometric lead titration, the samples were prepared by adding 30 µL, 90 µL, 180 µL of 10^{-4} M $Pb(NO_3)_2$ to 30 mL water to obtain the Pb^{2+} concentrations 10^{-7} M, 3×10^{-7} M, and 6×10^{-7} M, respectively. Pb^{2+}-selective electrodes were used as endpoint detectors and Pb^{2+}-selective emulsion as titration reagents.

References

(1) Hahn, R. B.; Allam, S. I. Anal. Chem. 1967, 39, 1880.

(2) Scott, L. E.; Orvig, C. Chem. Rev. 2009, 109, 4885.

(3) Buccella, D.; Horowitz, J. A.; Lippard, S. J. J. Am. Chem. Soc. 2011, 133, 4101.

(4) Pandey, U.; Dhami, P. S.; Jagesia, P.; Venkatesh, M.; Pillai, M. R. A. Anal. Chem. 2008, 80, 801.

(5) Peper, S.; Ceresa, A.; Bakker, E.; Pretsch, E. Anal. Chem. 2001, 73, 3768.

(6) Ansari, S. A.; Pathak, P.; Mohapatra, P. K.; Manchanda, V. K. Chem. Rev. 2012, 112, 1751.

(7) Rosario-Amorin, D.; Ouizem, S.; Dickie, D. A.; Wen, Y.; Paine, R. T.; Gao, J.; Grey, J. K.; Bettencourt-Dias, A. d.; Hay, B. P.; Delmau, L. H. Inorg. Chem. 2013, 52, 3063.

(8) Reilley, C. N.; Schmid, R. W. Anal. Chem. 1958, 30, 947.

(9) Schwarzenbach, G.; Flaschka, H. Complexometric titrations; Methuen: London, 1969.

(10) Christian, G. D. Analytical Chemistry; 6 ed.; John Wiley & Sons, Inc., 2004.

(11) Yin, P.; Li, T.; Forgan, R. S.; Lydon, C.; Zuo, X.; Zheng, Z. N.; Lee, B.; Long, D.; Cronin, L.; Liu, T. J. Am. Chem. Soc. 2013, 135, 13425.

(12) Reilley, C. N.; Schmid, R. W.; Sadek, F. S. J. Chem. Educ. 1959, 36, 555.

(13) Berlin, M.; Ullrebg, S. Nature 1963, 197, 84.

(14) Bakker, E.; Bühlmann, P.; Pretsch, E. Chem. Rev. 1997, 97, 3083.

(15) Xie, X.; Mistlberger, G.; Bakker, E. J. Am. Chem. Soc. 2012, 134, 16929.

(16) Bakker, E.; Pretsch, E. Angew. Chem. Int. Ed. 2007, 46, 5660.

(17) Xie, X.; Mistlberger, G.; Bakker, E. Anal. Chem. 2013, 85, 9932.

(18) Xie, X.; Bakker, E. ACS Appl. Mater. Interfaces 2014, 6, 2666.

(19) Xie, X.; Zhai, J.; Bakker, E. Anal. Chem. 2014, 86, 2853.

(20) Qin, Y.; Peper, S.; Bakker, E. Electroanalysis 2002, 14, 1375.

Chapter 3. Ion-selective Optode Nanospheres as Heterogeneous Indicator Reagents in Complexometric Titrations

This work has been published in *Anal. Chem.*, **2015**, *87* (5), 2827-2831

Abstract

Traditionally, optical titrations of inorganic ions are based on a rapid and visible colour change at the endpoint with water soluble organic dyes as indicators. Adequate selectivity is required for both the indicator and the complexing agent, which is often limited. We present here alternative, heterogenous ionophore based ion selective nanospheres as indicators and chelators for optical titrations. The indicating nanospheres rely on a weaker extraction of the analyte of interest by ion-exchange, owing to the additional incorporation of a lipophilic pH indicator in the nanosphere core. Ca^{2+} titration was demonstrated as a proof-of-concept. Both the chelating and the indicating nanospheres showed good selectivity and a wide working pH range.

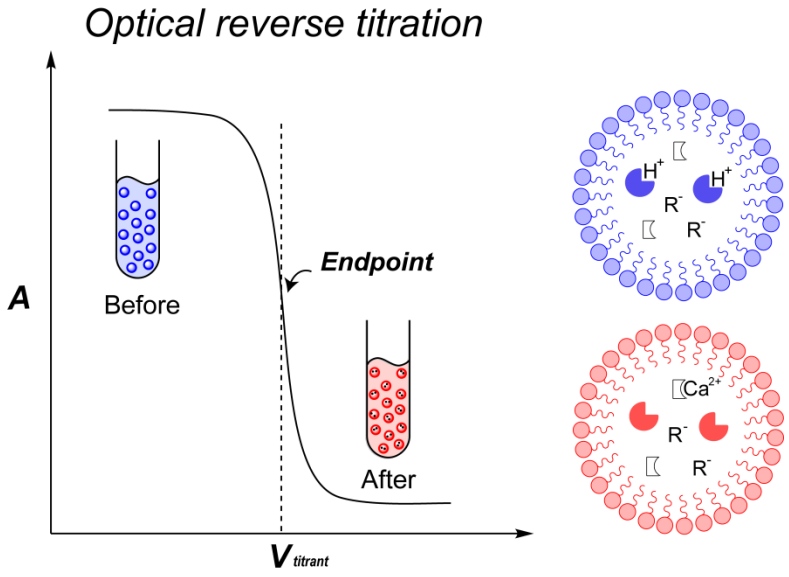

Introduction

Complexometric titration is a mature analytical technique that is being taught all over the world in analytical science.[1,2] Titrations are routinely used to determine ion concentration, speciation as well as complexation reactions in various fields such as environmental, clinical and bioanalytical chemistry.[3-6]

Water soluble organic compounds have been applied as chelators for complexometric titrations for over sixty years.[2,3,7] However, their pH dependent complexing ability and rather rigid selectivity remains an issue.[1,2,8] We have recently introduced colloidal titration reagents that may dramatically increase the available chemical toolbox of possible titration reagents, alleviate the need for pH control, and eliminate the requirement of a defined and singular reaction stoichiometry.[9]

The titration endpoint may typically be detected with optical indicators or electrochemical sensors.[6,10] An optical indicator, also a chelating agent, is easy to handle compared with electrochemical sensors owing to the convenient visual colour change at the endpoint. Organic dyes that directly bind to the analyte ion are typically used as optical indicators in chelometry. Current examples include phenolphthalein,[11] methyl red,[12] fast sulphon black,[13] Eriochrome Black T,[14] and murexide.[15]

As an optical indicator, the metal-indicator complex must be at least 10 to 100 times less stable than the metal-chelator complex so that the chelator can effectively displace the ion from the indicator complex. An indicator should have good selectivity, rapid and visible change in colour and be water soluble and stable. Not all available optical indicators can fulfil these requirements.[1]

Numerous indicators are weak acids, such as Eriochrome Black T, a classical indicator for determination of water hardness.[14] As a weak acid, its colour will also depend on the sample pH. In addition, the stability of metal-indicator complex and metal-chelator complex are pH dependent as well, and these types of experiments require careful pH control.[2]

Moreover, some optical indicators do not exhibit good selectivity. For example, murexide is used as an indicator for several metal ions including Ca^{2+}, Cu^{2+}, Ni^{2+}, and Co^{2+}.[15,16] A bias in the observed endpoint may arise in cases where these ions coexist in the sample.

Ionophore based optical ion sensors (optodes) have been known for many years.[17-19] However, their application as endpoint indicator for titration applications has not yet been put forward. The sensor must exhibit sufficient sensitivity to act as endpoint indicator. It is also known that the optode response is pH dependent, and therefore it requires pH control. Recently, an exhaustive sensing mode for ion selective optodes has been proposed.[19,20] The exhaustive nanosensors exhibited low detection limit, short response time and may largely overcome any pH cross-response.

Here, we report for the first time that titrimetric analysis can be performed with ion selective nanospheres acting both as chelators and indicators, thereby moving the conventional homogeneous titration in aqueous phase to a heterogeneous emulsion based organic–aqueous environment. pH independent titrations for Ca^{2+} were achieved by using exhaustive calcium-selective optical nanospheres as endpoint indicator while calcium selective nanospheres containing no chromoionophore was used as chelators.

Experimental Section

Reagents:

Pluronic F-127 (F127), o-nitrophenyl octyl ether (o-NPOE), dodecyl o-nitrophenyl ether (o-NPDDE), tetrahydrofuran (THF), sodium tetrakis-[3,5-bis(trifluoromethyl)phenyl]borate (NaTFPB), potassium tetrakis[3,5-bis(trifluoromethyl)phenyl]borate (KTFPB), calcium ionophore II (ETH 129), chromoionophore I (CH1), calcium ionophore IV, poly(vinyl chloride) (PVC), sodium hydrogen carbonate ($NaHCO_3$), hydrochloric acid (HCl), nitric acid (HNO_3, super pure) and calcium chloride ($CaCl_2$) were obtained from Sigma-Aldrich. Standard reference material (1643e, trace elements in water) was obtained from the National Institute of Standard and Technology (NIST).

Preparation of chelating and indicating nanospheres:

To prepare the chelating nanospheres, typically 2.27 mg of ETH129, 1.24 mg of KTFPB, 8.0 mg of o-NPDDE, and 3.0 mg of F127 were dissolved in 2.0 mL of THF to form a homogeneous solution. 0.5 mL of the THF solution was pipetted and injected into 3 mL

of deionized water on a vortex with a vortexing speed of 1000 rpm. Compressed air was blown on the surface of the resulting nanosphere emulsion for 30 min to remove THF. To prepare the indicating nanospheres, typically 5.66 mg of calcium ionophore IV, 0.75 mg of CH1, 1.78 mg of NaTFPB, 8.0 mg of o-NPOE, and 5.0 mg of F127 were dissolved in 3.0 mL of THF to form a homogeneous solution. The same procedure as mentioned above was used to fabricate the nanospheres.

Instrumentation:

Optical titration signals were measured with a UV−visible absorption spectrometer (SPECORD 250 plus, Analytic Jena, AG, Germany).

Optical titration:

2.5 mL or 3 mL of the chelating nanospheres (complexing agent) and 20 μL of the indicating nanospheres (indicator) were mixed in a cuvette. The optical reverse titrations were performed by step-wise aliquoting 10^{-3} M $CaCl_2$ or the standardized sample into the titration cuvette, each followed with recording of absorption spectrum.

Results and Discussion

Scheme 1 shows the principle of the reverse titration of calcium. A small amount of indicating nanospheres was mixed with excess amount of chelating nanospheres. The titrant (Ca^{2+} containing aqueous samples) was then dosed to the nanosphere emulsion. The indicating nanospheres contained calcium ionophore IV, CH1, NaTFPB, embedded in the hydrophobic nanosphere core made of o-NPOE and F127. The chelating nanospheres had similar sensing components (KTFPB, ETH 129 and o-NPDDE),[9] but lacked the chromoionophore. Different ionophores and matrices were used here to help ensure that the chelating particles exhibit a higher calcium affinity than the indicating particles. The different matrices may also reduce the exchange of components between the two types of particles.

Compared with conventional titrations, both the complexation reaction and the endpoint indication have been moved from the aqueous phase to an organic phase. With more titrant (Ca^{2+}) added, the chelating particles will eventually become saturated, resulting in

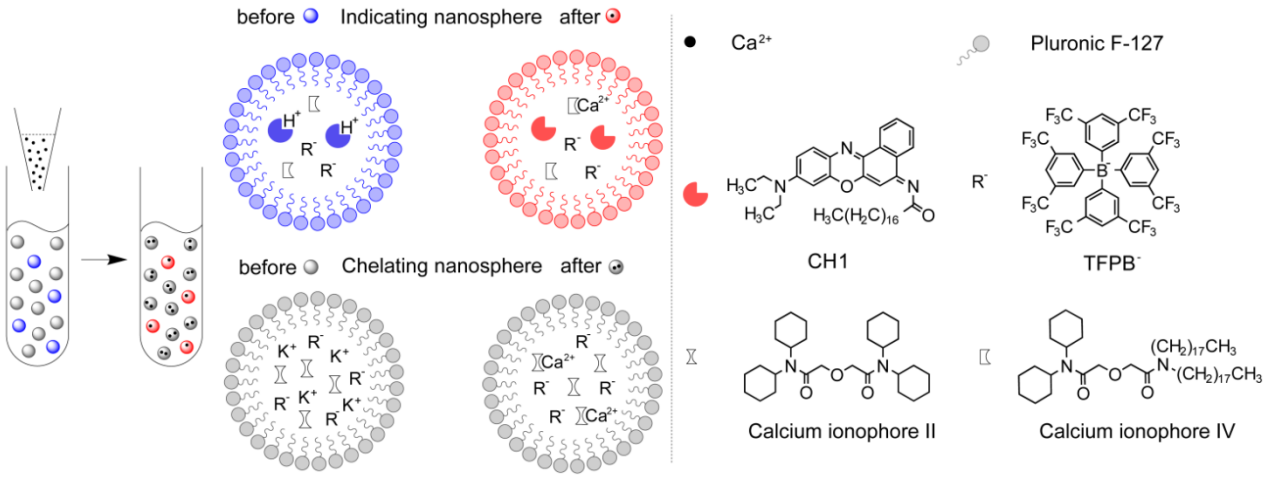

Scheme 1. Schematic illustration of ion-selective nanospheres as optical indicator and chelator for complexometric titration.

an increase of the free calcium concentration in solution. At that point, calcium will be extracted into the indicating particles and causes the deprotonation of CH1, which then results in a change in absorbance and colour. The amount of Ca^{2+} added can be quantified by the total amount of ion-exchanger (TFPB) if ionophore is in sufficient excess.

The nanospheres are fabricated by a precipitation method,[21] where the hydrophobic sensing components self-assemble into the nanosphere core. The typical average diameter of the nanospheres is less than 100 nm, but may grow with increasing particle concentration.[9,21] The indicating nanospheres have been reported as exhaustive nanosensors that are extremely sensitive to the analyte.[19,20] For instance, with small nanosphere quantities, 10^{-7} M of Ca^{2+} is able to cause complete deprotonation of CH1, thereby changing the colour of the nanosphere emulsion from blue to red.

For the calcium-selective chelating nanospheres, the working mechanism can be understood with the extraction process between the aqueous (aq) and organic nanospheric (ns) phase as shown in eq 1.

$$Ca^{2+}(aq) + 2M^{+}(ns) + 3L(ns) \rightleftharpoons CaL_3^{2+}(ns) + 2M^{+}(aq) \qquad (1)$$

Where M^+ is the initial counter ion of the ion exchanger in the nanosphere, L is the calcium ionophore that forms complexes of the type CaL_3^{2+}.

For the indicating nanospheres that contain an additional chromoionophore (*Ind*), a similar extraction process is shown in eq 2, where $HInd^+$ is the protonated chromoionophore.

$$Ca^{2+}(aq) + 2HInd^{+}(ns) + 3L(ns) \rightleftharpoons CaL_3^{2+}(ns) + 2H^{+}(aq) + Ind(ns) \quad (2)$$

The indicating nanospheres are subjected to an additional competition between hydrogen ions and calcium. By lowering the sample pH and/or the acidity of the chromoionophore, the calcium uptake capability should be weakened to a significant extent. Therefore, the difference in calcium affinity between the two varieties of nanospheres makes them promising candidates as indicators and complexants in complexometric titrations.

The relationship between primary ion (Ca^{2+}) concentration in the sensing phase and the sample solution can be quantified on the basis of ion-exchange theory. Both the indicating and the chelating nanospheres contain an excess of ionophore relative to ion exchanger. The mole fraction of Ca^{2+} (in the complex form) in the chelating nanospheres and the indicating nanospheres can be described by eq 3 and eq 4, respectively, where $[CaL_3^{2+}]^{cs}$ and $[R^-]^{cs}$ are the concentrations of Ca^{2+} and TFPB in the chelating nanospheres, respectively. $[Ca^{2+}]^{aq}$, $[J^+]^{aq}$ and $[J^{+'}]^{aq}$ are the concentration of Ca^{2+} and interfering ions in the sample solution, respectively. $K^{cs}_{Ca^{2+},J^+}$ is the selectivity coefficient for the chelating nanosphere while $[CaL_3^{2+}]^{is}$, $[R^-]^{is}$ and $K^{is}_{Ca^{2+'},J^{+'}}$ are the corresponding values for the indicating nanospheres.

$$\frac{2[CaL_3^{2+}]^{cs}}{[R^-]^{cs}} = \frac{2[Ca^{2+}]^{aq} + (K^{cs}_{Ca^{2+},J^+}[J^+]^{aq})^2}{2[Ca^{2+}]^{aq}} - \frac{\sqrt{4[Ca^{2+}]^{aq}(K^{cs}_{Ca^{2+},J^+}[J^+]^{aq})^2 + (K^{cs}_{Ca^{2+},J^+}[J^+]^{aq})^4}}{2[Ca^{2+}]^{aq}} \quad (3)$$

$$\frac{2[CaL_3^{2+}]^{is}}{[R^-]^{is}} = \frac{2[Ca^{2+}]^{aq} + (K^{is}_{Ca^{2+'},J^{+'}}[J^{+'}]^{aq})^2}{2[Ca^{2+}]^{aq}} - \frac{\sqrt{4[Ca^{2+}]^{aq}(K^{is}_{Ca^{2+'},J^{+'}}[J^{+'}]^{aq})^2 + (K^{is}_{Ca^{2+'},J^{+'}}[J^{+'}]^{aq})^4}}{2[Ca^{2+}]^{aq}} \quad (4)$$

The total amount of Ca^{2+} can be divided into three fractions, those in the chelating nanospheres, in the indicating nanospheres and in the sample solution, as shown in eq 5.

$$[Ca^{2+}]^{titrant}V^{titrant}_{Ca^{2+}} = [CaL_3^{2+}]^{cs}V^{cs} + [CaL_3^{2+}]^{is}V^{is} + [Ca^{2+}]^{aq}V_T \quad (5)$$

where $[Ca^{2+}]^{titrant}$ is the concentration of Ca^{2+} in the titrant, $V^{titrant}_{Ca^{2+}}$ is the volume of the titrant, V_{cs} and V_{is} are the volumes of the chelating nanospheres and the indicating nanospheres, respectively, V_T is the total volume.

Base on charge balance, the relationship between the protonated CH1 ($HInd^+$) in the indicating nanospheres and ion exchanger TFPB is shown in eq 6.

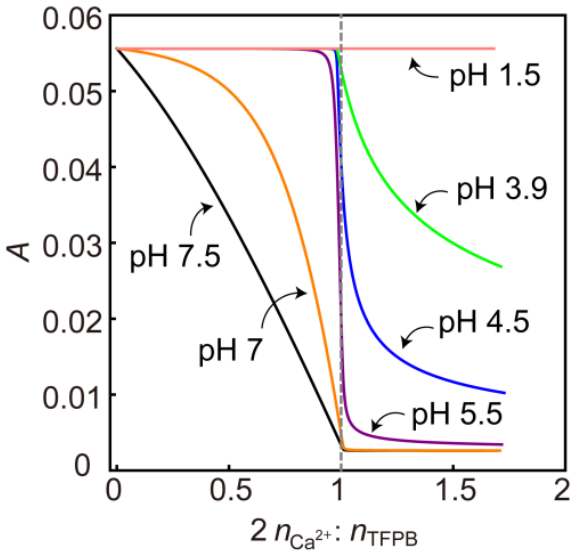

Figure 1. Theoretical optical reverse titration curves for calcium in different pH conditions. A is the absorbance at protonated wavelength. The dashed vertical line indicates the expected endpoint.

$$[HInd^+]^{is} = [R^-]^{is} - 2[CaL_3^{2+}]^{is} \quad (6)$$

where [HInd$^+$]is is the concentration of the protonated CH1 in the indicating nanospheres. The optical signal, absorbance (A), in this case, is expressed in eq 7.

$$A = \varepsilon_{HInd^+} b[HInd^+]^{is} + \varepsilon_{Ind} b([Ind_T]^{is} - [HInd^+]^{is}) \quad (7)$$

where [Ind$_T$]is is the total concentration of CH1, ε_{HInd^+} and ε_{Ind} are the molar extinction coefficients, and b is the optical path length.

Eq 8 is obtained after inserting eq 6 to eq 7:

$$A = \varepsilon_{Ind} b([Ind_T]^{is} - [R^-]^{is} + 2[CaL_3^{2+}]^{is}) + \varepsilon_{HInd^+} b([R^-]^{is} - 2[CaL_3^{2+}]^{is}) \quad (8)$$

Finally, $V_{Ca^{2+}}^{titrant}$ as a function of A can be obtained by solving equations (3), (4), (5) and (8). (see eq S1 in supporting information)

The optical reverse titration for Ca^{2+} at different pH can now be predicted, as shown in Figure 1. The vertical dashed line indicates the expected endpoint. At acidic pHs, sigmoidal titration curves are expected. With increasing pH, the s-shape curves change to two linear lines. Note that at very low pH (pH 1.5), the titration curve is flat because CH1 cannot be deprotonated even in the presence of excess amount of Ca^{2+}. At pH 7.5, the endpoint can be determined at the intersection of two lines. Figure S1 and S2 show the simulation of the concentration of Ca^{2+} in the chelating nanospheres, the indicating nanospheres and aqueous phase during the addition of titrant at pH 7.5 and pH 5.5,

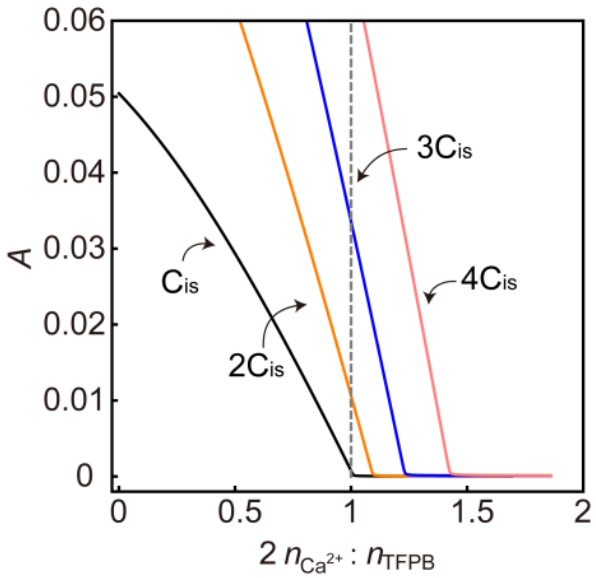

Figure 2. Theoretical reverse titration curves for calcium at pH 7.5 by using different amount of indicating nanospheres. C_{is} represents a fixed concentration of indicating nanospheres. A is the absorbance at protonated wavelength. The dashed vertical line indicates the expected endpoint.

respectively. A linear relationship between Ca^{2+} exchanged into the indicating nanospheres and the volume of titrant was obtained, meaning that the indicating nanospheres are working in the exhaustive mode at pH 7.5 (Figure S1b), Therefore, a linear relationship between the absorbance A and $2n_{Ca^{2+}} : n_{TFPB}$ (Figure 1) was obtained. This lack of s-shaped curve is understood by a proportionality between calcium content in the two types of particles, while the calcium level in the aqueous solution remains insignificant before the endpoint. At pH 5.5, the Ca^{2+} exchanged into the indicating nanospheres as function of volume of titrant assumes an s-shaped curve (Figure S2b) which signifies a sigmoidal relationship between A and $2n_{Ca^{2+}} : n_{TFPB}$ (Figure 1).

Figure 2 shows the theoretical titration curves simulated with different amounts of indicating nanospheres (different C_{is}) at pH 7.5. The titration endpoint gradually moves further away from the expected endpoint with increasing amount of indicating nanospheres. This is because the indicating nanospheres will consume analytes themselves. In this situation, not only the concentration of ion exchanger in the chelating nanospheres but also that in the indicating nanospheres should be accounted for. Figure 3 shows the experimental optical reverse titration curve (a) and absorption spectra (b) for Ca^{2+}. The titration was performed in non-buffered water. 10^{-3} M $CaCl_2$ solution (titrant)

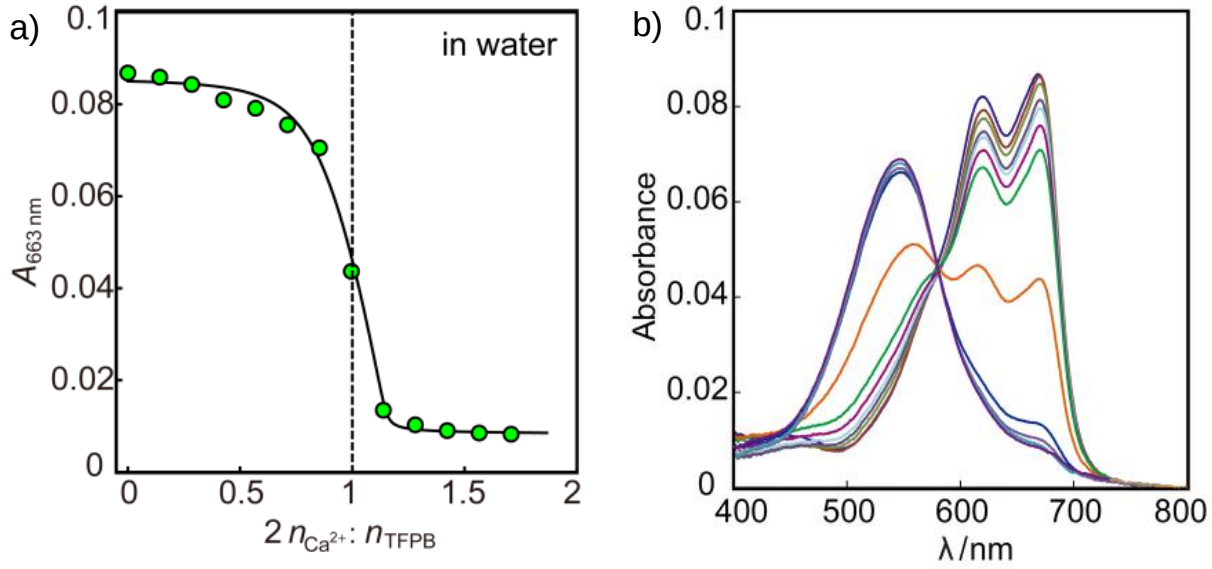

Figure 3. (a) Reverse titration curve for calcium titration using 10^{-3} M $CaCl_2$. Endpoint indicator: exhaustive Ca^{2+}-selective nanospheres. Chelator: nanospheres containing ETH 129 and TFPB. (b) Absorption spectra recorded at each titration point.

was gradually added to the mixed nanosphere emulsion. Before addition of any Ca^{2+}, the emulsion exhibited a blue colour owing to the complete protonation of CH1. As more Ca^{2+} being added, the protonation peak gradually decreased because of a small increase in the free Ca^{2+} level. At first, the decrease was quite small and gradual because most of the titrant was consumed by the chelating nanospheres. After saturation of the indicating nanospheres, the free Ca^{2+} concentration increase could be detected by the indicating nanospheres, giving a sharp transition with a very small error (ca. 1%). Indeed, the endpoint was obtained at 70 µL ± 0.5 µL (standard deviation) while the expected value was at 70.3 µL. The result corresponds satisfactorily to the expected theoretical s-shaped curve. Note that the sharpness of the transition highly depends on the interaction between the indicator and the analyte, which is defined by the optode response function as explained below.

Conventional titration using organic chelators and indicators usually requires pH control because any pH change could influence the effective binding strength of the chelator or the indicator molecule. The chelating nanospheres do not suffer from this disadvantage because the calcium ionophores are not pH sensitive in a wide pH range. In addition, the exhaustive indicating nanospheres have been known to be pH independent within a defined window of pH.[19] Figure 4 shows that the Ca^{2+} titration in different pH conditions.

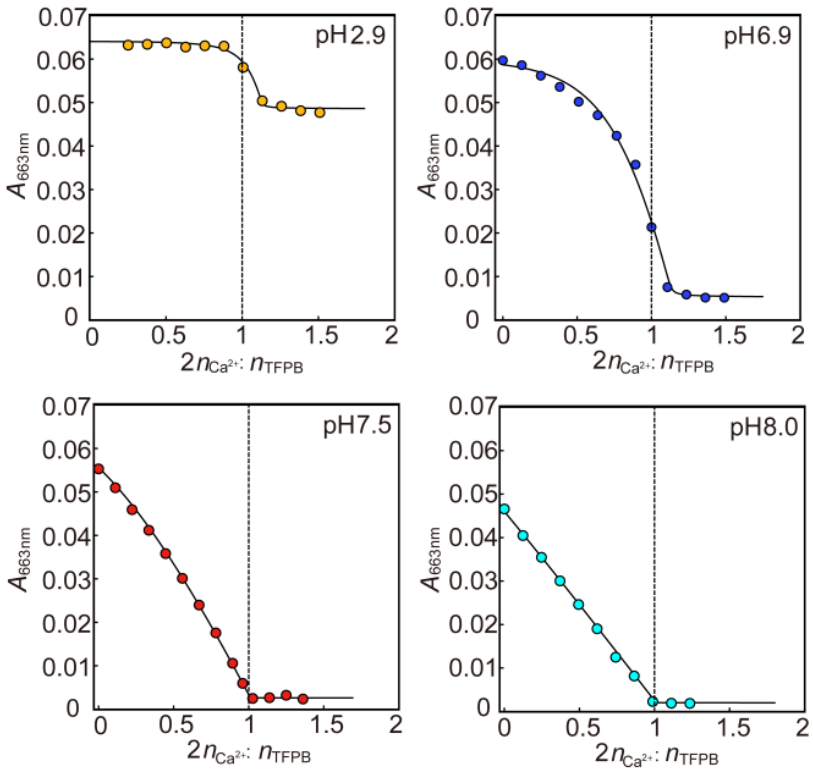

Figure 4. Experimental optical reverse titration curves for calcium in different pH solution. The dashed vertical lines indicate the expected endpoint. The pH 2.9 solution was prepared diluting HNO_3. The pH 6.9, pH 7.5 and pH 8.0 buffer solutions were prepared adjusting 10^{-3} M $NaHCO_3$ with HCl solution.

Even at very low pH value (pH 2.9, HNO_3), an accurate endpoint can still be obtained. Admittedly, under these acidic conditions, the absorbance change is much smaller than at more elevated pH because CH1 cannot undergo complete deprotonation. Indeed, chromoionophores with different basicities are available, providing the opportunity for a tunability of the working pH window and sensitivity of the indicating particles. Note that there exist no traditional calcium chelators and optical indicators that allow one to titrate calcium at this pH.

CH1 deprotonates more readily if the optical titration is performed at higher pH (Figure 4). The endpoint was at the transition point of the s-shaped titration curve, which gradually became more linear with increasing pH (as discussed above). At pH 7.5 and pH 8.0, the endpoint is found at the intersection of two linear curves (compare to Figure 1). The titration curves correspond indeed well to theoretical expectations and the errors are very small (ca. 1%). Further work will aim to improve the sharpness of the observed endpoint further to match those with potentiometric detection.[9]

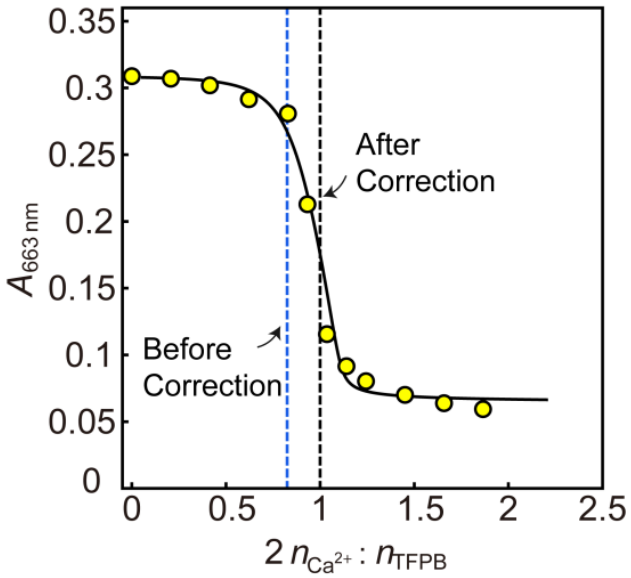

Figure 5. Optical reverse titration curve for calcium in non-buffered sample solution containing larger amount of indicating nanospheres. C_{TFPB} (chelating nanospheres) = 5.2×10^{-5} M, C_{TFPB} (indicating nanospheres) = 1.2×10^{-5} M, V_{total} = 3 ml. 10^{-3} M $CaCl_2$ stocking solution was used as titrant. Black and blue dashed vertical lines indicate the expected endpoint with and without considering the TFPB in the indicating nanospheres.

The consumption of analyte by the indicating nanospheres can be neglected if the amount of the indicating nanospheres is sufficiently small. However, if a high amount of indicating nanospheres was used, the ion exchanger in the indicating nanospheres cannot be ignored. Figure 5 shows the optical reverse titration for calcium with a large amount of indicating nanospheres. When the total amount of ion exchanger in both the chelating and the indicating nanospheres is accounted for, the error was very small (ca. 1.1%). If only those in the chelating particles were taken into account, the error was to be 17.9%.

In order to know if the sensing components in chelating and indicating nanospheres will exchange with each other, the change of absorbance of a mixture of two types of nanospheres was observed over time in 10 mM tris-HCl buffer at pH 7. One type of nanospheres contained only CH1 and the other just NaTFPB, while the matrix of the nanospheres were the same. If the components exchange, some nanospheres containing both CH1 and NaTFPB will appear. At such experimental conditions, CH1 will become fully protonated in the mixed nanospheres, while it remains fully deprotonated in the nanospheres containing CH1 only since no ion exchanger exists. As shown in Figure 6, the absorbance peak at 531 nm (deprotonation peak) and 663 nm (protonation peak) only showed a small change during 30 minutes. Note that one titration process takes less than

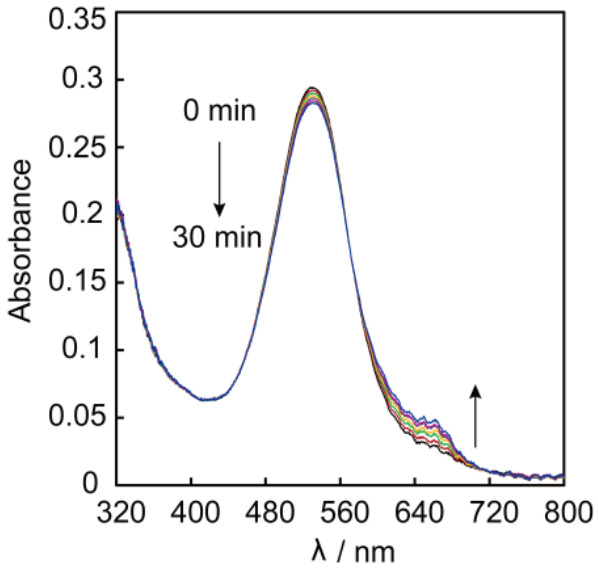

Figure 6. Time response of two types of nanospheres mixed in 10 mM tris-HCl buffer solution at pH 7. One contains only CH1 and the other only NaTFPB. The final concentration for CH1 and NaTFPB is 1.27×10^{-5} M and 1.58×10^{-5} M, respectively.

5 min. This confirms that the interchange of the components in the chelating and the indicating nanospheres is negligible.

The calcium level in a standardized reference sample (synthetic sample with standardized ion concentration) was determined. As shown in Figure 7, the result from the optical titration was found to be in agreement with the value of the standardized sample. This

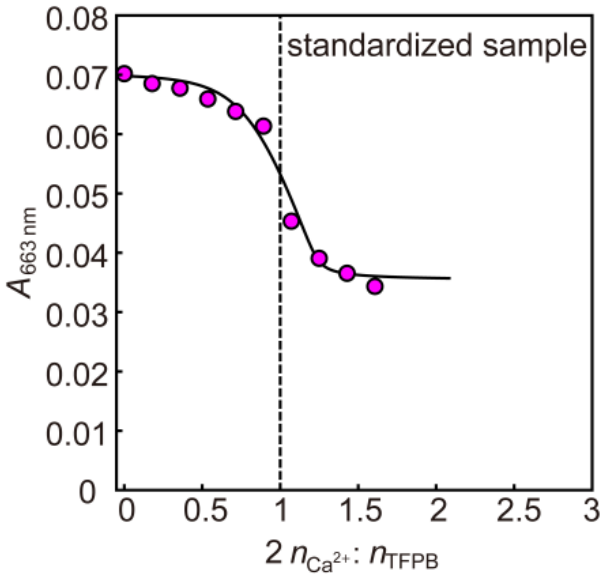

Figure 7. Reverse titration of Ca^{2+}-selective nanospheres using standard reference material 1643e as titrant. The dashed vertical line indicates the expected endpoint. C_{TFPB} (chelating nanospheres) = 3.61×10^{-5} M, V_{total} = 2.5 mL. The standardized concentration of calcium in reference material 1643e is 8.06×10^{-4} M.

also suggests that the selectivity of the calcium selective nanospheres is sufficient for routine analysis of fresh water.

In conclusion, we proposed here for the first time the use of ion-selective nanospheres as optical indicator as well as complexing agents for complexometric titrations. The titrations can be performed in a wide range of pH, which is impossible to achieve with existing calcium chelators. The nanospheres showed excellent selectivity and sensitivity for calcium. The calcium level in standardized sample was successfully assessed.

Supporting Information

Equation S1 shows the relationship between the volume of titrant $V_{Ca^{2+}}^{titrant}$ and absorbance A (see main text for derivation).

$$[Ca^{2+}]^{titrant}V_{Ca^{2+}}^{titrant} = [CaL_3^{2+}]^{is}V^{is} + \frac{2[CaL_3^{2+}]^{is}(K_{Ca^{2+},J^{+'}}^{is}[J^{+'}]^{aq})^2[R^-]^{is}V_T(\varepsilon_{HInd^+}b-\varepsilon_{Ind}b)^2}{(A-\varepsilon_{Ind}b[Ind_T]^{is})^2} +$$
$$\frac{(A-\varepsilon_{Ind}b[Ind_T]^{is})^2[R^-]^{cs}V^{cs}}{8[CaL_3^{2+}]^{is}(K_{Ca^{2+},J^{+'}}^{is}[J^{+'}]^{aq})^2[R^-]^{is}(\varepsilon_{HInd^+}b-\varepsilon_{Ind}b)^2}\{(K_{Ca^{2+},J^+}^{cs}[J^+]^{aq})^2 + \frac{4[CaL_3^{2+}]^{is}(K_{Ca^{2+},J^{+'}}^{is}[J^{+'}]^{aq})^2[R^-]^{is}(\varepsilon_{HInd^+}b-\varepsilon_{Ind}b)^2}{(A-\varepsilon_{Ind}b[Ind_T]^{is})^2} -$$
$$\sqrt{(K_{Ca^{2+},J^+}^{cs}[J^+]^{aq})^4 + \frac{8[CaL_3^{2+}]^{is}(K_{Ca^{2+},J^+}^{cs}[J^+]^{aq})^2(K_{Ca^{2+},J^{+'}}^{is}[J^{+'}]^{aq})^2[R^-]^{is}(\varepsilon_{HInd^+}b-\varepsilon_{Ind}b)^2}{(A-\varepsilon_{Ind}b[Ind_T]^{is})^2}}\}$$

eq S1

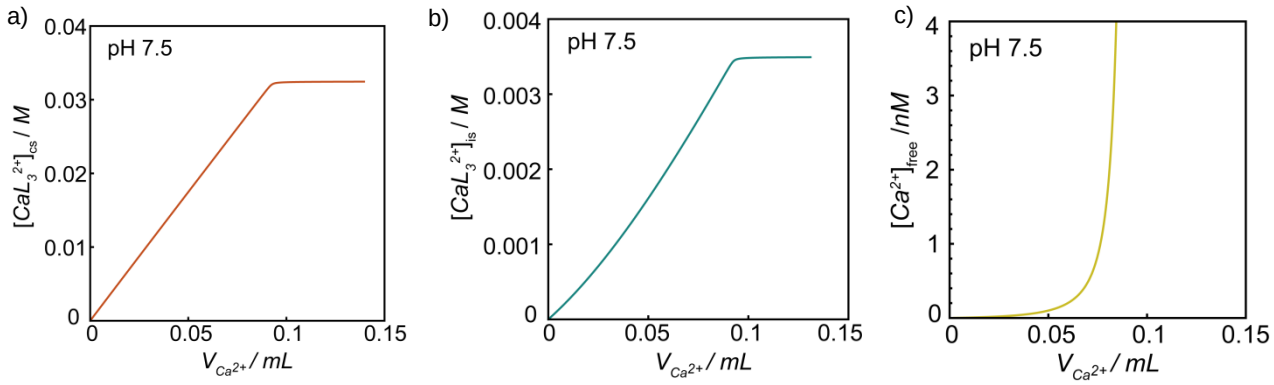

Figure S1. Theoretical concentration of calcium in (a) the chelating nanospheres, (b) the indicating nanospheres and (c) the aqueous phase as the volume of titrant increases at pH 7.5.

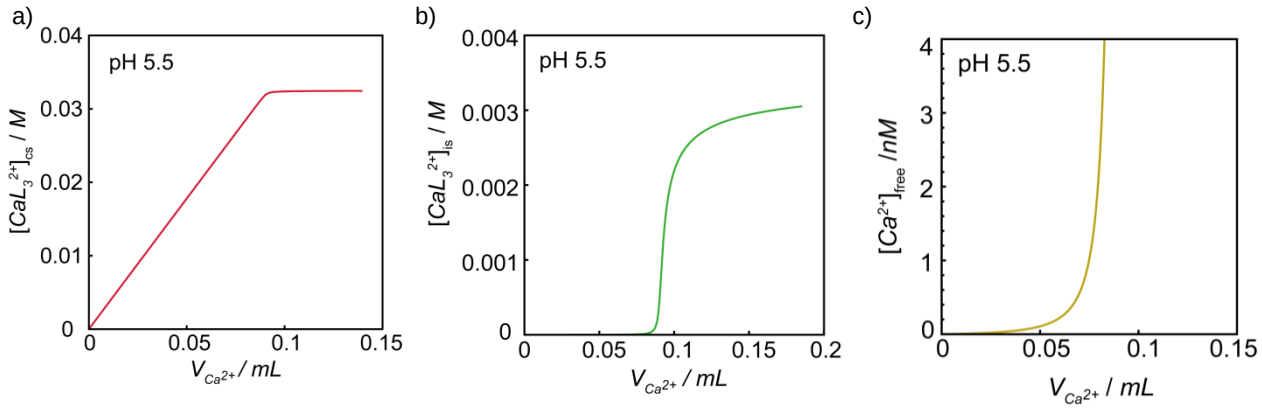

Figure S2. Theoretical concentration of calcium in (a) the chelating nanospheres, (b) the indicating nanospheres and (c) the aqueous phase as the volume of titrant increases at pH 5.5.

References

(1) Schwarzenbach, G.; Flaschka, H. Complexometric titrations; Methuen: London, 1969.

(2) Christian, G. D. Analytical Chemistry; 6 ed.; John Wiley & Sons, Inc., 2004.

(3) Scott, L. E.; Orvig, C. Chem. Rev. 2009, 109, 4885.

(4) Buccella, D.; Horowitz, J. A.; Lippard, S. J. J. Am. Chem. Soc. 2011, 133, 4101.

(5) Pandey, U.; Dhami, P. S.; Jagesia, P.; Venkatesh, M.; Pillai, M. R. A. Anal. Chem. 2008, 80, 801.

(6) Peper, S.; Ceresa, A.; Bakker, E.; Pretsch, E. Anal. Chem. 2001, 73, 3768.

(7) Yin, P.; Li, T.; Forgan, R. S.; Lydon, C.; Zuo, X.; Zheng, Z. N.; Lee, B.; Long, D.; Cronin, L.; Liu, T. J. Am. Chem. Soc. 2013, 135, 13425.

(8) Reilley, C. N.; Schmid, R. W.; Sadek, F. S. J. Chem. Educ. 1959, 36, 555.

(9) Zhai, J.; Xie, X.; Bakker, E. Chem. Commun. 2014, 50, 12659.

(10) Reilley, C. N.; Schmid, R. W. Anal. Chem. 1958, 30, 947.

(11) Duso, A. B.; Chen, D. D. Y. Anal. Chem. 2002, 74, 2938.

(12) Krüger, R.; Pfenninger, A.; Fournier, I.; Glückmann, M.; Karas, M. Anal. Chem. 2001, 73, 5812.

(13) Trimukhe, K. D.; Varma, A. J. Carbohydr. Polym. 2008, 71, 66.

(14) Harvey, A. E.; Komarmy, J. M.; Wyatt, G. M. Anal. Chem. 1953, 25, 498.

(15) Männel-Croisé, C.; Meister, C.; Zelder, F. Inorg. Chem. 2010, 49, 10220.

(16) Afshar, M. G.; Crespo, G. A. Anal. Chem. 2012, 84, 8813.

(17) Bakker, E.; Bühlmann, P.; Pretsch, E. Chem. Rev. 1997, 97, 3083.

(18) Xie, X.; Mistlberger, G.; Bakker, E. J. Am. Chem. Soc. 2012, 134, 16929.

(19) Xie, X.; Bakker, E. ACS Appl. Mater. Interfaces 2014, 6, 2666.

(20) Xie, X.; Zhai, J.; Bakker, E. Anal. Chem. 2014, 86, 2853.

(21) Xie, X.; Mistlberger, G.; Bakker, E. Anal. Chem. 2013, 85, 9932.

Chapter 4. Anion-Exchange Nanospheres as Titration Reagents for Anionic Analytes

This work has been published in *Anal. Chem.*, **2015**, *87* (16), 8347-8352

Abstract

We present here anion-exchange nanospheres as novel titration reagents for anions. The nanospheres contain a lipophilic cation for which the counter ion is initially Cl^-. Ion exchange takes place between Cl^- in the nanospheres and a more lipophilic anion in the sample, such as ClO_4^- and NO_3^-. Consecutive titration in the same sample solution for ClO_4^- and NO_3^- were demonstrated. As an application, the concentration of NO_3^- in spinach was successfully determined using this method.

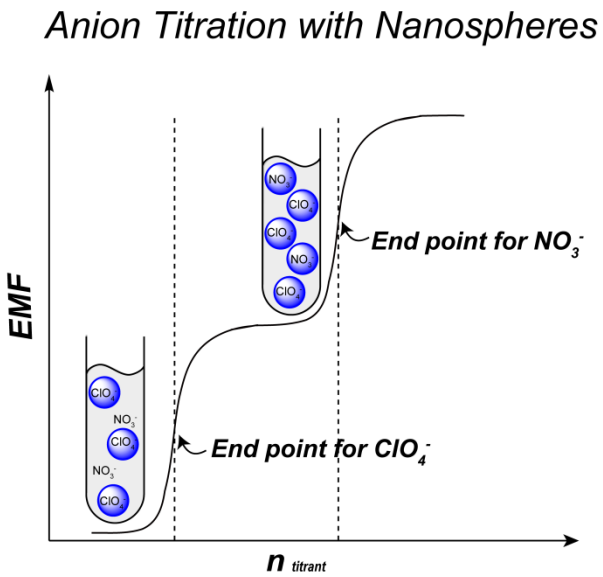

Introduction

Complexometric titration is a method for quantitative chemical analysis that has been extensively used in analytical chemistry, environmental chemistry and biotechnology for many decades.[1-4] Typically, water soluble organic compounds are used as chelators while electrodes and organic dyes serve as indicators.[5-8]

The complexometric titration for cations has been well established using organic chelators such as ethylenediaminetetraacetic acid (EDTA).[4] While the chemical analysis of anions is equally important, good chelators for anionic species are virtually non-existent. For instance, nitrate and phosphate are key nutrients for living plants and animals.[9] An oversupply of nutrients may have a negative impact on plants and fish as well as the environment. One example is eutrophication, which may cause a variety of problems such as algal blooms, aquatic animal death and water pollution.[10,11]

Recently, ionophore based ion selective nanosphere emulsions were introduced as chelators and indicators in the complexometric titration for cations.[12,13] The nanospheres contained an ionophore and a cation exchanger while the matrix was made of plasticizer and a surfactant Pluronic F-127 (F127). As the nanospheres are added to the sample solution the ionophore promotes the extraction of the target ion by replacing the original counter ion of the cation exchanger.

We report here for the first time that emulsions of nanospheres exhibiting a lipohilic core containing an anion exchanger may serve as titration reagents for anionic species. As these nanospheres are free of ionophore, the resulting selectivity must obey the so-called Hofmeister selectivity sequence, with more lipophilic ions preferred over hydrophilic ones typically in the order

$R^- > ClO_4^-, SCN^- > I^- > NO_3^- > Br^- > Cl^- > F^-$

where R^- denotes an organic anion.

A chloride counter ion confined to the nanosphere core is expected to spontaneously exchange with sample anions placed on its left in the sequence shown above. This principle is used here to demonstrate consecutive and separate titrations of perchlorate and nitrate as proof-of-concept examples. As an early application, the nitrate

concentration in spinach extract was successfully determined and confirmed by ion chromatography.

Experimental Section

Reagents

Pluronic F-127 (F127), dodecyl 2-nitrophenyl ether (o-NPDDE), tetrahydrofuran (THF), poly (vinyl chloride) (PVC), tetradodecylammonium chloride ($TDDA^+Cl^-$), chromoionophore VI (CHVI), Dowex® Marathon™ MSA chloride form (anion exchange resin), sodium perchlorate (NaClO4), sodium nitrate (NaNO3), sodium thiocyanate (NaSCN), saccharin, aspirin and sodium chloride (NaCl) were obtained from Sigma-Aldrich. Spinach was purchased from a local supermarket in Switzerland.

Preparation of anion exchange nanospheres

Typically, 3.05 mg of $TDDA^+Cl^-$, 5 mg of F127 and 8.0 mg of o-NPDDE were dissolved in 2.0 mL of THF to form a homogeneous solution. 0.6 mL of this THF solution was pipetted and injected into 2 mL of deionized water vortexing at 1000 rpm. Compressed air was blown on the surface for at least 30 min to remove THF.

Membranes and Electrodes

The ion selective membrane was prepared by dissolving the mixture composed of 3.75 mg of $TDDA^+Cl^-$, 50 mg of PVC and 100 mg of o-NPDDE in 1.5 mL of THF. The cocktail solution was then poured into a glass ring (22 mm in diameter) placed on a glass slide and dried overnight at room temperature under a dust-free environment. Small disks were punched off from the cast film and conditioned for 1 day in 10^{-3} M $NaClO_4$. The conditioned membranes were mounted separately in Ostec electrode bodies (Ostec, Sargans, Switzerland). The inner filling solution was composed of 10^{-3} M NaCl and 1g/ml anion exchange resin.

Instrumentation

Potentiometric titration signals were recorded on an EMF-16 precision electrochemistry EMF interface from Lawson Laboratories, Inc. A double-junction Ag/AgCl was used as reference electrode (Metrohm AG, Switzerland).

For potentiometric titration for ClO_4^-, the samples were prepared by diluting 15 μL, 32.5 μL 10^{-2} M $NaClO_4$ and 5 μL 10^{-1} M $NaClO_4$ in 5 mL water to obtain 3×10^{-5} M, 6.5×10^{-5} M and 10^{-4} M ClO_4^-, respectively. For NO_3^- titration, the sample was prepared by diluting 5 μL 10^{-1} M $NaNO_3$ in 5 mL water to get 10^{-4} M NO_3^-. For consecutive titration for 5×10^{-5} M ClO_4^- and 10^{-4} M NO_3^-, the sample was prepared by diluting 2.5 μL 10^{-1} M $NaClO_4$ and 5 μL 10^{-1} M $NaNO_3$ in 5 ml water.

Spinach extract was prepared by boiling 100 g of spinach leaf for 5 h followed by filtration to obtain the stock solution. Subsequently, 30 μL of spinach extract was added to 5 mL water to obtain the final titration sample. An anion-exchanger based ion selective electrode (see above) was used as indicator.

Results and Discussion

The principle of anion titration using ion exchange nanospheres is put forward in Scheme 1. The nanosphere cores are prepared by self-assembly of $TDDA^+Cl^-$, o-NPDDE and F127 in water using a previously developed method.[14] The counter ion of $TDDA^+$ is initially Cl^-, which is expected to be readily displaced by a more lipophilic anion A^- such as perchlorate and nitrate.

For an anionic titrant, the working principle is understood by the following ion exchange process (eq 1) between the aqueous phase (aq) and the organic nanospheric phase (ns),

$$Cl^-(ns) + A^-(aq) \rightleftharpoons Cl^-(aq) + A^-(ns) \quad (1)$$

Where Cl^- is the initial counter ion of ion exchanger in nanosphere and A^- is the more lipophilic target anion.

The relationship between the target anion concentrations in the nanospheres and the aqueous part of the sample solution is described by eq 2,

$$\frac{[A^-]^{ns}}{[TDDA^+]^{ns}_{titrant} V^{ns}_{titrant} / (V^{ns}_{titrant} + V_0)} = \frac{[A^-]^{aq}}{[A^-]^{aq} + K^{ns}_{A^-,J^-}[J^-]^{aq}} \quad (2)$$

where $[A^-]^{ns}$ is the concentration of anion A^- in the nanospheres, $[TDDA^+]^{ns}_{titrant}$ is the concentration of ion exchanger in the nanosphere stock solution, $V^{ns}_{titrant}$ is the volume of the nanosphere stock solution added into the sample, V_0 is the volume of water before addition of target ions and nanospheres, $[A^-]^{aq}$ and $[J^-]^{aq}$ are the concentration of A^- and interfering ion J^- in the solution, $K^{ns}_{A^-,J^-}$ is the selectivity coefficient of the nanospheres for A^- over J^-.

As shown in eq 3, the total number of moles of target anion A^- may either be localized in the nanospheres or in the aqueous sample solution:

$$[A^-]V_{A^-} = [A^-]^{ns}(V^{ns}_{titrant} + V_0) + [A^-]^{aq}(V_0 + V^{ns}_{titrant}) \quad (3)$$

Here, $[A^-]$ is the concentration of A^- in the stock solution and V_{A^-} is the volume of stock solution added to V_0.

Ion selective electrodes with response to the target anion were used as endpoint detectors. The relationship between the electromotive force (EMF) and concentration (activity, more strictly) of the target ion in the sample solution is given by eq 4,

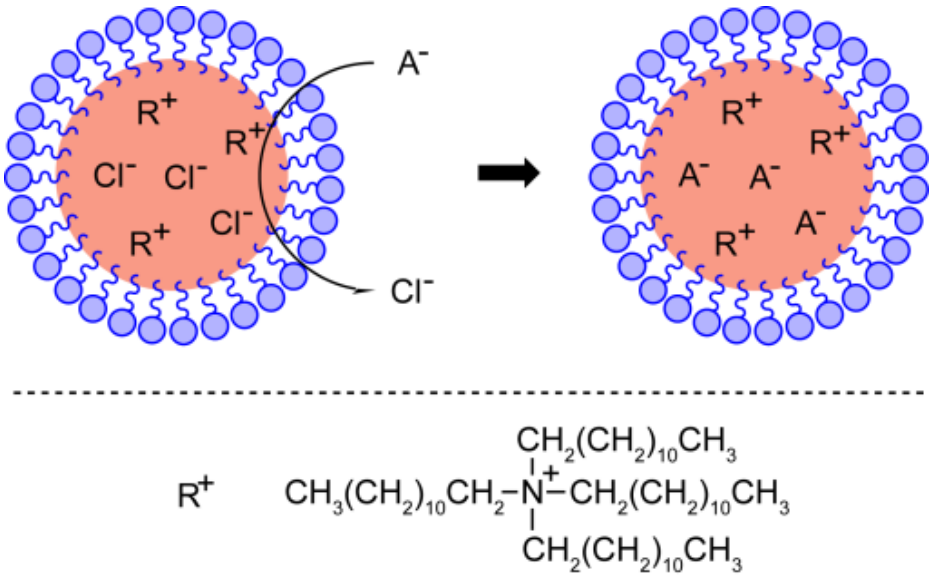

Scheme 1. Illustration of ion selective nanospheres as anionic titration reagents and the structure of the anion exchanger used in this work. The nanosphere core consists of the surfactant F127 and the plasticizer o-NPDDE. A^- is more lipophilic ion than Cl^-.

$$EMF = E_0 + s\lg[A^-]^{aq} \quad (4)$$

where E_0 is a constant potential and s the electrode slope, ideally –59.2 mV for a monovalent anion.

By combining eq 2, 3 and 4, the EMF can be obtained as a function of n_{TDDA^+} ($V^{ns}_{titrant}[TDDA^+]^{ns}_{titrant}$) (see eq S1 in supporting information) and used to predict the titration curve.

Figure 1 shows the potentiometric titration for ClO_4^- in non-buffered water with $TDDA^+Cl^-$ doped nanospheres as titrant. An anion selective membrane electrode containing the anion exchanger $TDDA^+Cl^-$ in o-NPDDE plasticized PVC was used as indicator. The inner solution of the electrode was 1 mM NaCl with additional anion exchange resin to maintain an inward perchlorate flux from the sample solution toward the inner solution.[15] For this reason, the electrodes exhibited a super Nernstian response slope to ClO_4^- in the range of 10^{-6} M to 10^{-4} M (Figure 2a), which further increased the

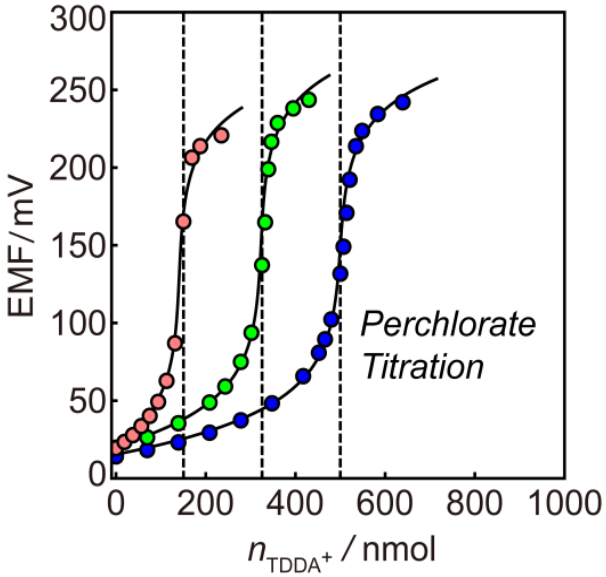

Figure 1. Potentiometric titration curves and theoretical fit for 3×10^{-5} M (pink), 6.5×10^{-5} M (green) and 10^{-4} M (blue) ClO_4^- in non-buffered solutions (amount of ClO_4^- in solution: 150 nmol, 325 nmol and 500 nmol). The dashed vertical lines show the expected endpoints.

Parameters: E_0 = -253 mV, V_0 = 5 mL, $K^{ns}_{A^-,J^-}[J^-]^{aq} = 7\times10^{-9}$ M, [A^-] = 0.01 M. For 3×10^{-5} M ClO_4^-: V_{A^-}= 15 uL, $[TDDA^+]^{ns}_{titration}=8\times10^{-4}$ M. For 6.5×10^{-5} M ClO_4^-: V_{A^-} = 32.5 uL, $[TDDA^+]^{ns}_{titration}=6.956\times10^{-4}$ M. For 10^{-4} M ClO_4^-: V_{A^-} = 50 uL, $[TDDA^+]^{ns}_{titration}=4.66\times10^{-4}$ M

sensitivity of the titration.[5] Three different concentrations of ClO_4^- were chosen for the titration experiment shown in Figure 1. Upon volumetric addition of the nanosphere emulsion to the sample solution, the extent of ClO_4^- extracting into the nanospheres and replacing the chloride ions is dictated by ion-exchange capacity of the nanosphere emulsion and the volume. The ion-exchange capacity means the amount of exchangeable ions per volume of particle stock suspension. For a titration experiment with a given concentration of analyte, changing the concentration of $TDDA^+$ in nanosphere stock solution will not affect the expected endpoint but only result in different final volume of the nanosphere stock solution required to reach the endpoint.

At the endpoint, the concentration of ClO_4^- in the sample solution is depleted, giving a sudden increase in the EMF signal. The sharp titration curves corresponded very well to the theoretical expectations from eq S1 with the endpoints calculated from the ion exchanger concentration in the nanospheres, giving errors of less than 1%. The level of the analyte could also be determined with ISEs directly, e.g., using external calibration as shown in Figure S1. Note that direct measurements with ISEs rely to a great extent on the sensor calibration. If the electrode exhibits a Nernstian response in the range of interest, the operation will be relatively straightforward, although uncertainties in activity

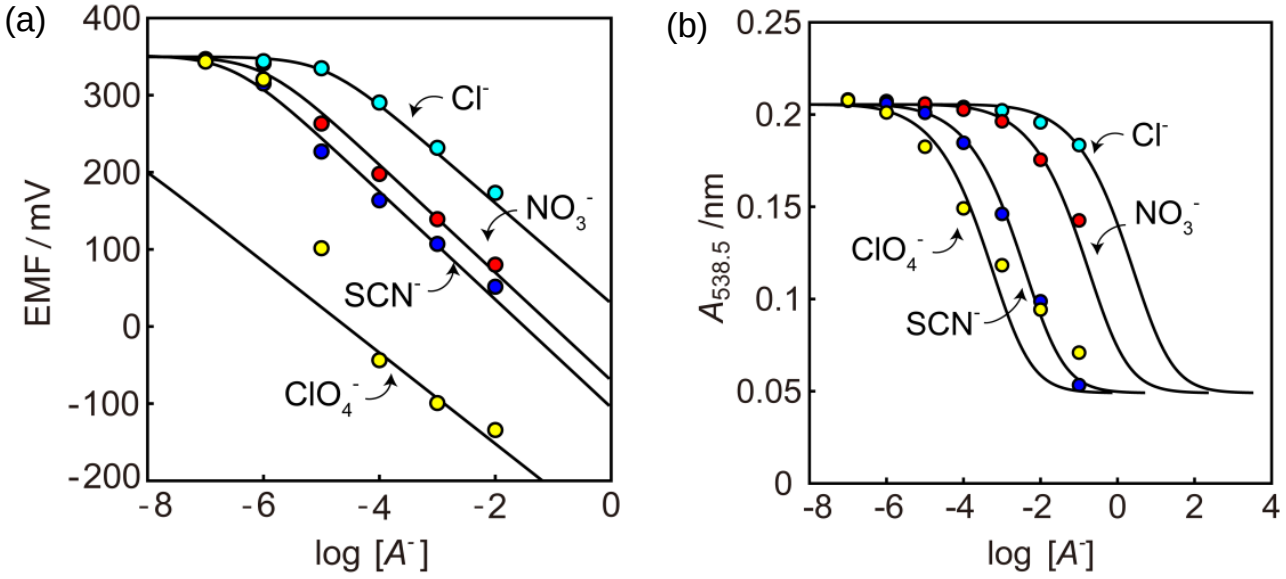

Figure 2. Selectivity of (a) $TDDA^+$ doped anionic selective electrode membrane in non-buffered water and (b) anion exchange nanospheres containing the optical reporter dye CHVI and $TDDA^+$ in pH 5.6 MES-NaOH buffer solution.

coefficients and liquid junction potentials may need to be accounted for. The calibration for an electrode exhibiting a super Nernstian electrode is more complicated and may result in unacceptably large errors. In contrast, the sensitivity can even be improved with a super Nernstian electrode when used as endpoint indicator in potentiometric titrations.

Both the nanospheres and the indicating electrode membrane contained $TDDA^+$. The selectivity pattern for the indicating electrodes was found to be similar to that of the ion selective nanospheres, with ClO_4^- ($\log K^{opt}_{ClO_4^-,Cl^-}$ = -5.1) > SCN^- ($\log K^{opt}_{SCN^-,Cl^-}$ = -2.3) > NO_3^- ($\log K^{opt}_{NO_3^-,Cl^-}$ = -1.7) > Cl^- in the concentration range from 10^{-6} M to 10^{-2} M (Figure 2a). To better visualize the selectivity pattern for the titrating reagents, the nanospheres were doped with additional H^+-selective chromoionophore (CHVI) in addition to $TDDA^+$. The use of CHVI gave rise to an optical signal that was quantified in absorbance mode. The principle is analogous to that of ion selective optodes: hydrogen ions and anions will be co-extracted into the nanospheres, resulting in an absorbance change of CHVI. The ability to extract anions is different between the optical nanospheres containing CHVI and the ones only doped with $TDDA^+Cl^-$. For the nanospheres with optical readout, the ability to extract anions is not only related to the lipophilicity of the anions but also to the

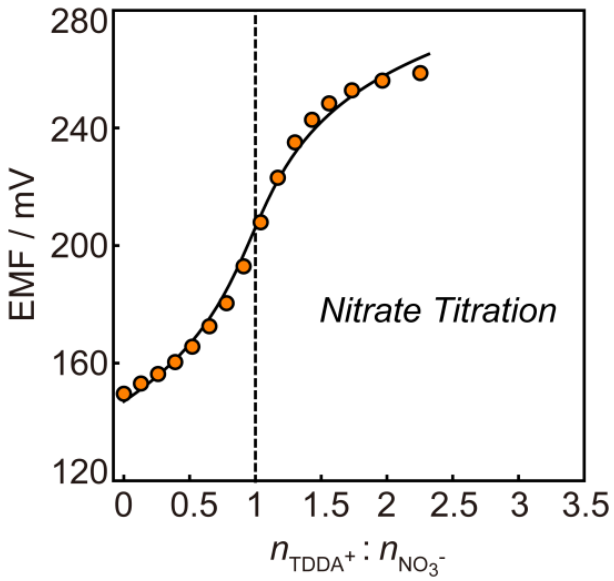

Figure 3. Potentiometric titration and theoretical fit for 10^{-4} M NO_3^- in non-buffered solution with ion selective nanospheres as titration reagents. The dashed vertical line indicates the expected endpoint. Parameters: E_0 = -89 mV, $[A^-]$ = 0.1 M, V_{A^-} = 5 uL, V_0 = 5 mL, $K^{ns}_{A^-,J^-}[J^-]^{aq}$ = 1.23×10^{-6} M, $[TDDA^+]^{ns}_{titration}$ = 1.445×10^{-3} M.

basicity of the H^+ indicator (CHVI). Nonetheless, assuming no interaction between the anions and the chromoionophore, the selectivities between the two cases are expected to be comparable. Figure 2b shows the following selectivity pattern with ClO_4^- ($\log K^{opt}_{ClO_4^-,Cl^-}$ =-3.7) > SCN^- ($\log K^{opt}_{SCN^-,Cl^-}$ = -2.8) > NO_3^- ($\log K^{opt}_{NO_3^-,Cl^-}$ = -1.2) > Cl^-. This resembles the one observed in Figure 2a for the anion-exchange electrode despite the different sensing matrices used and the possibility of additional ion pair formation with the protonated indicator in the optode nanospheres.

Figure 3 shows that in the absence of perchlorate, the nanospheres can be used to titrate nitrate as well. To our knowledge, there has been no titration reagents reported for perchlorate and nitrate so far. The titration curve corresponds satisfactorily to the theoretical expectation with a very small error of ca. 1%.

For environmental applications in sea water and fresh water, chloride is one of the most abundant interfering anions.[16] Figure 4 demonstrates a ClO_4^- titration in 10 mM NaCl background solution. With such a high concentration of Cl^- as background, the titrations were still able to give accurate results. The titration endpoint again corresponded to theoretical expectations with a small error of ca. 1%.

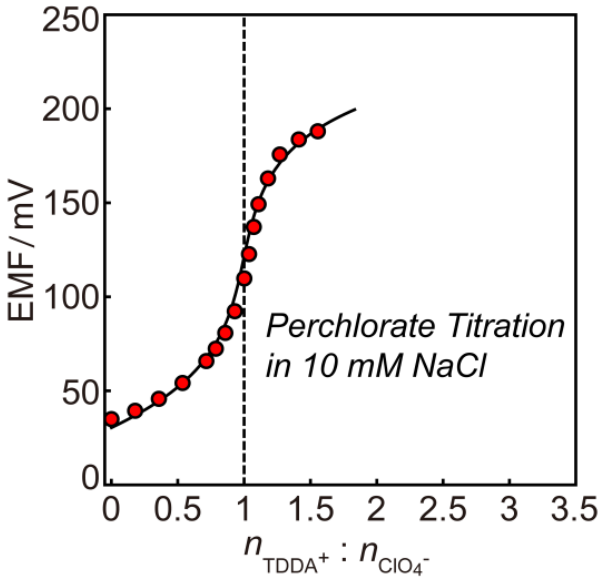

Figure 4. Potentiometric titration curve for 10^{-4} M ClO_4^- in 10 mM NaCl solution fit with theoretical curve. The dashed vertical line shows the expected endpoint. Parameters: E_0 = -204 mV, [A^-] = 0.1 M, V_{A^-} = 5 uL, V_0= 5 mL, $K^{ns}_{A^-,J^-}[J^-]^{aq}$ = 1.1×10^{-7} M, $[TDDA^+]^{ns}_{titration} = 8.94\times10^{-4}$ M.

Ionophore based ion selective nanospheres exhibited excellent selectivity toward one analyte,[17,18] but they have so far not been explored for the titration of several distinct ions that coexist in solution. We now demonstrate this for the first time for the anion-exchanger-doped nanospheres developed here. Figure 5 shows a consecutive titration of ClO_4^- and NO_3^-. The selectivity series of the detecting electrode is similar to that of the nanospheres (see Figure 2a and b). Both ion selective nanospheres (titrant) and electrodes (indicator) contribute to the visualization of the endpoint separation. The endpoints for ClO_4^- and NO_3^- shown in Figure 5 are clearly separated, giving an error of less than ca. 3%. The corresponding first derivative of the titration curve is shown in Figure S2 to better visualize the endpoints. The derivation of the theoretical equation for consecutive titration is similar to that for single ion titration (eq S7). The results were in satisfactory agreement with the theoretical s-shaped curve.

Figure 6 shows the calculated titration curves (a, c) and their second derivatives (b, d) for monovalent anions, using selectivity coefficients $\log K^{ns}_{NO_3^-,Cl^-}$ = -2.3 and $\log K^{ns}_{ClO_4^-,Cl^-}$ = -5.0 extracted from the nitrate titration (Figure 3) and perchlorate titration curves shown in Figure 4. A concentration increase of interfering ions results in a less pronounced

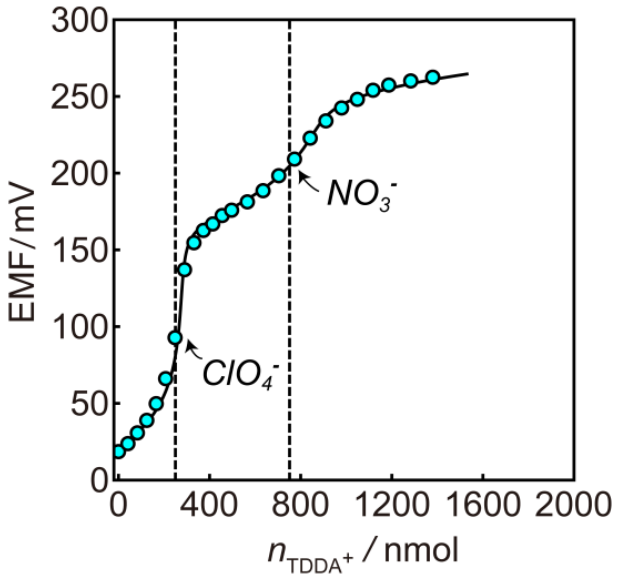

Figure 5. Potentiometric consecutive titration for 5×10^{-5} M ClO_4^- and 10^{-4} M NO_3^- in non-buffered water (amount of ClO_4^- in solution: 250 nmol, amount of NO_3^- in solution: 500 nmol). Titrant: $TDDA^+Cl^-$ doped nanospheres. Indicator: anion selective electrode. $[TDDA^+]^{ns}_{titration}$ =1.38×10^{-3} M.

endpoint. Compared with the selectivity of the optode nanospheres shown in Figure 2b, the titrating nanospheres appear to be better suited for the detection of lipophilic ions. This difference is perhaps likely due to the additional chromoionophore (CHVI) in the optode nanospheres that may contribute to an unwanted stabilization of the chloride ion.

A higher selectivity for A^- over J^- may tolerate a higher concentration of interfering ions, see Figure 6 (e). With the selectivity coefficients $\log K^{ns}_{A^-,J^-}$ = -2.3, a better than 90% accuracy is achieved with at most $10^{-2.83}$ M interfering ion concentration. Similarly, with a selectivity coefficient $\log K^{ns}_{A^-,J^-}$ = -5.0 (perchlorate), the titration may tolerate a $10^{-0.24}$ M back ground level of chloride. Note that any interfering anions with the same selectivity coefficient should have the same influence on the accuracy shown in Figure 6.

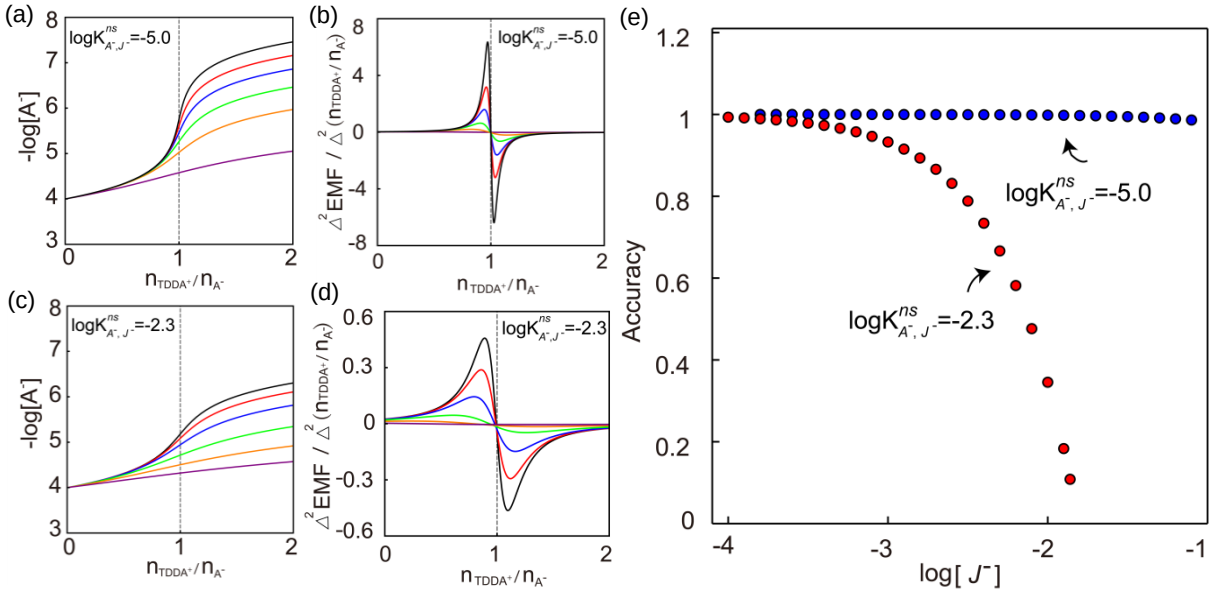

Figure 6. Theoretical titration curves (a, c) and secondary differentiation of the titration curves (b, d) for 10^{-4} M primary anions A^- with different concentrations of interference ion J^- with indicated selectivity coefficients for A^- over J^-. (e) Deviation from 100 % accuracy as a function of the interfering ion J^- concentration for ion exchange nanospheres with indicated selectivity coefficient.

For (a) and (b), parameters are as follows: E_0 = -204 mV, [A$^-$] = 0.1 M, V_{A^-}= 5 uL, V_0= 5 mL, $K^{ns}_{A^-,J^-}$ = 1.1×10^{-5}, $[TDDA^+]^{ns}_{titration}$ = 8.94×10^{-4} M. Concentration of interference ion $[J^-]^{aq}$: $10^{-2.5}$ M (black),$10^{-2.2}$ M (red),$10^{-1.9}$ M (blue), $10^{-1.5}$ M (green), 10^{-1} M (orange) and 1 M (purple). For (c) and (d), parameters are as follows: E_0 = -89 mV, [A$^-$] = 0.1 M, V_{A^-} = 5 uL, V_0 = 5 mL, $K^{ns}_{A^-,J^-}$ = $10^{-2.3}$ M, $[TDDA^+]^{ns}_{titration}$ = 1.445×10^{-3} M. Concentration of interference ion $[J^-]^{aq}$: 10^{-4} M (black),$10^{-3.8}$ M (red),$10^{-3.5}$ M (blue), 10^{-3} M (green), $10^{-2.5}$ M (orange) and 10^{-2} M (purple). The parameters for (e) are the same as above.

With a known selectivity coefficient and concentration of primary anion, the maximum tolerable interference concentration of can therefore be predicted. With a given ClO_4^- concentration, the maximum tolerable concentrations of different organic anions can vary according to the lipophilicity of the anions. For perchlorate titration, the maximum tolerable concentration for aspirin is higher than that with saccharin, as shown in Figure S3. Consecutive titration for ClO_4^- and saccharin was successful with anion selective nanospheres as titrant (Figure S4). Because the lipophilicity of ClO_4^- is higher than saccharin (Figure S5), the first and the second endpoints corresponded to ClO_4^- and saccharin, respectively. Most multivalent anions such as sulfate and phosphate are usually very hydrophilic and should not cause significant interference to the titration of lipophilic anions.

Figure 7 displays the calculated deviation of the endpoint from 100% accuracy as a

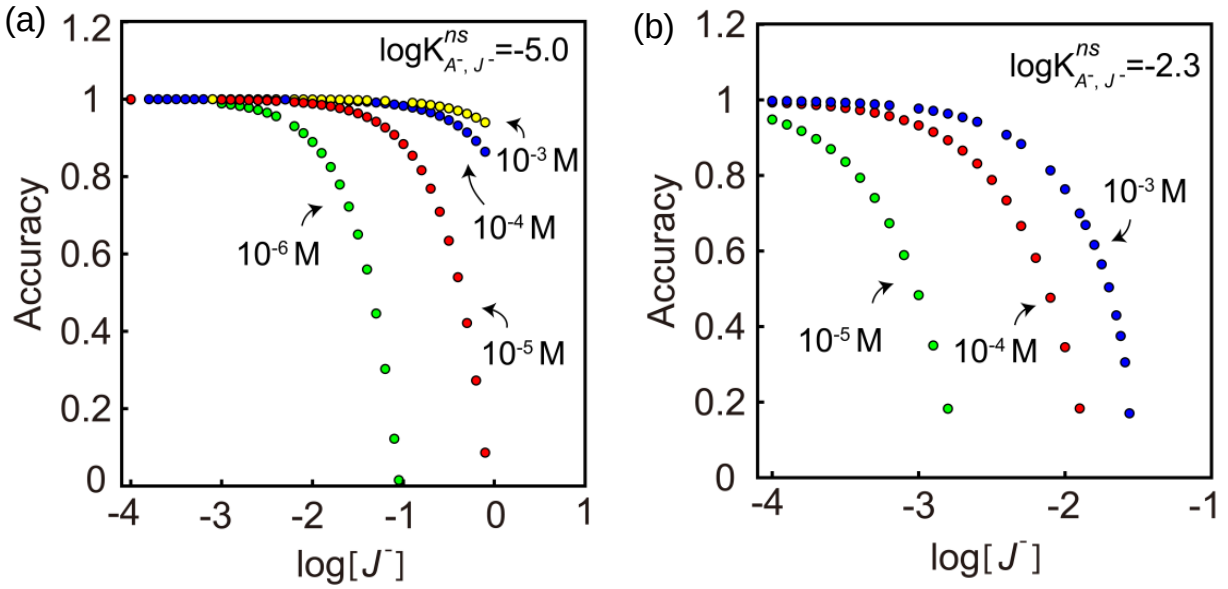

Figure 7. Deviation of the calculated endpoint from 100 % accuracy as a function of the interfering ion J^- concentration for ion exchange nanospheres with the indicated selectivity coefficients and analyte anion concentrations (A^-). Parameters for (a) : E_0 = -204 mV, [A^-] = 0.1 M, V_0 = 5 mL, $K^{ns}_{A^-,J^-}$ = 1.1×10^{-5} M, $[TDDA^+]^{ns}_{titration}$ = 8.94×10^{-4} M. V_{A^-} = 0.05 uL, V_{A^-} = 0.5 uL, V_{A^-} = 5 uL and V_{A^-} = 50 uL corresponding to the concentrations of primary ion [A^-]: 10^{-6} M (green), 10^{-5} M (red),10^{-4} M (blue), 10^{-3} M (yellow), respectively. Parameters for (b): E_0 = -89 mV, [A^-] = 0.1 M, V_0= 5 mL, $K^{ns}_{A^-,J^-}$ = 10$^{-2.3}$ M, $[TDDA^+]^{ns}_{titration}$ = 1.445×10^{-3} M. V_{A^-} = 0.5 uL, V_{A^-}= 5 uL and V_{A^-} = 50 uL corresponding to the concentrations of primary ion [A^-]: 10^{-5} M (green), 10^{-4} M (red), 10^{-3} M (blue), respectively.

function of the different interfering ion J^- concentration for the titration of analyte anions at the indicated concentrations. Both Figure 7a and b demonstrate that increasing the concentration of primary ions will tolerate higher levels of interference.

As an initial application, the ion exchange nanospheres were used to titrate the nitrate concentration in spinach extract, which was obtained by boiling and filtration and was diluted prior to titrimetric analysis. The concentration of NO_3^- in the extract was determined as 18.0 mM $\pm$ 0.1 mM (standard deviation) using the methodology developed

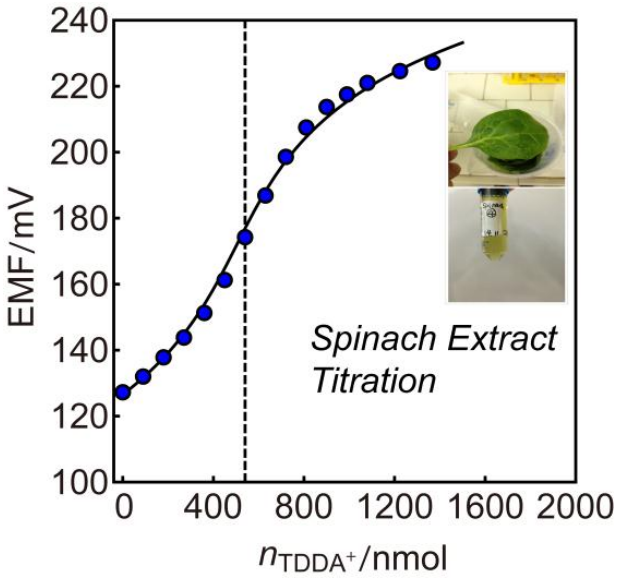

Figure 8. Potentiometric titration curve and theoretical fit for NO_3^- in spinach extract. n_{TDDA+} (end point) = 540 nmol, V_{total} = 5 mL. The dashed vertical line shows the expected endpoint. Parameters: E_0 = -108 mV, $[A^-]$ = 1.8×10^{-2} M, V_{A-} = 30 uL, V_0= 5 mL, $K^{ns}_{A^-,J^-}[J^-]^{aq}$ = 2.9×10^{-6} M, $[TDDA^+]^{ns}_{titration}$ = 1.8×10^{-3} M.

here (Figure 8), while ion chromatography using external calibration (Figure S6) gave 17.7 mM $\pm$ 0.1 mM (standard deviation). The data is fit with eq S1 using the parameters shown in the caption of Figure 8.

It is expected that the titration error will increase with increasing concentration of interfering ions in any real sample. Here, as shown by the ion chromatographic analysis of the spinach extract, the main interfering ion was Cl^- (see Figure S7). In the diluted spinach extract with concentration of 1.08×10^{-4} M NO_3^-, the chloride concentration was in the low milimolar range and did not interfere with the nitrate determination.

In conclusion, this work describes for the first time the titration of anions with anion-exchanger-doped nanosphere emulsions as titration reagents. The nanospheres exhibit a Hofmeister selectivity pattern and utilize readily sourced and inexpensive materials. Separate as well as consecutive titrations for perchlorate and nitrate were demonstrated. The concentration of NO_3^- in spinach extract was successfully determined using this method.

Supporting Information

Eq S1 shows the relationship between the volume of titrant $V_{titrant}^{ns}$ and EMF (see main text for derivation).

$$EMF = E_0 - sLog_{10}[\frac{x_0 + \sqrt{y_0 + x_0^{\,2}}}{2(V_0 + V_{titrant}^{ns})}] \qquad \text{eq S1}$$

Where $x_0 = [A^-]V_{A^-} - K_{A^-,J^-}^{ns}[J^-]^{aq}(V_0 + V_{titrant}^{ns}) - [TDDA^+]_{titrant}^{ns}V_{titrant}^{ns}$

and $y_0 = 4[A^-]V_{A^-}K_{A^-,J^-}^{ns}[J^-]^{aq}(V_0 + V_{titrant}^{ns})$

By inserting $n_{TDDA^+} = V_{titrant}^{ns}[TDDA^+]_{titrant}^{ns}$ into equation S1, the EMF as a function of n_{TDDA^+} is obtained.

Theoretical equation for the consecutive titration of two anions

$$\frac{[A^-]^{ns}}{[TDDA^+]_{titrant}^{ns}V_{titrant}^{ns}/(V_{titrant}^{ns} + V_0)} = \frac{[A^-]^{aq}}{[A^-]^{aq} + K_{A^-,J^-}^{ns}[J^-]^{aq}} \qquad \text{eq S2}$$

$$\frac{[J^-]^{ns}}{[TDDA^+]_{titrant}^{ns}V_{titrant}^{ns}/(V_{titrant}^{ns} + V_0)} = \frac{[J^-]^{aq}}{[J^-]^{aq} + K_{J^-,A^-}^{ns}[A^-]^{aq}} \qquad \text{eq S3}$$

$$[A^-]V_{A^-} = [A^-]^{ns}(V_{titrant}^{ns} + V_0) + [A^-]^{aq}(V_0 + V_{titrant}^{ns}) \qquad \text{eq S4}$$

$$[J^-]V_{J^-} = [J^-]^{ns}(V_{titrant}^{ns} + V_0) + [J^-]^{aq}(V_0 + V_{titrant}^{ns}) \qquad \text{eq S5}$$

$$EMF = E_0 - s_0 \log_{10}\left\{[A^-]^{aq} + K_{A^-,J^-}^{ns}[J^-]\right\} \qquad \text{eq S6}$$

By combining equations S2, S3, S4, S5 and S6, the EMF as a function of $V_{titrant}^{ns}$ is obtained.

$$\text{EMF} = \text{E}_0 - s_0 Log_{10}[\frac{x_1 + \sqrt{y_1 + x_1^{\,2}} + K_{A^-,J^-}^{ns}(x_2 + \sqrt{y_2 + x_2^2})}{2(V_0 + V_{titrant}^{ns})}] \qquad \text{eq S7}$$

where $x_1 = [A^-]V_{A^-} - K_{A^-,J^-}^{ns}[J^-]^{aq}(V_0 + V_{titrant}^{ns}) - [TDDA^+]_{titrant}^{ns}V_{titrant}^{ns}$,

$y_1 = 4[A^-]V_{A^-}K_{A^-,J^-}^{ns}[J^-]^{aq}(V_0 + V_{titrant}^{ns})$, $x_2 = [J^-]V_{J^-} - K_{J^-,A^-}^{ns}[A^-]^{aq}(V_0 + V_{titrant}^{ns}) - [TDDA^+]_{titrant}^{ns}V_{titrant}^{ns}$

and $y_2 = 4[J^-]V_{J^-}K_{J^-,A^-}^{ns}[A^-]^{aq}(V_0 + V_{titrant}^{ns})$.

By inserting $n_{TDDA^+} = V^{ns}_{titrant}[TDDA^+]^{ns}_{titrant}$ into eq S7, the EMF as a function of n_{TDDA^+} is obtained.

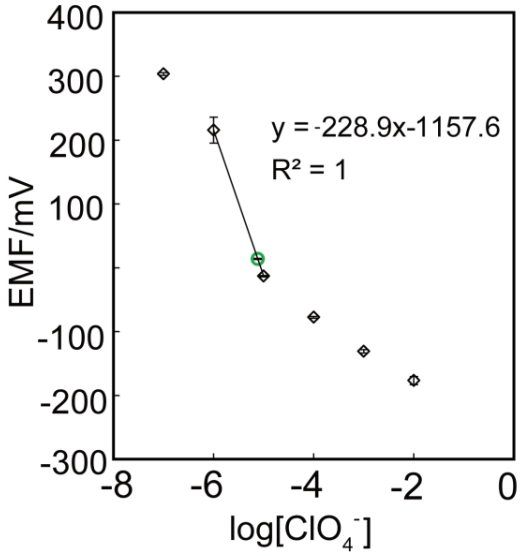

Figure S1. Potentiometric response of $TDDA^+$ doped anionic electrode to ClO_4^-. The green circle indicates the EMF of the ClO_4^- sample solution (13.99 ± 0.91) which corresponds to a log[ClO_4^-] of -5.12. Compared with the prepared real concentration (log[ClO_4^-]= -5.3), the error is ca. 3.4%.

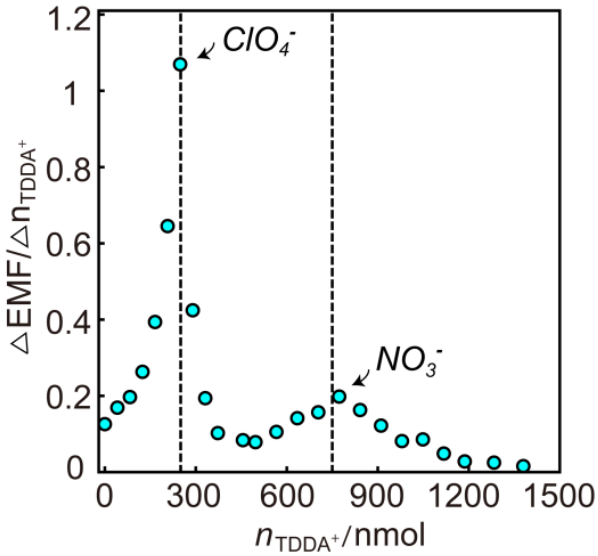

Figure S2. The first differentiation of consecutive titration for ClO_4^- and NO_3^- as shown in Figure 5. The dashed vertical lines indicate the expected endpoints.

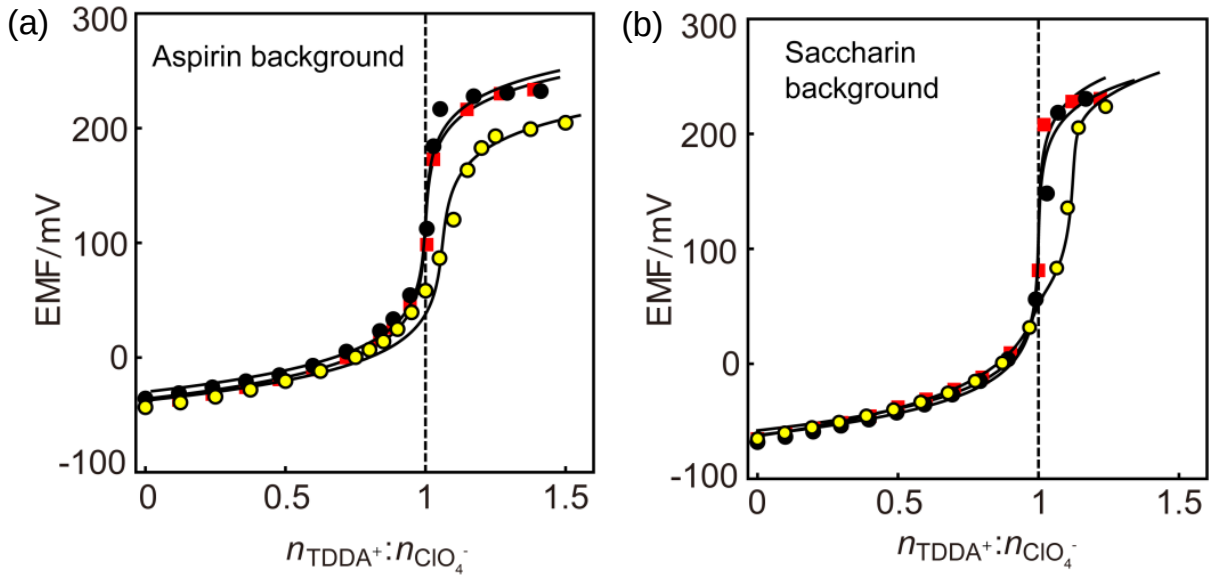

Figure S3. Potentiometric titration curves for 10^{-4} M ClO_4^- with different background of interfering anions. (a) Red: without aspirin. Black: 10^{-5} M aspirin. Yellow: 10^{-4} M aspirin. (b) Red: without saccharin. Black: 10^{-6} M saccharin. Yellow: 10^{-5} M saccharin. The dashed vertical line indicates the expected endpoints. Aspirin and saccharin stock solutions were adjusted by NaOH to reach pH 7.0 before use.

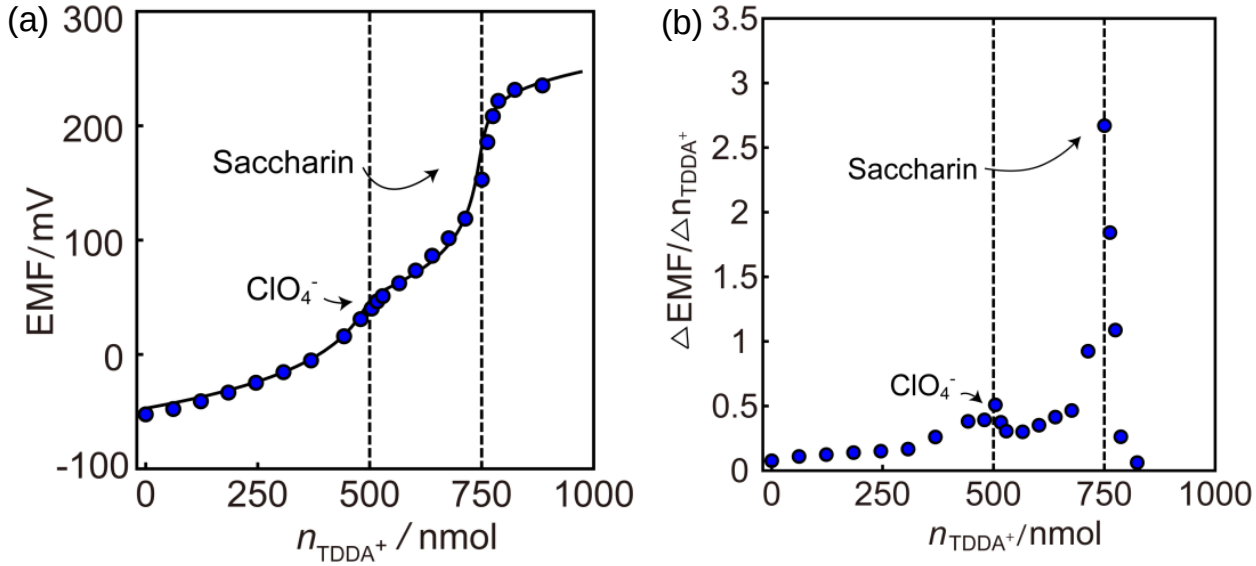

Figure S4. (a) Potentiometric consecutive titration for 10^{-4} M ClO_4^- and 5×10^{-5} M saccharin in non-buffered water fit with theoretical curve and (b) corresponding first differentiation of the titration curve (amount of ClO_4^- in solution: 500 nmol, amount of saccharin in solution: 250 nmol, total volume: 5 ml). The dashed vertical line shows the expected endpoint. Titrant: $TDDA^+Cl^-$ doped nanospheres. Indicator: anion selective electrode. $[TDDA^+]^{ns}_{titrant} = 1.23\times10^{-3}$ M. Saccharin stock solution was adjusted by NaOH to reach pH 7.0 before use.

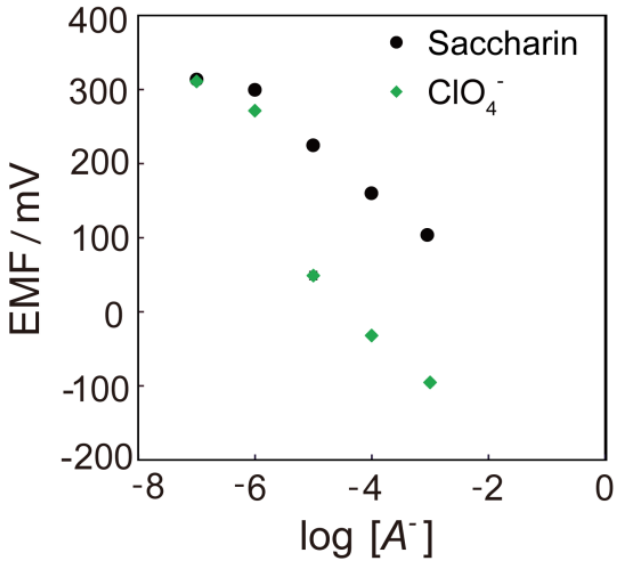

Figure S5. Selectivity of $TDDA^+$ doped anionic selective electrode membrane for ClO_4^- and saccharin in non-buffered water. Saccharin stock solution was adjusted by NaOH to reach pH 7.0 before use.

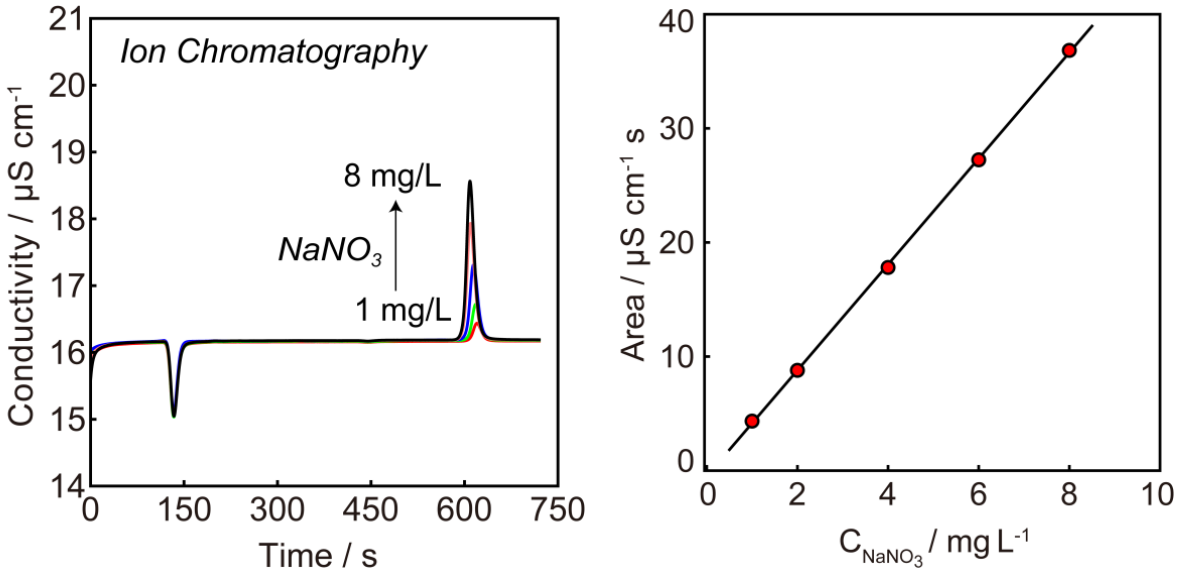

Figure S6. Ion chromatography time trace graph (left) and calibration curve (right) for different concentrations of NO_3^- (1 mg/L, 2 mg/L, 4 mg/L, 6 mg/L and 8 mg/L).

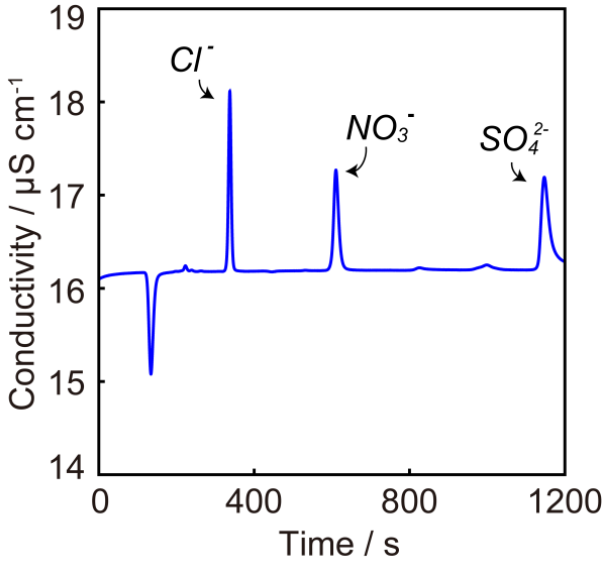

Figure S7. Ion chromatographic time trace for the injection of spinach extract solution.

References

(1) Yapper, M. C.; DuPré, D. B. J. Chem. Educ. 1997, 74, 1422.

(2) Hudson, R. J. M.; Rue, E. L.; Bruland, K. W. Environ. Sci. Technol. 2003, 37, 1553.

(3) Buccella, D.; Horowitz, J. A.; Lippard, S. J. J. Am. Chem. Soc. 2011, 133, 4101.

(4) Schwarzenbach, G.; Flaschka, H. Complexometric titrations; Methuen: London, 1969.

(5) Peper, S.; Ceresa, A.; Bakker, E.; Pretsch, E. Anal. Chem. 2001, 73, 3768.

(6) Hamidi-Asl, E.; Daems, D.; Wael, K. D.; Camp, G. V.; Nagels, L. J. Anal. Chem. 2014, 86, 12243.

(7) Yin, P.; Li, T.; Forgan, R. S.; Lydon, C.; Zuo, X.; Zheng, Z. N.; Lee, B.; Long, D.; Cronin, L.; Liu, T. J. Am. Chem. Soc. 2013, 135, 13425.

(8) Christian, G. D. Analytical Chemistry; 6 ed.; John Wiley & Sons, Inc., 2004.

(9) Davidson, E. A.; Howarth, R. W. Nature 2007, 449, 1000.

(10) Smetacek, V.; Zingone, A. Nature 2013, 504, 84.

(11) William M. Lewis, J.; Wurtsbaugh, W. A.; Paerl, H. W. Environ. Sci. Technol. 2011, 45, 10300.

(12) Zhai, J.; Xie, X.; Bakker, E. Anal. Chem. 2015, 87, 2827.

(13) Zhai, J.; Xie, X.; Bakker, E. Chem. Commun. 2014, 50, 12659.

(14) Xie, X.; Mistlberger, G.; Bakker, E. Anal. Chem. 2013, 85, 9932.

(15) Bakker, E.; Pretsch, E. Angew. Chem. Int. Ed. 2007, 46, 5660.

(16) Chester, R. Marine Geochemistry; 2 ed.; Wiley-Blackwell: London, 2000.

(17) Bakker, E.; Bühlmann, P.; Pretsch, E. Chem. Rev. 1997, 97, 3083.

(18) Bühlmann, P.; Pretsch, E.; Bakker, E. Chem. Rev. 1998, 98, 1593.

Chapter 5. Solvatochromic Dyes as pH-Independent Indicators for Ionophore Nanosphere-Based Complexometric Titrations

This work has been published in *Anal. Chem.*, **2015**, *87* (24), 12318-12323

Abstract

For half a century, complexometric titrations of metal ions have been performed with water soluble chelators and indicators that typically require careful pH control. Very recently, ion selective nanosphere emulsions were introduced that exhibit ion-exchange properties and are doped with lipophilic ionophores originally developed for chemical ion sensors. They may serve as novel, highly selective and pH independent complexometric reagents. While ion optode emulsions have been demonstrated as useful indicators for such titrations, they exhibit a pH-cross response that unfortunately complicates the identification of the endpoint. We present here pH independent optode nanospheres as indicators for complexometric titrations, with calcium as an initial example. The nanospheres incorporate an ionic solvatochromic dye (SD), ion exchanger and ionophore. The solvatochromic dye will be only expelled from the core of the nanosphere into the aqueous solution at the endpoint at which point it results in an optical signal change. The

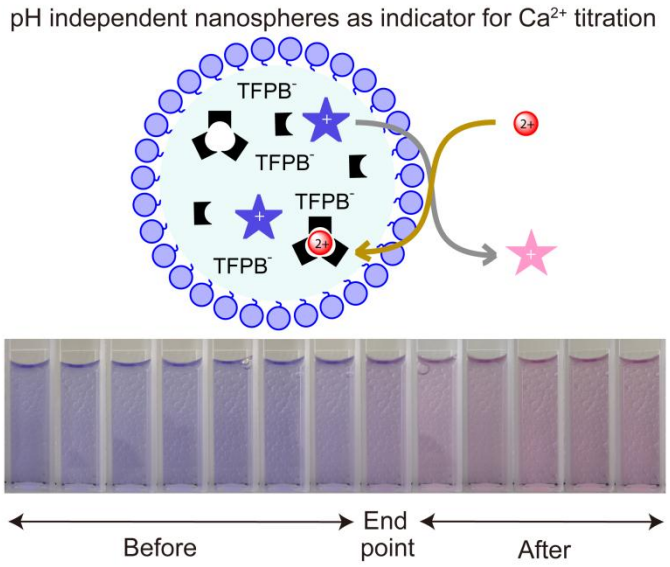

titration curves are demonstrated to be pH independent and with sharper endpoints than with previously reported chromoionophore-based optical nanospheres as indicator. The calcium concentration in mineral water was successfully determined using this method.

Introduction

Complexometric titration is an established and inexpensive technique for the quantification of metal ions in solution that compares well with other analytical techniques such as mass spectrometry (MS), ion chromatography (IC) and nuclear magnetic resonance (NMR).[1-4] Conventional complexometric titrations require water soluble chelators and indicators.[2] Highly selective ionophores cannot be adapted to this platform because they are very lipophilic and therefore water insoluble. Recently, ion selective nanoemulsions containing chromoionophores and ionophores as novel titration reagents (indicators and chelators) have been introduced.[5-7] Hydrophobic ionophores can be easily embedded into nanoemulsions, thereby extending the available reagent toolbox for complexation titrations.

The endpoint of a titration experiment can be monitored using ion selective electrodes or indicating dyes. Most of the indicating dyes also exhibit a response to sample pH changes, such as Eriochrome Black T and Murexide, and thus careful control of the sample pH is required.[8,9] To overcome this, ion selective optical nanosphere emulsions, miniaturized versions of ion optodes, have recently been demonstrated as endpoint indicators.[6] The nanospheres contain lipophilic sensing components including ion exchanger, ionophore and chromoionophore (lipophilic pH indicator). The signal change in absorbance or fluorescence mode depends on the competition between the hydrogen ion and the cationic analyte or coextraction of anionic analyte and hydrogen ion. The endpoint can be visualized in a specific range of pH, outside of which the transition becomes insufficiently sharp. This unsatisfactory behavior is caused by the simple fact that the response of the indicating nanospheres is pH dependent.

Ion-selective optical sensing films independent of sample pH have been previously reported by replacing the chromoionophores with solvatochromic dyes (SDs).[10-15] The sensor was based on hydrogel entrapped plasticizer droplets containing ionophores and SDs. The analyte ion could be exchanged or co-extracted with SDs into the droplet, causing an optical signal change in the SDs.[11,13,15,16] Changing the polarity of the solvent will induce a change in the ground and excited states of the SD and result in a change in the absorbance or fluorescence spectrum.[16-19] These dyes are used to probe the solvent

polarity and are also developed as research tools for the measurement of cell membrane potential changes, for cell imaging applications, and biosensors.[20-25] Here we present ion selective optical nanospheres incorporating SDs as pH independent endpoint indicators in the complexometric titration of Ca^{2+} as an initial model system. The endpoints can be easily identified in a very wide range of pH by recording absorbance or fluorescence, and are accompanied by a colour change visible to the naked eye.

Experimental Section

Reagents

Pluronic F-127 (F127), bis(2-ethylhexyl)sebacate (DOS), sodium tetrakis-[3,5-bis(trifluoromethyl)phenyl]borate (NaTFPB), potassium tetrakis[3,5-bis(trifluoromethyl)phenyl]borate (KTFPB), calcium ionophore II (ETH 129), calcium ionophore IV, 3,3′-dibutylthiacarbocyanine iodide (SD2), calcium chloride ($CaCl_2$), sodium hydroxide (NaOH), 2-amino-2-(hydroxymethyl)-1,3-propanediol (Tris), tetrahydrofuran (THF), methanol and hydrochloric acid (HCl) were obtained from Sigma-Aldrich. The charged solvatochromic dye (SD1) was synthesized in house.[26]

Preparation of chelating and indicating nanospheres

To prepare the chelating nanospheres, typically 1.75 mg of ETH129, 1.34 mg of KTFPB, 2.14 mg of DOS, and 1.5 mg of F127 were dissolved in 2.0 mL of THF to form a homogeneous solution. 0.5 mL of the THF solution was pipetted and injected into 3 mL of deionized water on a vortex with a vortexing speed of 1000 rpm. Compressed air was blown on the surface of the resulting nanosphere emulsion for 30 min to remove THF.

To prepare the indicating nanospheres, typically 1.61 mg of calcium ionophore IV, 0.21 mg of SD1, 0.64 mg of NaTFPB, 8.0 mg of DOS, and 5.0 mg of F127 were dissolved in 1 mL of THF to form a homogeneous solution. 0.1 mL of the THF solution was pipetted and injected into 4 mL of deionized water on a vortex with a vortexing speed of 1000 rpm. Compressed air was blown on the surface of the resulting nanosphere emulsion for 30 min as well to remove THF.

Instrumentation

Optical titration signals were measured with the UV−visible absorption spectrometer (SPECORD 250 plus, Analytic Jena, AG, Germany). Fluorescence signals were measured with a fluorescence spectrometer (Fluorolog-3, Horiba Jobin Yvon).

Optical titration

0.8 mL of the chelating nanospheres (complexing reagent) and 0.15 ml of the indicating nanospheres (indicator) were mixed in a cuvette and diluted with water to reach a final volume of 2 ml. The optical reverse titrations were performed by volumetric dosing of 10^{-3} M $CaCl_2$ or real sample into the titration cuvette, each step followed with recording the absorption or fluorescence spectrum.

Results and Discussion

Scheme 1 shows the principle of ion selective nanospheres as chelator and indicator for

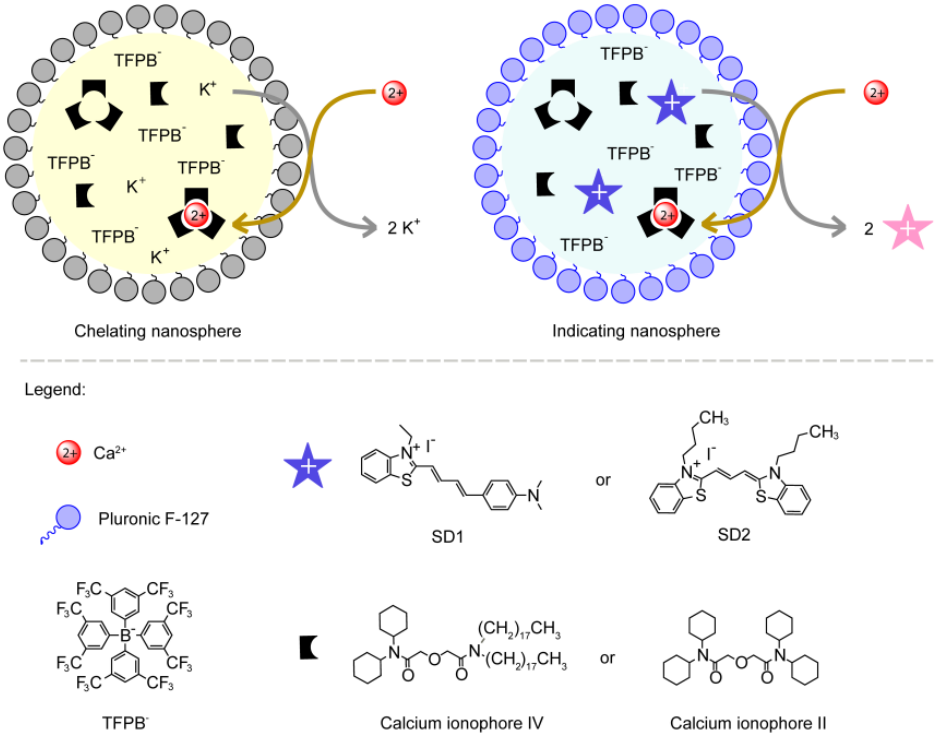

Scheme 1. Schematic illustration of ion selective nanospheres as chelators and indicators in the complexometric titration of calcium. Chelating nanospheres contain calcium ionophore II and cation exchanger. Indicating nanosphere contain calcium ionophore IV, cation exchanger and solvatochromic dye (SD1 or SD2).

calcium titration. The chelating and indicating nanospheres contain calcium ionophore IV or calcium ionophore II and the cation exchanger $TFPB^-$ embedded in the hydrophobic core made of DOS and F127. The indicating nanospheres contain additionally positively charged solvatochromic dye (SD1 or SD2) as the signal reporter. Dynamic light scattering (DLS) shows that the average diameter of the indicating nanosphere is 210 ± 3 nm. The polydispersity index (PDI) was determined as 0.27 ± 0.03 indicating a relatively narrow size distribution.

Calcium can be extracted into the chelating nanospheres by exchanging with the counter ion of $TFPB^-$. In the indicating nanospheres, SD1 is able to partition between the core of the nanosphere and the aqueous solution. When no Ca^{2+} is present in the solution, SD1 resides mainly within the core of the nanospheres, exhibiting a blue colour. At the endpoint only, SD1 is exchanged by Ca^{2+} into the aqueous solution and the colour will turn red.

Both the chelating and indicating nanospheres function on the basis of ion exchange as follows. For the chelating nanosphere, calcium will be extracted by the calcium ionophore into the organic phase to replace the initial counter ion of the ion exchanger, M^+:

$$Ca^{2+}(aq) + 3L(ns) + 2M^{+}(ns) \rightleftharpoons CaL_3^{2+}(ns) + 2M^{+}(aq) \quad (1)$$

where L is the calcium ionophore and CaL_3^{2+} the complex formed between Ca^{2+} and L. For the indicating nanospheres, the initial counter ion of the ion exchanger is the positively charged solvatochromic dye, SD^+. Therefore, the appropriate process can be expressed as:

$$Ca^{2+}(aq) + 2SD^{+}(ns) + 3L(ns) \rightleftharpoons CaL_3^{2+}(ns) + 2SD^{+}(aq) \quad (2)$$

Both chelating and indicating nanospheres contain a molar excess of ionophore relative to ion exchanger. The relationship between the primary ion (Ca^{2+}) concentration in the nanospheres and sample solution can be quantified by ion exchange theory.[27] The mole fraction of extracted (and complexed) Ca^{2+} in the chelating nanospheres and the indicating nanospheres are described by eq 3 and eq 4, respectively.

$$\frac{2[CaL_3^{2+}]^{cs}}{[TFPB^-]^{cs}} = \frac{2[Ca^{2+}]^{aq} + (K^{cs}_{Ca^{2+},J^+}[J^+]^{aq})^2}{2[Ca^{2+}]^{aq}} - \frac{\sqrt{4[Ca^{2+}]^{aq}(K^{cs}_{Ca^{2+},J^+}[J^+]^{aq})^2 + (K^{cs}_{Ca^{2+},J^+}[J^+]^{aq})^4}}{2[Ca^{2+}]^{aq}} \quad (3)$$

$$\frac{2[CaL_3^{2+}]^{is}}{[TFPB^-]^{is}} = \frac{2[Ca^{2+}]^{aq} + (K^{is}_{Ca^{2+\prime},SD^+}[SD^+]^{aq})^2}{2[Ca^{2+}]^{aq}} - \frac{\sqrt{4[Ca^{2+}]^{aq}(K^{is}_{Ca^{2+\prime},SD^+}[SD^+]^{aq})^2 + (K^{is}_{Ca^{2+\prime},SD^+}[SD^+]^{aq})^4}}{2[Ca^{2+}]^{aq}} \quad (4)$$

where $[CaL_3^{2+}]^{cs}$ and $[TFPB^-]^{cs}$ are the concentrations of Ca^{2+} complex and ion exchanger in the chelating nanospheres, $[Ca^{2+}]^{aq}$ and $[J^+]^{aq}$ the concentrations of Ca^{2+} and interfering ion J^+ in aqueous phase, and $K^{cs}_{Ca^{2+},J^+}$ the selectivity coefficient of chelating nanosphere for Ca^{2+} over the cation initially present in the nanospheres, J^+. In eq 4, $[CaL_3^{2+}]^{is}$, $[TFPB^-]^{is}$, $K^{is}_{Ca^{2+\prime},SD^+}$ are the corresponding values for the indicating nanospheres, and $[SD^+]^{aq}$ is the concentration of SD^+ in aqueous phase.

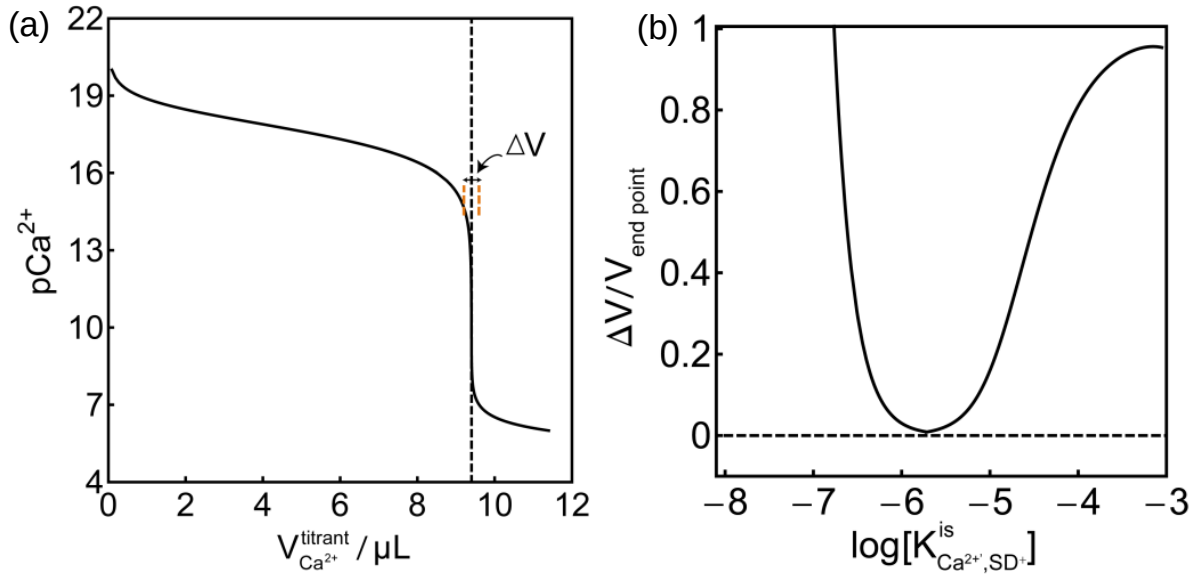

Figure 1. (a) Theoretical relationship between the free calcium concentration remaining in the sample (pCa^{2+}) and the volume of the titrant ($CaCl_2$) in the presence of chelating nanospheres. The dashed vertical line marks the expected endpoint. (b) Theoretical estimate for the sharpness of the transition as a function of $\log K^{is}_{Ca^{2+\prime},SD^+}$ in the presence of the chelating and indicating nanospheres. ΔV is the volume of the titrant required to alter the phase ratio of the SDs from 9 : 1 to 1 : 9. Parameters: V_T = 2 mL, $K^{is}_{Ca^{2+\prime},SD^+}[SD^+]^{aq} = 2.35\times10^{-3}$ M, V_{cs} = 8 μL, $[Ca^{2+}]^{titrant} = 10^{-3}$ M, $K^{cs}_{Ca^{2+},J^+}[J^+]^{aq} = 10^{-12}$ M, V_{is} = 1 μL, $[TFPB^-]^{is} = 10^{-6}$ M, $[SD^+]^{is} = 0.9[TFPB^-]^{is}$ or $[SD^+]^{is} = 0.1[TFPB^-]^{is}$.

The mass conservation for calcium is written as:

$$[Ca^{2+}]^{titrant} V_{Ca^{2+}}^{titrant} = [CaL_3^{2+}]^{cs} V_{cs} + [CaL_3^{2+}]^{is} V_{is} + [Ca^{2+}]^{aq} V_T \quad (5)$$

Here, $[Ca^{2+}]^{titrant}$ and $V_{Ca^{2+}}^{titrant}$ are the concentration of titrant and the volume added into the sample, respectively. V_T is the total volume and V_{cs} and V_{is} are the volumes of chelating and indicating nanospheres, respectively.

The relationship between absorbance, *A*, and $[CaL_3^{2+}]^{is}$ is found as:

$$A = \frac{V_{is}}{V_T}\{([SD^+]_T^{is} - 2[CaL_3^{2+}]^{is})\varepsilon_1 b + 2[CaL_3^{2+}]^{is}\varepsilon_2 b\} \quad (6)$$

Where $[SD^+]_T^{is}$ is the total concentration of charged solvatochromic dye SD^+ in indicating nanosphere, ε_1 and ε_2 are the molar absorptivities of SD^+ in the nanosphere and aqueous solution, respectively, and *b* is the optical path length of the suspension.

The $V_{Ca^{2+}}^{titrant}$ as a function of $[CaL_3^{2+}]^{is}$ is now obtained by solving equations (3), (4) and (5) (see eq 7). The absorbance as a function of $2n_{Ca^{2+}} : n_{TFPB^-} = 2V_{Ca^{2+}}^{titrant}[Ca^{2+}]^{titrant} : [TFPB^-]^{cs} V_{cs}$ is obtained by inserting eq 6 into eq 7.

$$V_{Ca^{2+}}^{titrant} = \frac{1}{[Ca^{2+}]^{titrant}}\{[CaL_3^{2+}]^{is} V_{is} + \frac{yV_T}{x^2} + \frac{[TFPB]^{cs} x^2 V_{cs}(z^2 + \frac{2y}{x^2} - \sqrt{z^4 + \frac{4yz^2}{x^2}})}{4y}\} \quad (7)$$

where $x = 2[CaL_3^{2+}]^{is} - [TFPB^-]^{is}$, $y = 2[CaL_3^{2+}]^{is}[TFPB^-]^{is}(K_{Ca^{2+'},SD^+}^{is}[SD^+]^{aq})^2$, $z = K_{Ca^{2+},J^+}^{cs}[J^+]^{aq}$

.

During the reverse titration process, the free Ca^{2+} concentration in the aqueous phase will gradually increase. Figure 1a shows the modeled relationship between the free calcium remaining in the aqueous phase (pCa^{2+}) and the volume of $CaCl_2$ titrant in the presence of chelating nanospheres. The chelating nanospheres impose a very low free calcium concentration before the endpoint. After saturating the chelating nanospheres, the calcium concentration will dramatically increase. A good indicator should abruptly change colour at the endpoint. ΔV shown in Figure 1a indicates the volume of titrant required to change the phase ratio of the SDs from 9 : 1 to 1 : 9, thereby encompassing the region of visible colour change. The smaller the $\Delta V/V_{end\ point}$ is, the sharper the transition will be. For an extremely sharp transition and a small associated error, the indicator should be most sensitive at the endpoint. For SD-based nanospheres, the optical response depends on the

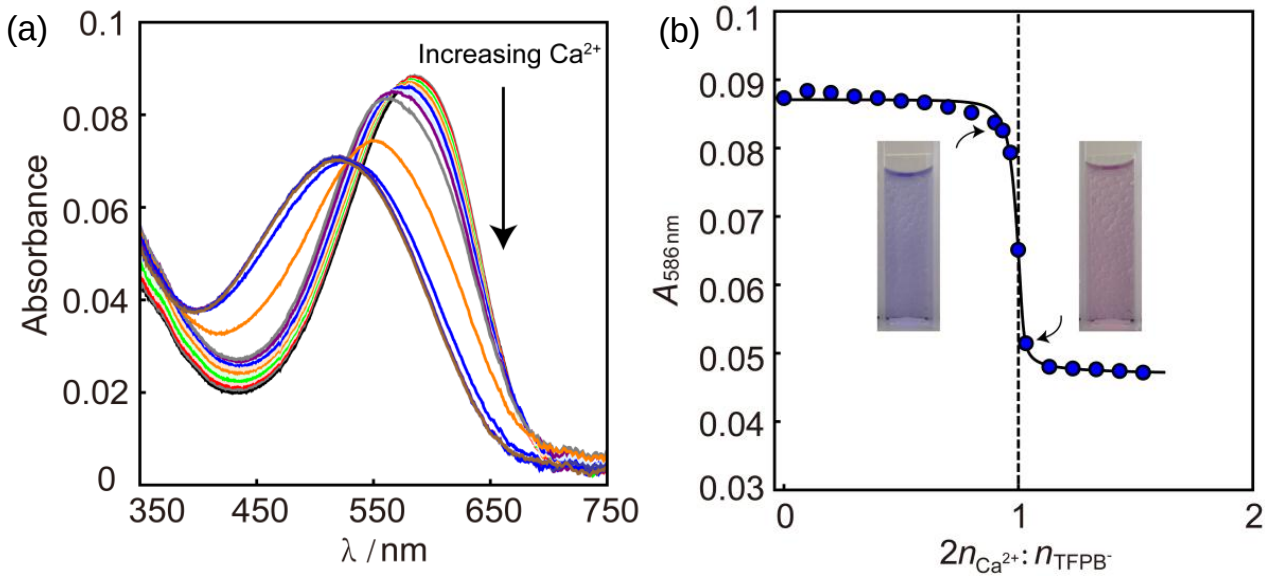

Figure 2. (a) Absorption spectra and (b) corresponding titration curve for the reverse titration for calcium using10^{-3} M $CaCl_2$ as titrant without pH control. Endpoint indicator: SD1-based Ca^{2+}-selective nanospheres. Chelator: nanospheres containing ETH 129 and $TFPB^-$. The dashed vertical line indicates the expected endpoint. Fitting parameters: V_T = 2 ml, $[TFPB^-]^{is}$ = $3.29\times10^{-6.02}$ M, V_{is} = 1.5 µL, $[TFPB^-]^{cs}$ =2.35×10^{-5} M, V_{cs} = 8 µL, $[Ca^{2+}]^{titrant}$ = 10^{-3} M, $K^{cs}_{Ca^{2+},J^+}[J^+]^{aq}$ =$10^{-7.12}$ M, $K^{is}_{Ca^{2+\prime},SD^+}[SD^+]^{aq}$ =$10^{-5.5}$ M.

selectivity of Ca^{2+} over SD^+. A more hydrophilic SD^+ results in the smaller $K^{is}_{Ca^{2+\prime},SD^+}$ value. Therefore, the lipophilicity of the SD^+ dyes will influence the transition and the accuracy of the titration. Figure 1b shows how the $\Delta V/V_{end\ point}$ is influenced by the selectivity coefficient $\log K^{is}_{Ca^{2+\prime},SD^+}$. For a titration with a given amount of chelator and Ca^{2+}, an optimal range of selectivity will exist.

The utility of the chelating nanospheres have been demonstrated in our previous work.[5,6] Here, the titration was performed by mixing chelating and indicating nanospheres. The sample or standard solution containing Ca^{2+} was then volumetrically dosed into the suspension. During the titration process, Ca^{2+} is first consumed by the chelating nanospheres. After saturating the chelating nanospheres, the Ca^{2+} will be extracted into the indicating nanospheres to replace the solvatochromic dye and cause the blue shift in the absorption spectrum as shown in Figure 2a. The absorptivities of SD1 in various solvents have been previously reported by our group.[26] The absorptivity of SD1 in water (4.2×10^4 L mol^{-1} cm^{-1}) is much higher than some conventional indicators such as Murexide (1.3×10^4 L mol^{-1} cm^{-1}).[26,28] Here, only a small amount of SD1 was doped into

the nanospheres so that the amount of calcium consumed by indicating nanospheres can be neglected. The sharp transition of the titration curve can be easily identified visually or from the spectra (Figure 2b). The small value of $\Delta V/V_{\text{end point}}$ (ca. 6.4%) suggests that the lipophilicity of the SD1 in the indicating nanosphere is well matched to the titration of interest. The experimental data fit well with eq 7 and the errors between theoretical fit and the experimental datas are very small (Figure S1). Compared to the theoretically expected end point, the error was only ca. 1%.

H^+-selective chromoionophore-based ion-selective optical nanospheres were previously demonstrated to function as indicators for calcium titration. Unfortunately, the calcium response of the nanospheres also depends on sample pH. As a consequence, the titration curve went from sigmoidal to linear as the sample pH increased.[6] In practice, a sharp transition is much more preferred. SD-based optical nanospheres can overcome this pH

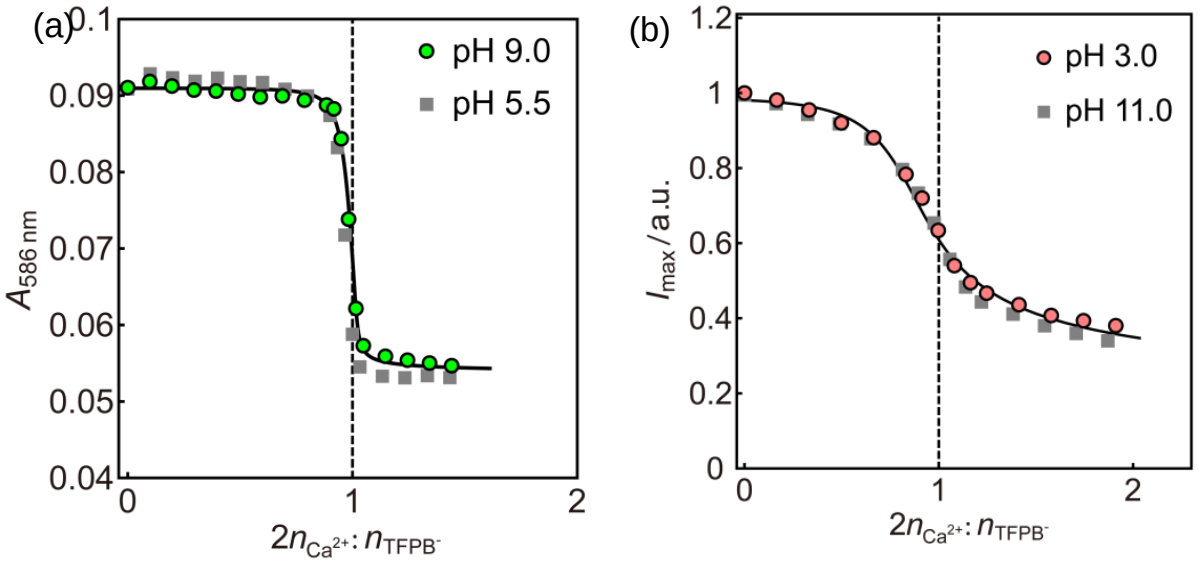

Figure 3. Optical reverse titration curves for calcium using solvatochromic dye SD1 (a) and SD2 (b) based optical nanospheres as indicator at the indicated pH values. (a) Endpoint indicator: SD1-based and Ca^{2+}-selective; pH 9.0: 10^{-3} M tris-H_2SO_4; pH 5.5: 10^{-3}M MES-NaOH; (b) Endpoint indicator: SD1-based Ca^{2+}-selective nanospheres. pH 3.0: 10^{-3} M HCl; pH 11.0:10^{-3}M NaOH. Chelator: nanospheres containing ETH 129 and $TFPB^-$. The dashed vertical line indicates the expected endpoint. Fitting parameters (a): V_T = 2 ml, $[TFPB^-]^{is} = 3.29\times10^{-6.15}$ M, V_{is} = 1.5 µL, $[TFPB^-]^{cs} = 2.35\times10^{-5}$ M, V_{cs} = 8 µL, $[Ca^{2+}]^{titrant} = 10^{-3}$ M, $K^{cs}_{Ca^{2+},J^+}[J^+]^{aq} = 10^{-7}$ M, $K^{is}_{Ca^{2+},SD^+}[SD^+]^{aq} = 10^{-5.5}$ M. (b) V_T = 3 ml, $[TFPB^-]^{is} = 1.1\times10^{-5}$ M, V_{is} = 1 µL, $[TFPB^-]^{cs} = 4.9\times10^{-4}$ M, V_{cs} = 19 µL, $[Ca^{2+}]^{titrant} = 10^{-3}$ M, $K^{cs}_{Ca^{2+},J^+}[J^+]^{aq} = 10^{-4.37}$ M, $K^{is}_{Ca^{2+},SD^+}[SD^+]^{aq} = 10^{-3.569}$M.

dependence as it has been demonstrated that they exhibit a dramatically lower pH cross-sensitivity.[10] As shown in Figure 3a, identical titration curves at pH 5.5 and pH 9.0 are observed using the solvatochromic dye SD1 as indicator. In fluorescence mode, SD2-based optical nanospheres also showed very similar titration curves at pH 3.0 and pH 11.0 (Figure 3b). Both the SD1 and SD2-based titration curves agreed well with the theory and the errors between theoretical fit and the experimental data were small (Figure S2). Note that under more acidic or basic pH conditions, hydrogen ions or hydroxide ions will eventually cause interference by ion-exchange and coextraction. Nonetheless, the reported pH range already accounts for most situations of practical importance, including physiological and environmental samples.

It is noted that the SD2-based titration curves are not as sharp as the SD1-based ones, which is explained with the much higher lipophilicity of SD2 compared to SD1. According to Figure 1b, this increase in lipophilicity will make $\log K^{is}_{Ca^{2+\prime},SD^+}$ deviate from the optimal range and cause an increase in $\Delta V/V_{\text{end point}}$ (Figure 1b) and thus make the transition less sharp.

Both the indicating and chelating nanospheres remain functional after one week. Figure 4

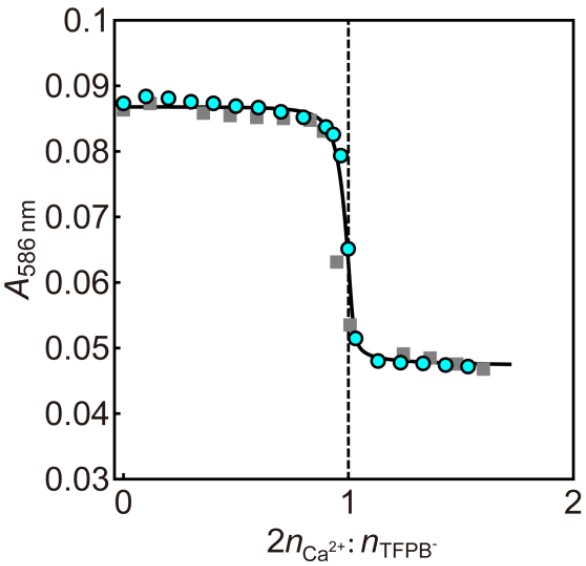

Figure 4. Complexometric titration curves using freshly prepared indicating and chelating nanosphere (green) and one-week-old indicating and chelating nanoshperes (gray). Endpoint indicator: SD1-based nanosphere. Chelator: nanospheres containing ETH 129 and $TFPB^-$. The dashed vertical line indicates the expected endpoint. Fitting parameters: $V_T = 2$ ml, $[TFPB^-]^{is} = 3.29\times10^{-6.02}$ M, $V_{is} = 1.5$ µL, $[TFPB^-]^{ns} = 2.35\times10^{-5}$ M, $V_{cs} = 8$ µL, $[Ca^{2+}]^{titrant} = 10^{-3}$ M, $K^{cs}_{Ca^{2+},J^+}[J^+]^{aq} = 10^{-7}$ M, $K^{is}_{Ca^{2+\prime},SD^+}[SD^+]^{aq} = 10^{-5.5}$ M.

compares titrations using freshly prepared nanospheres and one-week-old nanospheres, suggesting good stability. As an initial application, the calcium level in mineral water (purchased in a local Swiss supermarket) was determined as 13.0 mM ± 0.1 mM (standard deviation shown; n=3) using the nanospheres described in this work while atomic absorption spectroscopy (AAS) gave 12.6 mM ± 0.09 mM.

Compared with conventional complexometric titrations with water soluble reagents, our method exhibits better selectivity, a wider working pH range and increased versatility. While the reagents costs are currently higher, they will be reduced once the method becomes more widely accepted. The comparison of the characteristics is shown in Table S1.

In conclusion, we have described here solvatochromic dye based ion selective optical nanospheres as indicator for the complexometric titrations of cations, with calcium as initial example. Both chelating nanospheres and the SD-based indicating nanospheres operate independently of pH, which is in significant contrast to any other established complexometric titration procedure. Calcium titrations can now be performed without pH control in a wide range of pH. The calcium concentration in mineral water has been successfully determined, demonstrating the potential utility of this new class of ionophore-based reagents.

Supporting Information

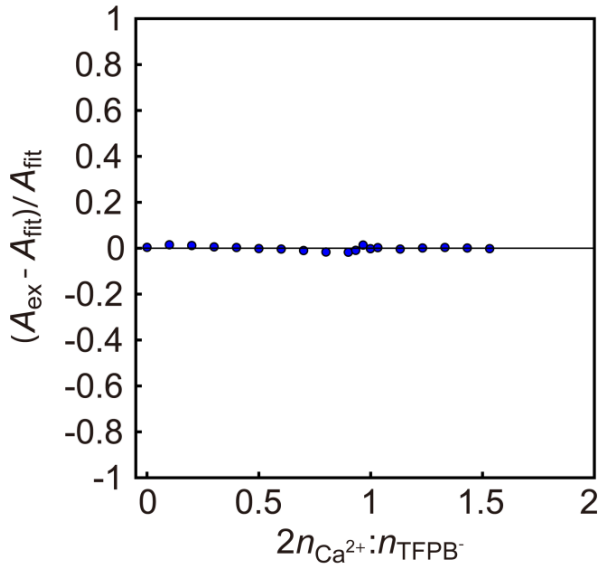

Figure S1. An estimation of the error between theoretical fit and the experimental data for Figure 2b. A_{ex} is the experimental absorbance at 586 nm and A_{fit} is the corresponding theoretical absorbance used to fit the data.

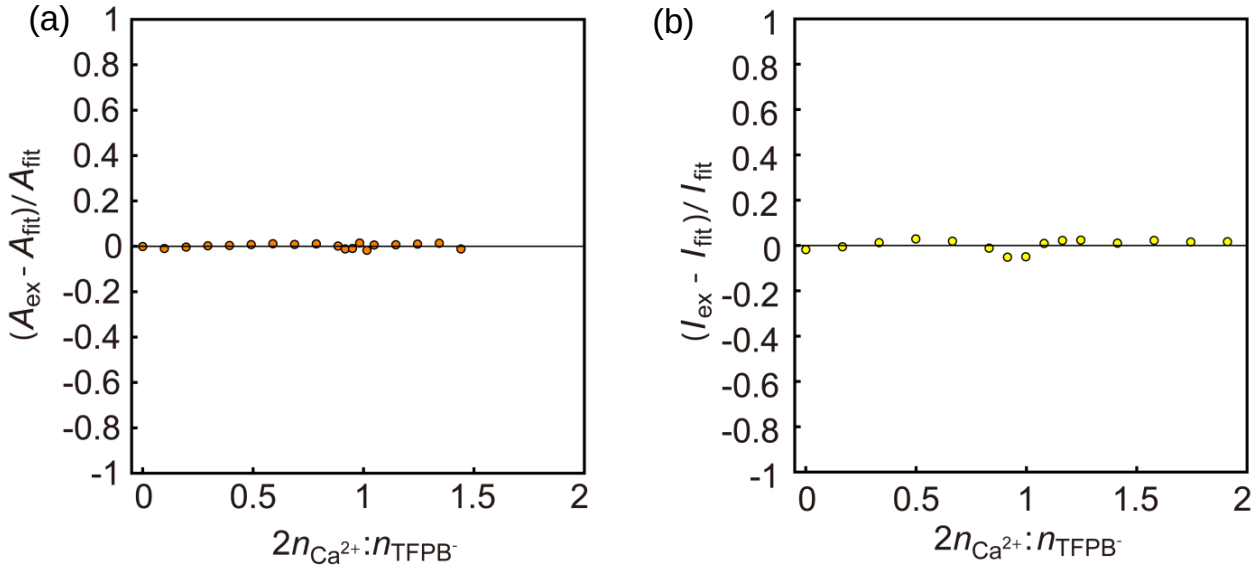

Figure S2. An estimation of the error between theoretical fit and the experimental data for Figure 3a (left, a) and Figure 3b, (right, b). (a) A_{ex} is the experimental absorbance at 586 nm and A_{fit} is the corresponding theoretical absorbance used to fit the data. (b) I_{ex} is the experimental maximum emission intensity and I_{fit} is the corresponding theoretical intensity used to fit the data.

Table S1. Comparision between the complexometric titration methods based on ion selective nanospheres and water soluble reagents.

	Nanosphere based	**Water soluble reagents**
Selectivity	high	low
Variety of the chelators and indicators	large	small
Working pH range	wide	narrow
Cost	high	low

References

(1) Ding, J.; Qin, W. *Biosens. Bioelectron.* **2013**, *47*, 559.

(2) Schwarzenbach, G.; Flaschka, H. *Complexometric titrations*; Methuen: London, 1969.

(3) Hamidi-Asl, E.; Daems, D.; Wael, K. D.; Camp, G. V.; Nagels, L. J. *Anal. Chem.* **2014**, *86*, 12243.

(4) Cui, L.; Puerto, M.; López-Salinas, J. L.; Biswal, S. L.; Hirasaki, G. J. *Anal. Chem.* **2014**, *86*, 11055.

(5) Zhai, J.; Xie, X.; Bakker, E. *Chem. Commun.* **2014**, *50*, 12659.

(6) Zhai, J.; Xie, X.; Bakker, E. *Anal. Chem.* **2015**, *87*, 2827.

(7) Zhai, J.; Xie, X.; Bakker, E. *Anal. Chem.* **2015**, *87*, 8347.

(8) Männel-Croisé, C.; Meister, C.; Zelder, F. *Inorg. Chem.* **2010**, *49*, 10220.

(9) Sun, S.; Tu, K.; Yan, X. *Analyst* **2012**, *137*, 2124.

(10) Xie, X.; Zhai, J.; Bakker, E. *J. Am. Chem. Soc.* **2014**, *136*, 16465.

(11) Huber, C.; Werner, T.; Krause, C.; Wolfbeis, O. S.; Leiner, M. J. P. *Anal. Chim. Acta* **1999**, *398*, 137.

(12) Chojnacki, P.; Werner, T.; Wolfbeis, O. S. *Microchim. Acta* **2004**, *147*, 87.

(13) Huber, C.; Klimant, I.; Krause, C.; Werner, T.; Wolfbeis, O. S. *Anal. Chim. Acta* **2001**, *449*, 81.

(14) Huber, C.; Werner, T.; Krause, C.; Wolfbeis, O. S. *Analyst* **1999**, *124*, 1617.

(15) Krause, C.; Werner, T.; Huber, C.; Wolfbeis, O. S. *Anal. Chem.* **1999**, *71*, 1544.

(16) Krause, C.; Werner, T.; Huber, C.; Wolfbeis, O. S. *Anal. Chem.* **1999**, *71*, 5304.

(17) Reichardt, C. *Chem. Rev.* **1994**, *94*, 2319.

(18) Machado, V. G.; Stock, R. I.; Reichardt, C. *Chem. Rev.* **2014**, *114*, 10429.

(19) Dsouza, R. N.; Pischel, U.; Nau, W. M. *Chem. Rev.* **2011**, *111*, 7941.

(20) Baranov, M. S.; Solntsev, K. M.; Baleeva, N. S.; Mishin, A. S.; Lukyanov, S. A.; Lukyanov, K. A.; Yampolsky, I. V. *Chem. Eur. J.* **2014**, *20*, 13234.

(21) Woodford, C. R.; Frady, E. P.; Smith, R. S.; Morey, B.; Canzi, G.; Palida, S. F.; Araneda, R. C.; Kristan, W. B.; Kubiak, C. P.; Miller, E. W.; Tsien, R. Y. *J. Am. Chem. Soc.* **2015**, *137*, 1817.

(22) Yang, M.; Song, Y.; Zhang, M.; Lin, S.; Hao, Z.; Liang, Y.; Zhang, D.; Chen, P. R. *Angew. Chem. Int. Ed.* **2012**, *51*, 7674.

(23) Demchenko, A. P. *Methods Appl. Fluoresc.* **2013**, *1*, 1.

(24) Cohen, L. B.; Salzberg, B. M.; Davila, H. V.; Ross, W. N.; Landowne, D.; Waggoner, A. S.; Wang, C. H. *J. Membrane Biol.* **1974**, *19*, 1.

(25) Wang, Q.; Lawrence, D. S. *J. Am. Chem. Soc.* **2005**, *127*, 7684.

(26) Xie, X.; Gutiérrez, A.; Trofimov, V.; Szilagyi, I.; Soldati, T.; Bakker, E. *Anal. Chem.* **2015**, *87*, 9954.

(27) Ceresa, A.; Radu, A.; Peper, S.; Bakker, E.; Pretsch, E. *Anal. Chem.* **2002**, *74*, 4027.

(28) Khan, T. K.; Gupta-Bhaya, P. *Talanta* **1997**, *44*, 2087.

Chapter 6. Ionophore-Based Titrimetric Detection of Alkali Metal Ions in Serum

This work has been submitted to *ACS Sens.*, **2017**, *2*, 606-612

Abstract

While the titrimetric assay is one of the most precise analytical techniques available, only a limited list of complexometric chelators is available as many otherwise promising reagents are not water soluble. Recent work demonstrated the successful titrimetry with ion-exchanging polymeric nanospheres containing hydrophobic complexing agents, so-called ionophores, opening an exciting avenue in this field. However, this method was limited to ionophores of very high affinity to the analyte and exhibited a relatively limited titration capacity. To overcome these two limitations, we report here on solvent based titration reagents. This heterogeneous titration principle is based on the dissolution of all hydrophobic recognition components in a solvent such as dichloromethane (CH_2Cl_2) where the ionophores are shown to maintain a high affinity to the target ions. HSV (hue, saturation, value) analysis of the images captured with a digital camera provides a convenient and inexpensive way to determine the endpoint. This approach is combined

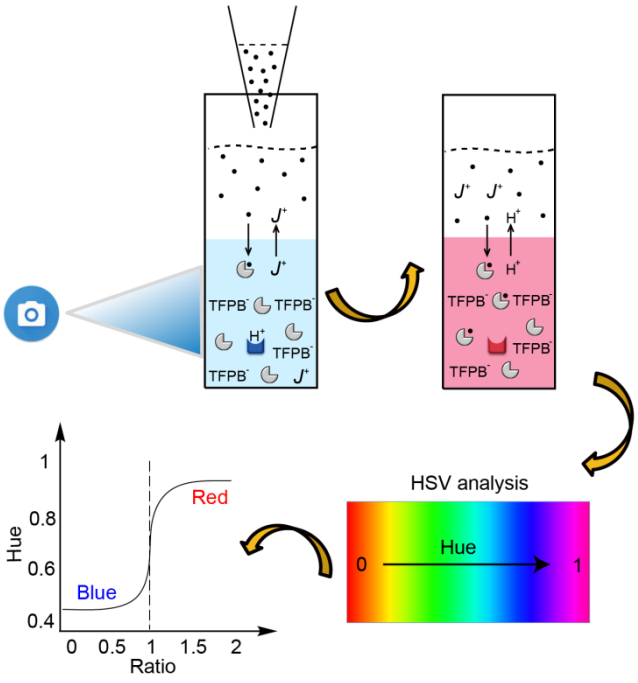

with an automated titration setup. The titrations of the alkali metals K^+, Na^+ and Li^+ in aqueous solution are successfully demonstrated. The potassium concentration in human serum without pretreatment was precisely and accurately determined as 4.38 mM $\pm$ 0.10 mM (automated titration), which compares favorably with atomic emission spectroscopy (4.47 mM $\pm$ 0.20 mM).

Keywords: Ionophore-based titration reagents, ion exchange principle, alkali metals, human serum, HSV analysis

Introduction

In complex biological systems such as human serum, the determination of inorganic metal ions is of key importance because their levels are closely associated with patient health.[1-3] Numerous techniques and methods have been established for real sample measurements, including potentiometric and optical chemosensors, titrimetry, ion chromatography, mass spectrometry and atomic spectroscopy.[4-9] An automated titration would be attractive because of the very high precision associated with such measurements. Its most significant challenge is to achieve sufficient selectivity for the target ion against interfering ones. For example, the measurement of K^+ (in the range of 3.5 mM to 5.5 mM) in human serum is difficult because of a high Na^+ background (135 mM to 145 mM) and the presence of other cations including Ca^{2+} (2.25 mM to 2.75 mM) and Mg^{2+} (0.7 mM to 1.1 mM).[4,5]

Complexometric titrations are normally performed in homogenous aqueous phase and for this reason chelators and indicators must be water soluble. Chelators such as ethylenediamine tetraacetic acid (EDTA) and its derivatives diethylene triamine pentaacetic acid (DTPA) and ethylene glycol tetraacetic acid (EGTA) have been widely used in complexometric titration since 1945.[10-15] Commercial available dyes such as Eriochrome Black T and Murexide are classical dyes and function as indicators for many metal ions.[13,16,17] A rather rigid selectivity sequence and the presence of protonatable groups make it normally necessary to pretreat the sample and to use masking reagents, which is undesired.

For lack of selective reagents, traditional titration methods for alkali metals such as K^+, Na^+ and Li^+ are indirect and often based on salt precipitation of metals such as Zn^{2+}, Co^{2+}, and Ni^{2+}. The metal can only then be determined with EDTA.[10,18] These methods are not applicable to complex physiological samples.

Recently, ion selective nanospheres, a new generation of titration reagents, moved the titration process from homogeneous to heterogeneous phase.[19-22] The use of non-polar nanospheres makes the chelators and indicators no longer limited to water soluble compounds. Ionophores with high selectivity to the desired metal ion can now conceivably be used in titrations, by simply doping them into the nanospheres. For

example, chelating nanospheres, made of surfactant Pluronic F-127 and plasticizer, contain ion exchanger and ionophore in their core. Based on the principle of ion-exchange, the concentration of titrated analyte can be calculated by that of the ion exchanger without considering the stoichiometry between ionophore and analyte. The indicating nanospheres are formulated with similar components to the chelating nanosphere but contain an additional chromoionophore (lipophilic pH indicator) or a solvatochromic dye. This new titration principle based on nanospheres of high selectivity has been successfully applied to Ca^{2+} and Pb^{2+} ions.[19,20,22] Unfortunately, however, it cannot easily be extended to ionophores with lower binding affinity such as those for K^+, Na^+ and Li^+, as the binding constants have been shown to be quite dramatically reduced in the more polar environment of the nanospheres compared to polymeric sensor materials.[23]

Two phase extractions have been widely used for separation, purification and recovery of target products in biotechnology, food chemistry and nuclear industry.[24-28] The two phases may be combinations of polymer/polymer, polymer/salt, polymer/water and solvent/water systems.[29-31] In liquid-liquid systems, the extractants or ligands can be dissolved into one of the liquid phase while the analytes are present in the other phase.[32] The dissolution of the ion exchanger together with the extractants/ligands was shown to enhance the extraction efficiency and gave a reduced extraction time.[26]

To the best of our knowledge, two-phase extraction systems based on the ion exchange principle have never been applied as titration reagents in complexometric titrations. We introduce here a family of ionophore-based water-immiscible titration reagents for K^+, Na^+ and Li^+. They function as both the chelator and indicator, dramatically simplifying the analytical procedure. These reagents not only extend the use of liphophilic compounds but also improve the capacity of the sensor components and maintain a higher affinity of the ionophore compared to nanosphere based reagents. The extraction of the analyte is rapid and the signals can be monitored by UV-visible spectroscopy or by analyzing the hue value from less expensive picture or movie acquisition data. A home-made automatic setup is introduced. The level of K^+ in human serum, without the need for sample pretreatment, is successfully determined.

Experimental Section

Reagents

Sodium tetrakis-[3,5-bis(trifluoromethyl)phenyl]borate (NaTFPB), potassium tetrakis[3,5-bis(trifluoromethyl)phenyl]borate (KTFPB), valinomycin (potassium ionophore I), 4-tert-butylcalix[4]arene tetraacetic acid tetraethyl ester (sodium ionophore X), N,N,N′,N′,N″,N″-hexacyclohexyl-4,4′,4″-propylidynetris(3-oxabutyramide) (lithium ionophore VIII), 9-(diethylamino)-5-(octadecanoylimino)-5H-benzo[a]phenoxazine (CHI), 2-amino-2-(hydroxymethyl)-1,3-propanediol (Tris), sodium chloride (NaCl), potassium chloride (KCl), lithium chloride (LiCl), calcium chloride ($CaCl_2$), magnesium chloride ($MgCl_2$), dichloromethane (CH_2Cl_2), hydrochloric acid (HCl) were obtained from Sigma-Aldrich. Human serum was provided by Hôpitaux Universitaires de Genève (HUG).

Preparation of ionophore-based titration reagents

Typically, for the potassium titration reagent, 0.90 mg NaTFPB and 1.60 mg potassium ionophore I were dissolved in 2.2 ml CH_2Cl_2 and mixed with 160 µL CHI stock solution, which was prepared by dissolving 0.20 mg CHI into 3 ml CH_2Cl_2. For the sodium titration reagent, 1.08 mg KTFPB and sodium ionophore X were dissolved in 2 ml CH_2Cl_2 and mixed with the CHI solution. For lithium titration reagent, 0.96 mg KTFPB and 2.30 mg lithium ionophore VIII were dissolved into 2 ml CH_2Cl_2 and mixed with the CHI solution.

Optical titration

Typically, 2 mL of ionophore-based titration reagent was added into a quartz cuvette and mixed with 2 mL (or 1 mL) pH 7.0 (or pH 7.4) 10^{-2} M Tris-HCl buffer solution. The cuvette was shaken until the colour of the solvent layer became blue. The back titration was performed by gradually adding 10^{-2} M analyte (KCl, NaCl, LiCl) or human serum into the cuvette, each step followed by sufficient shaking. For the home-made automated titration, 10^{-2} M KCl or human serum was delivered from a syringe pump into a glass vial

containing the titration reagent and buffer solution. The glass vial was kept vibrating throughout the experiment.

Instrumentation

Optical signals were measured with a UV−visible absorption spectrometer (SPECORD 250 plus, Analytic Jena, AG, Germany) or a digital camera (Canon EOS 5D Mark III). The home-made setup for automated titration was composed of a syringe pump (KD Scientific) and vortexer (Heidoph).

Results and Discussion

The ionophore-based titration reagents combining the functions of chelator and indicator are shown in scheme 1. The reagent contains excess amount of ion-exchanger (NaTFPB or KTFPB) and ionophore (potassium ionophore I, sodium ionophore X or lithium ionophore VIII) relative to a small amount of CHI (lipophilic pH indicator) in the organic

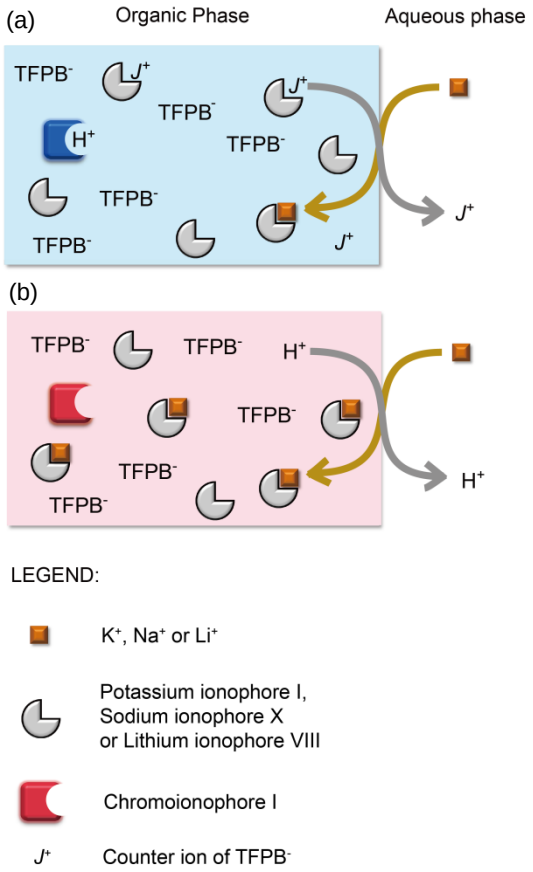

Scheme 1. The working principle of the solvent based titration reagents. (a) Before endpoint. (b) After endpoint.

phase (CH_2Cl_2). The aqueous phase is a pH buffered solution. As the analyte ion is added into the aqueous phase, it is extracted into the organic phase to form a complex with the ionophore, which causes the initial counter ion of the ion-exchanger to be exchanged out into the aqueous phase. Only after consuming all the counter ions of the ion exchanger, the analyte ions will be exchanged with the more tightly bound hydrogen ions in the organic phase. This causes the deprotonation of protonated CHI, resulting in a drastic colour change at the endpoint. The ionophore-based titration reagents function on the basis of the ion-exchange principle, which is briefly quantified here mathematically.

Before the endpoint, the titration process can be described by the overall equilibrium (1):

$$I^+(aq) + JL^+(org) \overset{K_1}{\rightleftharpoons} IL^+(org) + J^+(aq) \quad (1)$$

With the corresponding exchange constant K_1,

$$K_1 = \frac{[IL^+]_{org}[J^+]_{aq}}{[I^+]_{aq}[JL^+]_{org}} \quad (2)$$

Where I^+ is the analyte ion (K^+ or Na^+ or Li^+), L is the ionophore, and J^+ is the counter ion (interfering ion) of the $TFPB^-$. IL^+ and JL^+ are the complexed primary ion and interfering ion. NaTFPB is used for K^+ titration whereas KTFPB served as cation-exchanger salt for Na^+ and Li^+ titration. The stoichiometry of monovalent analyte ion with ionophore complex is 1:1, while $[IL^+]_{org}$, $[J^+]_{aq}$, $[I^+]_{aq}$ and $[JL^+]_{org}$ are molar concentrations of the indicated species.

At the endpoint, the process is described by equilibrium (3):

$$I^+(aq) + L(org) + Hind^+(org) \overset{K_2}{\rightleftharpoons} IL^+(org) + ind(org) + H^+(aq) \quad (3)$$

With the corresponding exchange constant K_2,

$$K_2 = \frac{[IL^+]_{org}[H^+]_{aq}[ind]_{org}}{[I^+]_{aq}[L]_{org}[Hind^+]_{org}} \quad (4)$$

Where Hind and ind are the protonated and deprotonated CHI, $[ind]_{org}$ and $[Hind^+]_{org}$ are the corresponding concentrations, and $[H^+]_{aq}$ is the concentration of hydrogen ions in aqueous phase. Based on this theory, the theoretical titration curves are obtained to fit the experimental data (see eq S1 to S9 in Supporting Information for details).

The experimental titration curves for K^+, Na^+ and Li^+ and the corresponding spectra are shown in Figure 1. The ionophore-based titration reagents were readily prepared by dissolving the corresponding ionophores, ion-exchanger and a very small amount of CHI

in CH_2Cl_2. The titrations were performed at pH 7.0 for K^+ and pH 7.4 for Na^+ and Li^+. As shown in Figure 1(a) and (d), KCl was gradually added into the aqueous phase and each step was recorded by absorbance after equilibration.

Based on the ion-exchange principle, the molar amount of ion exchanger corresponds to the one of K^+ that can be consumed by the reagent. The ionophore is in excess of the ion exchanger and for this reason the stoichiometry between the K^+ and potassium ionophore I does not necessarily need to be considered.

Before the endpoint, K^+ will be exchanged into the organic phase by the counter ion (Na^+) of the $TFPB^-$ and complexed with the potassium ionophore I. Here, CHI remains in the protonated state and the colour of the organic phase is blue. After consuming all the Na^+, K^+ will exchange into the organic phase by expelling hydrogen ions bound to the indicator into the aqueous phase. At the endpoint, therefore, the colour of the organic phase turns purple. Beyond the endpoint, CHI will become fully deprotonated and the

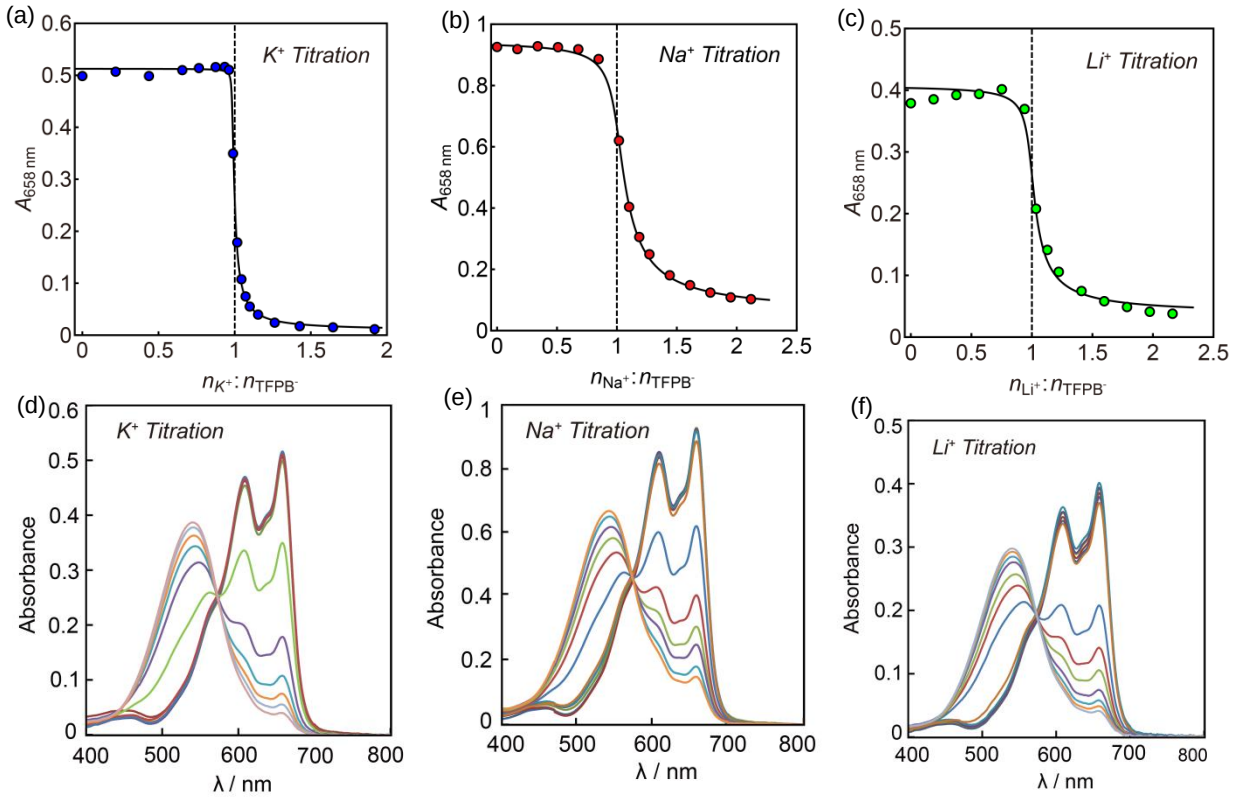

Figure 1. The optical reverse titration curves (a, b, c) and corresponding absorption spectra (d, e, f) for K^+, Na^+ and Li^+, respectively. Titrant: 10^{-2} M KCl or NaCl or LiCl. The dashed vertical lines indicate the expected endpoint. Buffer solution: 10^{-2} M Tris-HCl pH 7.0 for K^+ titration, 10^{-2} M Tris-HCl pH 7.4 for Na^+ and Li^+ titration. Absorption spectra recorded at each titration point.

colour will change to red. During the titration, the volume of added analyte solution, i.e., the increase of the total volume of aqueous phase should be taken into account, as done in our theoretical treatment (see SI for details).

Compared to ion selective nanosphere-based titration reagents (Figure S1), the titration curve for K^+ shown in Figure 1a is much sharper and more accurate with an error of less than 1%. The titration based on nanosphere reagents only exhibited accurate and sharp transition (Figure S1a) when the ionophore had a sufficiently high effective binding constant, as with calcium ionophore II for calcium. Indeed, our efforts to achieve nanosphere-based K^+ titrations with potassium ionophore I was not successful as the experimental endpoint was found to be far from the correct one, with an error of about 48%. The logarithmic effective binding constants (β) of potassium ionophore I in the nanospheres has recently been determined as 6.1 ± 0.1,[23] about 4 orders of magnitude lower than those reported earlier in PVC-DOS membrane ($\log\beta = 10.1 \pm 0.2$).[33] The corresponding value in CH_2Cl_2 was here experimentally determined as 10.2 ± 0.1 which is practically identical to that found in PVC-DOS by using a previously reported method.[34] It appears that only ionophores with high binding constants can be used for nanosphere-based titration reagents. Additionally, nanosphere-based titration reagents cannot be endowed with a high ion-exchange capacity, as increasing the nanosphere concentration results in aggregation and light scattering limitations. On the other hand, it is easier to dissolve sensor components in CH_2Cl_2 with the aim to increase the titration capacity and to allow for the analysis of even highly concentrated samples. In the configuration tested here, the equilibration time of the ionophore based assay was found to be around 4 s at the endpoint, likely limited by convective mixing.

For the Na^+ and Li^+ titrations shown in Figure 1 (b), (c) and (e), (f), the reagents contain similar sensor components as for the K^+ titration (see Experimental). Both titration curves are sharp and accurate with small errors of less than 1%. The different shapes of the titration curves are due to the difference in the complex formation constants. Here, potassium ionophore I exhibits the highest binding constant compared to sodium ionophore X and lithium ionophore VIII and thus the K^+ titration curve appears the sharpest.[33] All titration curves agree very well with theory (see supporting information).

The selectivity of the ionophore based reagents was evaluated, see Figure 2. To obtain sigmoidal calibration curves useful for visual selectivity analysis, the solvent contained ion exchanger and CHI at a 1:1 molar ratio instead of excess amount of ion exchanger over CHI, while maintaining an excess of ionophore. The response of the ion selective reagent to various cations is shown in Figure 2. The horizontal distance between the calibration curves for the primary ion and any interfering ion on the logarithmic concentration scale reflects the selectivity: the larger the separation, the more selective

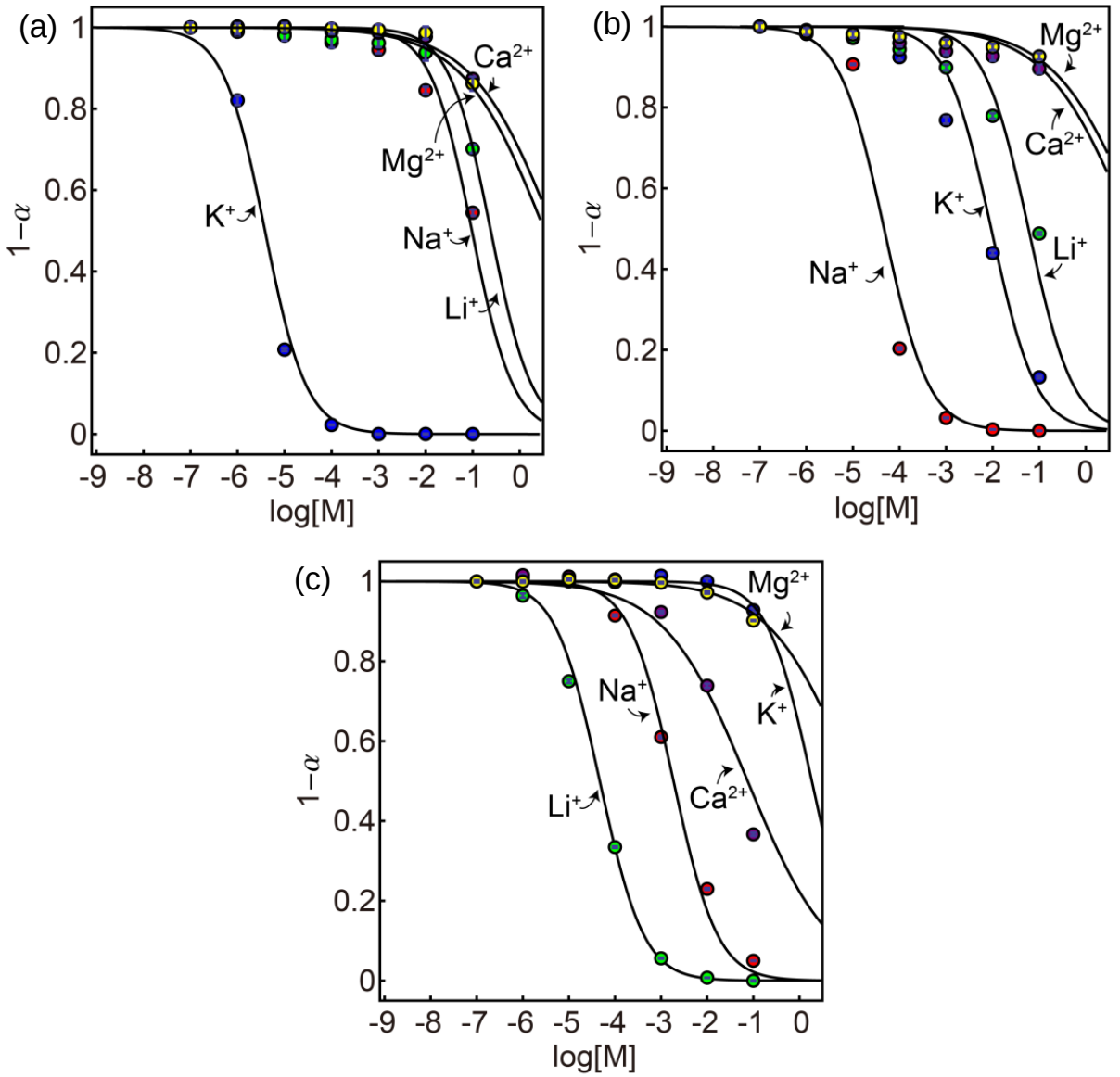

Figure 2. The response of the K^+ (a), Na^+ (b) and Li^+ (c) selective reagents to various interfering ions, respectively. Buffer solution: (a)10^{-2} M Tris-HCl pH 7.0, (b, c) 10^{-2} M Tris-HCl pH 7.4. The horizontal distance between the calibration curve for primary ion and any interfering ions represents $logK_1$.

the reagent. For example, the distance between K^+ and Na^+, K^+ and Li^+ are 4.4 and 4.8 logarithmic units (Figure 2a), respectively, and so the K^+ reagent can tolerate more Li^+ than Na^+ in the sample. The distance is also indicative of the exchange constant ($\log K_1$) between the primary ion I^+ and complexed interfering ion JL^+. The $\log K_1$ values obtained from Figure 2 were used for theoretical predictions.

The experimental K^+ titrations with a background of 10^{-2} M (with accurate endpoint) and 10^{-1} M NaCl (with less than 1 % error) are shown in Figures S2 (a) and (b). Theory predicts an error of 1.3% for a 0.15 M Na^+ background, which is adequate for K^+ titration in human serum.

Figure S3 (a) and (b) show the Na^+ titration and Li^+ titration in a background of 10^{-3} M KCl and 10^{-1} M KCl, respectively. Both titrations are successful and give acceptable errors: the theoretical error prediction for Na^+ titration in a 3.3 mM and 5.5 mM KCl background are 2.6 % and 4.4%, respectively.

For Li titration, the Li selective reagent can tolerate a very high concentration of KCl, giving a calculated error of 1.1 % for 10^{-1} M KCl. Unfortunately, it cannot tolerate a high concentration of Na^+ because of limited selectivity and is not suitable for Li^+ titration in serum.

The K^+ selective ionophore-based titration reagent was chosen as an initial example to demonstrate the titrimetric assay in human blood serum. Considering the major cationic interfering species Na^+ (135 mM to 145 mM), Ca^{2+} (2.25 mM to 2.75 mM) and Mg^{2+} (0.7 mM to 1.1 mM), the K^+ selective reagent showed no response to Ca^{2+} and Mg^{2+} in the concentrations of interest, leaving Na^+ as the major interference.[35] In agreement with predictions, endpoint analysis gave a potassium concentration of 4.32 ± 0.10 mmol/L (Figure S4), which agrees with the results from atomic emission spectrometry (AES: 4.47 ± 0.20 mmol/L). Figure 3 shows photographic images of the K^+ titration process. After each dose of KCl solution, the pictures were taken immediately after shaking but before separation of the two phases (Figure 3a). Figure 3b shows the corresponding pictures captured after complete phase separation.

The endpoints can equally be obtained by HSV (hue, saturation, value) analysis of images or videos captured with a digital camera, which is instrumentally convenient. HSV is a cylindrical-coordinate representation of pixels in an RGB (red, green, blue)

colour model where each pixel is defined by the hue (H), saturation (S) and value (V) coordinates in the colour space. The use of the hue from images in HSV colour space has been shown to be a robust parameter for quantitative analysis of the response of optical sensors.[36,37] The titration curves from pictures taken before and after phase separation are plotted as the computed hue value to the ratio of $n_{K^+} : n_{TFPB^-}$ and shown in Figures 3c and 3d, respectively. The hue signals were extracted from the pictures by software (Wolfram Mathematica). The titration curves appear the same and the transitions are very sharp, independent of the two phases being mixed or separated. The titration curves agree with the model and result in errors of less than 1%. Serum titrations were also performed by analyzing the hue signals from the images, see Figure S5. Based on the total amount of the NaTFPB in the titration reagent and the volume of added human serum at the

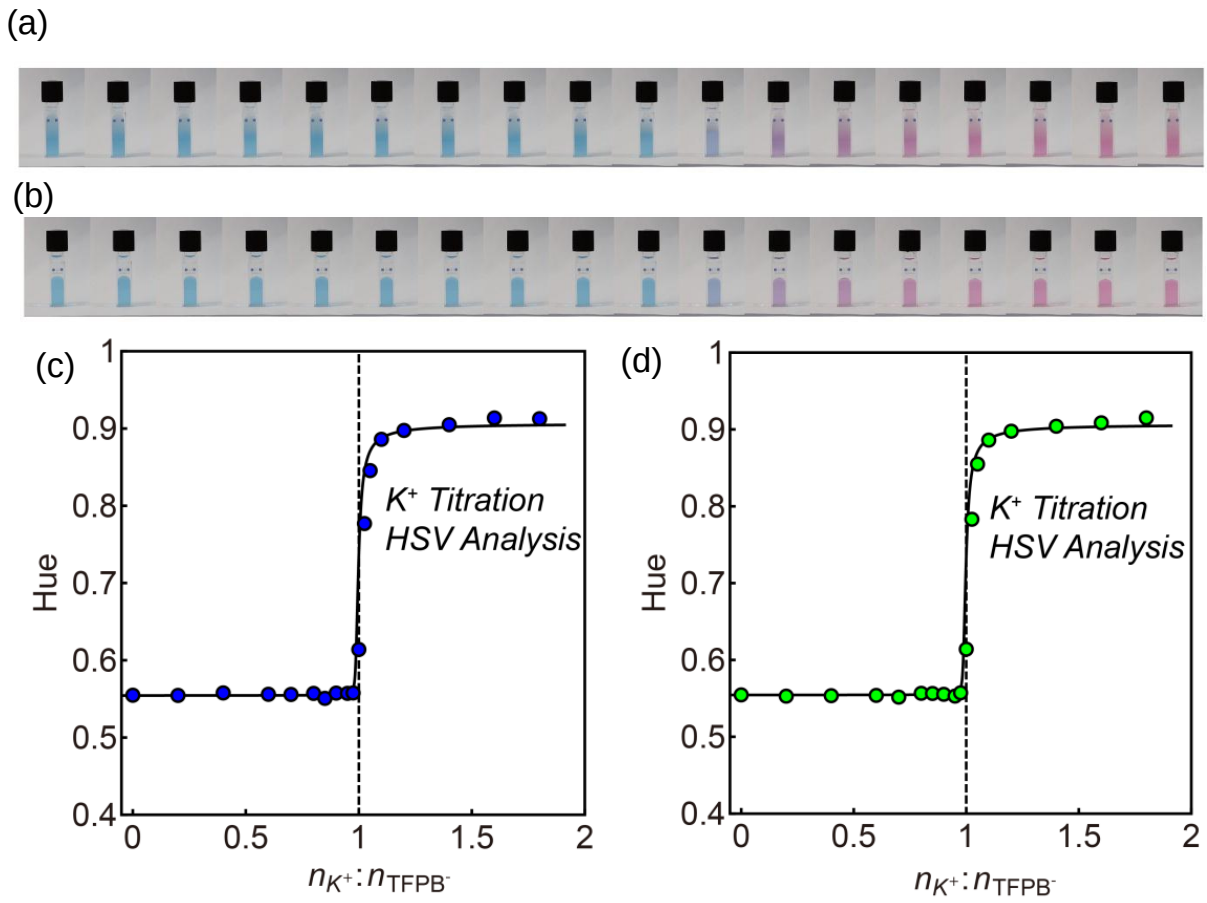

Figure 3. Pictures of the K^+ titration process after shaking (a) and after two phases separated (b) and the corresponding titration curves (c) and (d) based on the HSV analysis. The dashed vertical lines indicate the expected end points. Buffer solution: 10^{-2} M Tris-HCl pH 7.0.

endpoint, the level of K^+ was again determined as 4.40 ± 0.10 mmol/L.

From a practical point of view, an automated titration is preferred for routine analysis. For this purpose, a homemade automatic reverse titration setup was built, see Figure 4a, b. It comprises a syringe pump to inject accurate sample volumes and a vortex to efficiently mix the two phases (aqueous buffer and CH_2Cl_2). The syringe pump delivers precise volumes of the sample while a digital camera focuses on the coloured CH_2Cl_2 part to record consecutive images or a single movie. The K^+ titration curve from the movie hue signals is shown in Figure 4c. Sharp transitions were obtained successfully and the experimental endpoint agreed with the expected one. The K^+ level in undiluted human serum was also successfully determined with this home-made automatic titration setup as 4.38 ± 0.10 mmol/L (see Figure 4d and video in the supporting information).

In conclusion, we describe here for the first time the use of solvent based ion-selective

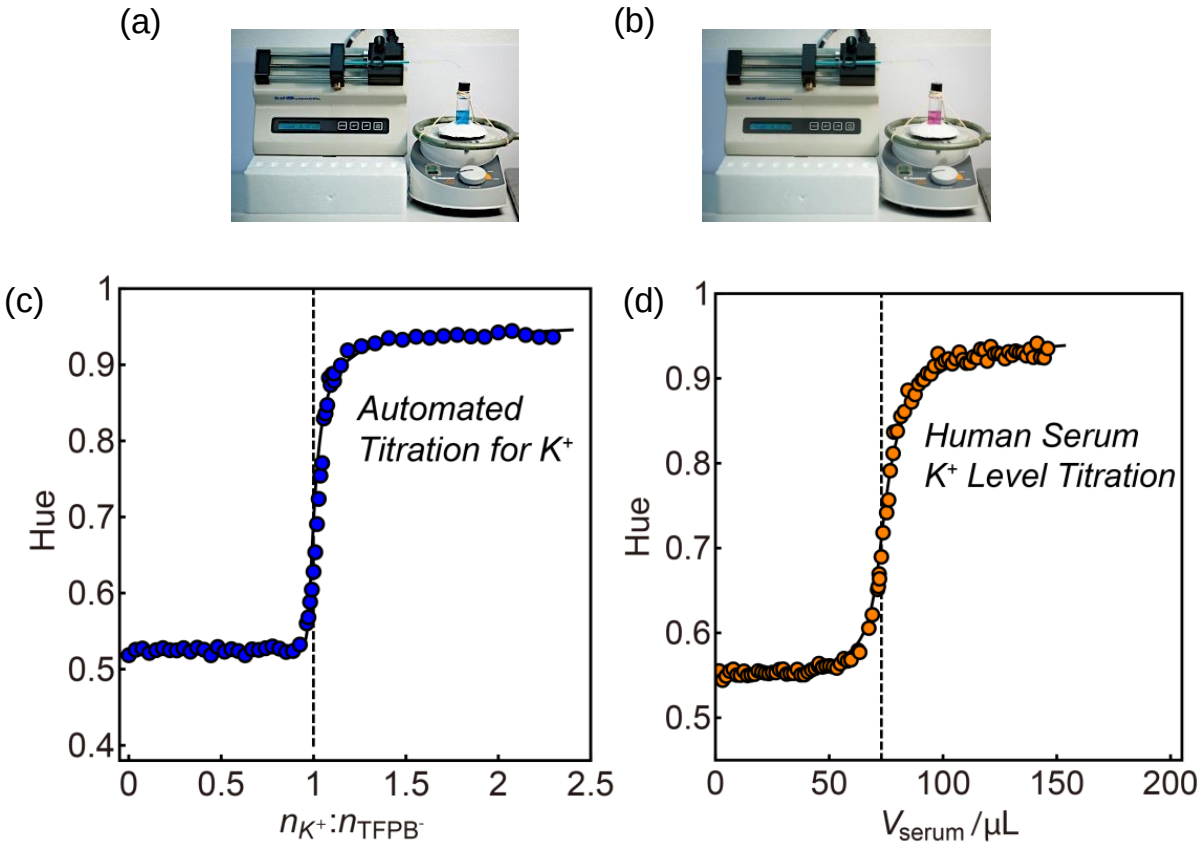

Figure 4. The setup of the automated titration. (a) Before titration, (b) after the endpoint. (c) Titration analysis for K^+ based on the hue signals retrieved from the frames in the video. (d) Serum titration based on the hue signals retrieved from the frames in the video. Organic phase: K^+ selective titration reagent. Aqueous phase: 10^{-2} M Tris-HCl pH 7.0 buffer solution. The volume of the added serum at the end point is V_{serum} = 73 µL.

ionophore titration reagents as combined chelator/indicator in complexometric titrations. This class of titration reagents exhibits higher binding constants and extraction capacity relative to the emulsion based approach reported earlier. Chemically selective K^+, Na^+, and Li^+ titrations were successfully demonstrated. The K^+ level in undiluted human blood serum was satisfactorily determined, which is promising for a possible clinical application. We note that with the current experimental setup, a complete K^+ titration in serum takes about 30 min, which need to be shortened for an application in routine practice.

Supporting Information

Detailed Theoretical Approach

$$I^+(org) + L(org) \rightleftarrows IL^+(org) \qquad K_1' = \frac{[IL^+]_{org}}{[L]_{org}[I^+]_{org}} \qquad \text{S1}$$

$$Hind^+(org) \rightleftharpoons H^+(org) + ind(org) \qquad K_2' = \frac{[H^+]_{org}[ind]_{org}}{[Hind^+]_{org}} \qquad \text{S2}$$

$$I^+(aq) + H^+(org) \rightleftharpoons I^+(org) + H^+(aq) \qquad K_3' = \frac{[I^+]_{org}[H^+]_{aq}}{[I^+]_{aq}[H^+]_{org}} \qquad \text{S3}$$

$$JL^+(org) \rightleftarrows J^+(org) + L(org) \qquad K_4' = \frac{[L]_{org}[J^+]_{org}}{[JL^+]_{org}} \qquad \text{S4}$$

$$I^+(aq) + J^+(org) \rightleftharpoons I^+(org) + J^+(aq) \qquad K_5' = \frac{[I^+]_{org}[J^+]_{aq}}{[I^+]_{aq}[J^+]_{org}} \qquad \text{S5}$$

Where K'_1 is formation constant between the primary ion (I^+) and ionophore (L), K'_2 is the dissociation constant of protonated CHI, K'_3 is the exchange constant between primary ion and proton, K'_4 is the dissociation constant of complexed interfering ion (JL^+), K'_5 is the exchange constant between primary ion and interfering ion.

I^+ is the monovalent primary ion (K^+ or Na^+ or Li^+), L is the ionophore for the K^+ or Na^+ or Li^+, IL^+ is the complexation of the primary ion and ionophore, $Hind^+$ and ind are the protonated and deprotonated form of the CHI, J^+ is the counter ion of the ion exchanger (also interference ions). $[IL^+]_{org}$ and $[JL^+]_{org}$ $[L]_{org}$ are the concentrations of complexed ionophore and free ionophore in solvent phase, $[Hind^+]_{org}$ and $[ind]_{org}$ are the concentrations corresponding for CHI. $[I^+]_{aq}$, $[H^+]_{aq}$ and $[J^+]_{aq}$ are concentrations of the

primary ions, proton and interfering ion in aqueous phase, respectively. $[I^+]_{org}$, $[H^+]_{org}$ and $[J^+]_{org}$ are the corresponded concentrations in organic phase.

The organic phase must maintain electroneutrality, resulting in the charge balance shown in eq S6:

$$[TFPB_T^-]_{org} = [IL^+]_{org} + [Hind^+]_{org} + [JL^+]_{org} + [J^+]_{org} + [I^+]_{org} + [H^+]_{org} \quad \text{S6}$$

The mass balances for the ionophore and CHI are written in eq S7 and S8:

$$[L_T]_{org} = [IL^+]_{org} + [L]_{org} + [JL^+]_{org} \quad \text{S7}$$

$$[ind_T]_{org} = [Hind^+]_{org} + [ind]_{org} \quad \text{S8}$$

Where $[L_T]_{org}$, $[TFPB_T^-]_{org}$ and $[ind_T]_{org}$ are the total concentrations of ionophore, ion exchanger and CHI in the organic phase, respectively, while $[L]_{org}$ is that of the uncomplexed ionophore in organic phase.

The total molar amount of the primary ion can be divided into three parts, free primary ions in aqueous phase, free and complexed in the organic phase:

$$[I^+]^{titrant} V_{I^+}^{titrant} = ([I^+]_{org} + [IL^+]_{org}) V_{org} + [I^+]_{aq} (V_{I^+}^{titrant} + V_{buffer}) \quad \text{S9}$$

where $[I^+]^{titrant}$ and $V_{I^+}^{titrant}$ are the concentration and volume of the added sample solution containing the analyte; V_{org} and V_{buffer} are the volumes of organic and aqueous phase.

The absorbance A is expressed on the basis of Beer's law as:

$$A = \varepsilon_{Hind^+} b [Hind^+]_{org} + \varepsilon_{ind} b ([ind_T]_{org} - [Hind^+]_{org}) \quad \text{S10}$$

Where ε_{Hind^+} and ε_{ind} are the molar extinction coefficients and b is the optical path length.

By solving eqs S1 to S10, a relationship between $V_{I^+}^{titrant}$ and absorbance A is obtained. This allows one to calculate the ratio of the amount of the primary ion and ion exchanger ($n_{I^+} : n_{TFPB^-}$) to absorbance A, which was used to describe the experimental titration data.

Additional Results

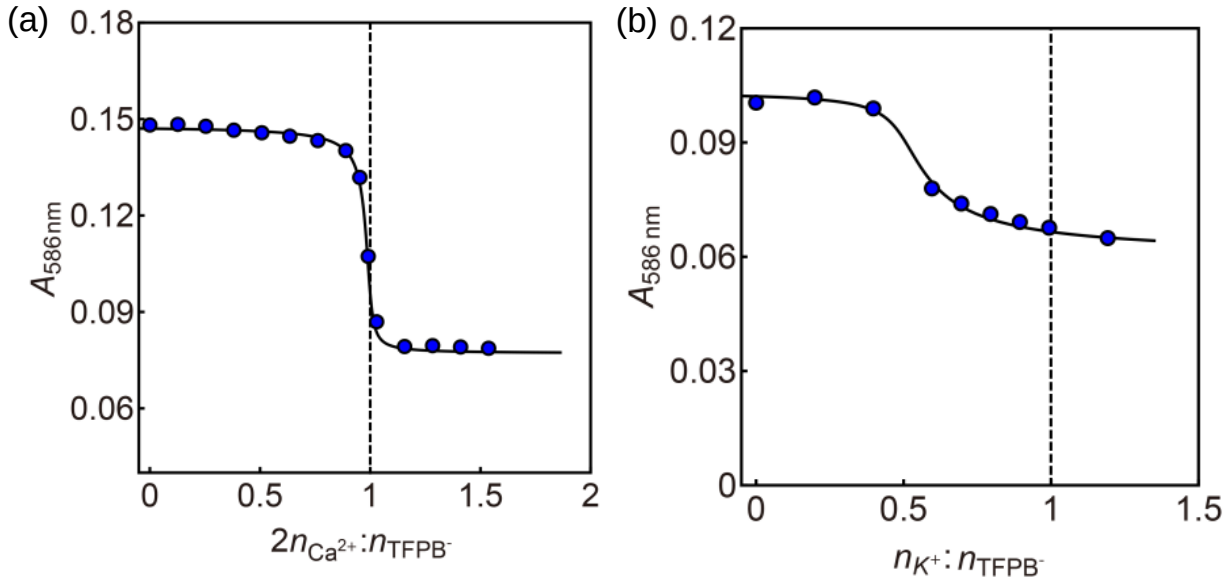

Figure S1. Optical reverse titration for (a) Ca^{2+} and (b) K^+ based on the nanospheres as chelator and indicator. The nanospheres contain ionophore (calcium ionophore II or potassium ionophore I), large amount of ion exchanger and small amount of solvatochromic dye. The core of the nanosphere is made of plasticizer and surfactant F127.

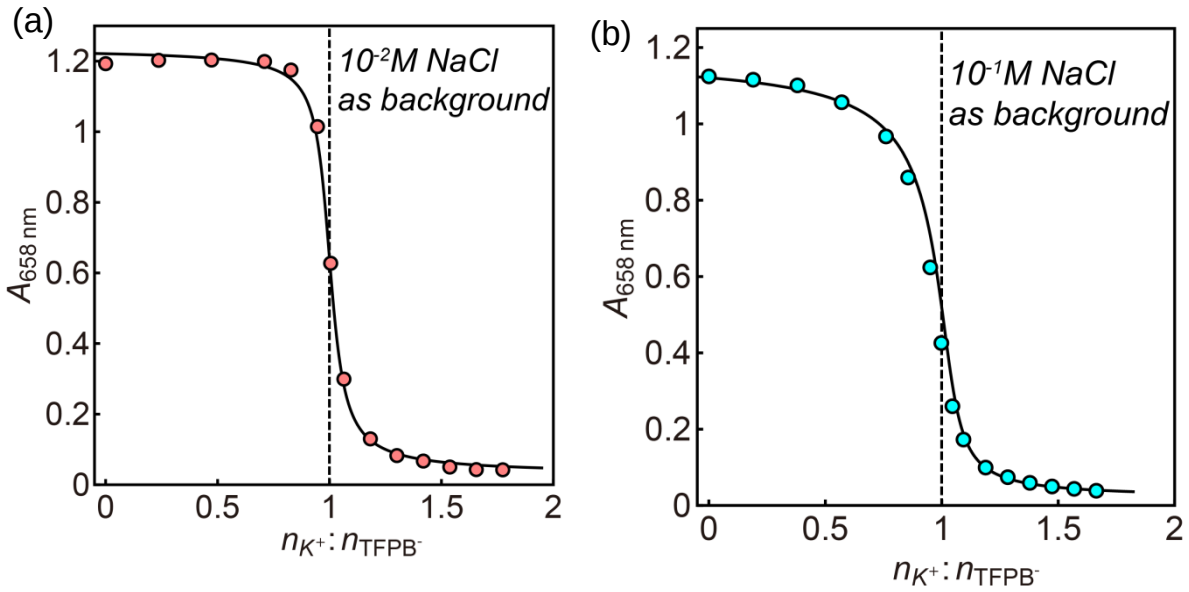

Figure S2: (a) Experimental titration curve for K^+ with 10^{-2} M and (b) 10^{-1} M Na^+ as background in 10^{-2} M Tris-HCl buffer solution (pH 7). The dashed vertical lines indicate the expected endpoint.

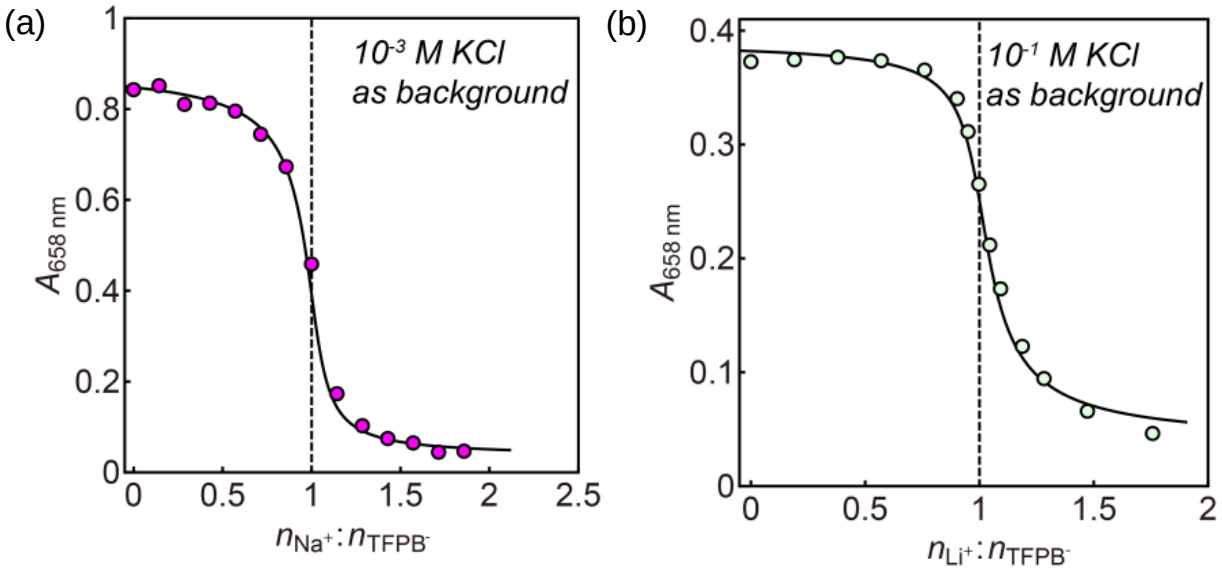

Figure S3. Optical reverse titration for Na^+ and Li^+ at the background of (a) 10^{-3} M KCl and (b) 10^{-1} M KCl, respectively. Buffer: (a) and (b) 10^{-2} M Tris-HCl pH 7.4 for Na^+ and Li^+ titration.

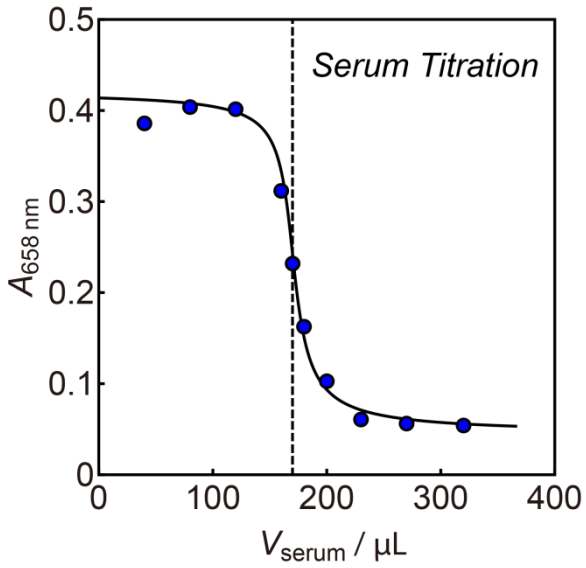

Figure S4. Optical reverse titration for determining the K^+ level in human serum. Organic phase: K^+ selective titration reagent. Aqueous phase: 10^{-2} M Tris-HCl pH 7.0 buffer solution. The volume of the added serum at the end point is V_{serum} = 170 μL.

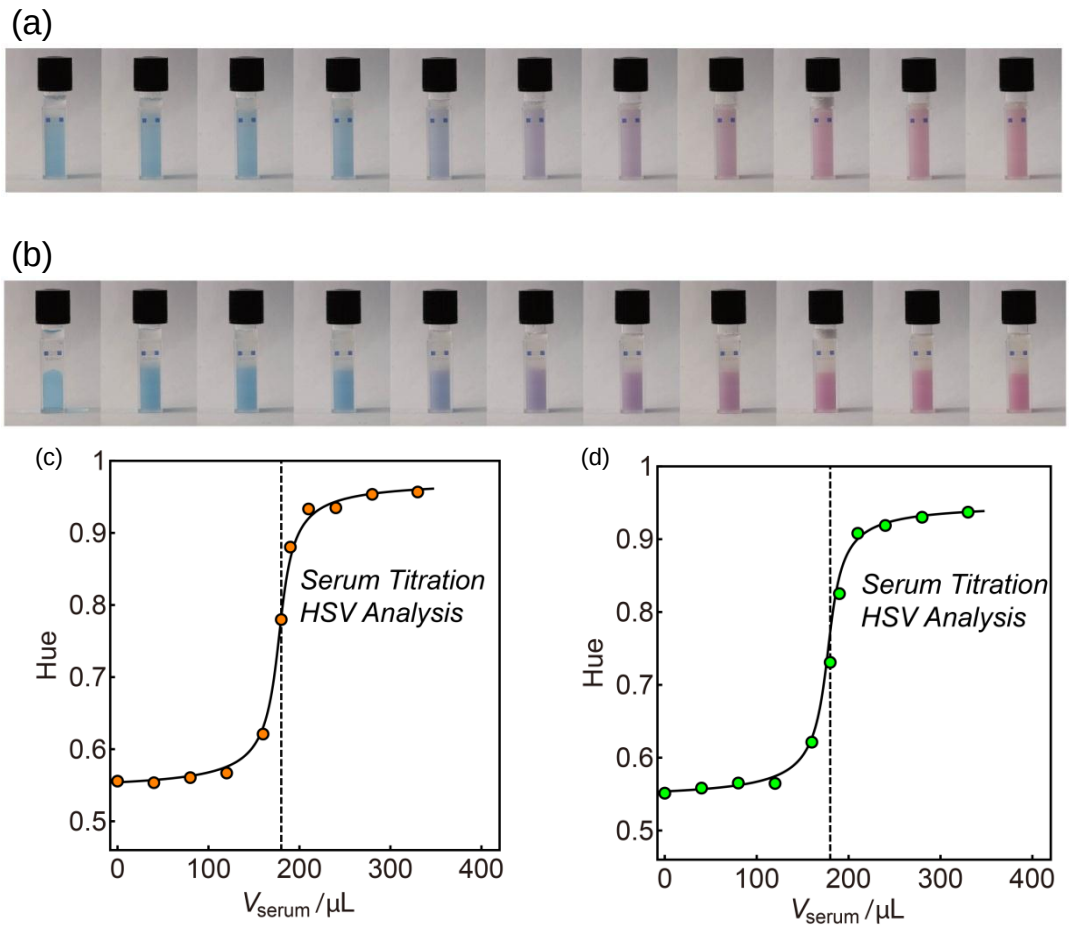

Figure S5. Serum titration based on analysis of hue signals retrieved from pictures. Pictures of the K^+ titration process after shaking (a) and after two phases separated (b) and the corresponding titration curves (c) and (d) based on the HSV analysis. Organic phase: K^+ selective titration reagent. Aqueous phase: 10^{-2} M Tris-HCl pH 7.0 buffer solution. The volume of the added serum at the endpoint is V_{serum} = 180 µL.

Additional movie file: Automatic titration of potassium in human serum by using home-made setup. Experimental parameters: V_{org} =1 mL, V_{buffer} =1 mL, $[H^+]_{aq}$ =10^{-7} M, V_{serum} = 73 uL (at the end point). The entire serum titration process takes currently about 30 min, longer than for water samples.

Link: http://pubs.acs.org/doi/suppl/10.1021/acssensors.7b00165

References

(1) Yu, S. P.; Canzoniero, L. M.; Choi, D. W. *Curr. Opin. Cell Biol.* **2001**, *13*, 405.

(2) Kuo, H.-C.; Cheng, C.-F.; Clark, R. B.; Lin, J. J.-C.; Lin, J. L.-C.; Hoshijima, M.; -Trân, V. T. B. N.; Gu, Y.; Ikeda, Y.; Chu, P.-H.; Jr., J. R.; Giles, W. R.; Chien, K. R. *Cell* **2001**, *107*, 801.

(3) Krishna, G. G.; Miller, E.; Kapoor, S. *N. Engl. J. Med.* **1989**, *320*, 1177.

(4) Zhang, S.; Zhang, R.; Ma, B.; Qiu, J.; Li, J.; Sang, Y.; Liu, W.; Liu, H. *RSC Adv.* **2016**, *6*, 41999.

(5) Yang, L.; Qing, Z.; Liu, C.; Tang, Q.; Li, J.; Yang, S.; Zheng, J.; Yang, R.; Tan, W. *Anal. Chem.* **2016**, *88*, 9285.

(6) Harrington, J. M.; Young, D. J.; Essader, A. S.; Sumner, S. J.; Levine, K. E. *Biol. Trace Elem. Res.* **2014**, *160*, 132.

(7) Chuang, F. S.; Sarbeck, J. R.; John, P. A. S.; Winefordner, J. D. *Mikrochim. Acta* **1973**, *61*, 523.

(8) Buchberger, W. W. *TrAC, Trends Anal. Chem.* **2001**, *20*, 296.

(9) Moody, G. J.; Saad, B. B.; Thomas, J. D. R. *Analyst* **1989**, *114*, 15.

(10) Schwarzenbach, G.; Flaschka, H. *Complexometric titrations*; Methuen: London, 1969.

(11) Salvatore, M. M.; Salvatore, F. *Word J. Chem. Educ.* **2015**, *3*, 5.

(12) Roy, N.; Nath, S.; Dutta, A.; Mondal, P.; Paul, P. C.; Singh, T. S. *RSC Adv.* **2016**, *6*, 63837.

(13) Karita, S.; Kaneta, T. *Anal. Chim. Acta* **2016**, *924*, 60.

(14) Bian, X.; Lockless, S. W. *Anal. Chem.* **2016**, *88*, 5549.

(15) Afshar, M. G.; Crespo, G. A.; Bakker, E. *Anal. Chem.* **2015**, *87*, 10125.

(16) Chakma, B.; Jain, P.; Singh, N. K.; Goswami, P. *Anal. Chem.* **2016**, *88*, 10316.

(17) Männel-Croisé, C.; Meister, C.; Zelder, F. *Inorg. Chem.* **2010**, *49*, 10220.

(18) Swain, B. *Sep. Purif. Technol.* **2017**, *172*, 388.

(19) Zhai, J.; Xie, X.; Bakker, E. *Chem. Commun.* **2014**, *50*, 12659.

(20) Zhai, J.; Xie, X.; Bakker, E. *Anal. Chem.* **2015**, *87*, 2827.

(21) Zhai, J.; Xie, X.; Bakker, E. *Anal. Chem.* **2015**, *87*, 8347.

(22) Zhai, J.; Xie, X.; Bakker, E. *Anal. Chem.* **2015**, *87*, 12318.

(23) Xie, X.; Bakker, E. *Anal. Chem.* **2015**, *87*, 11587.

(24) Leong, Y. K.; Lan, J. C.-W.; Loh, H.-S.; Ling, T. C.; Ooi, C. W.; Show, P. L. *J. Sep. Sci.* **2016**, *39*, 640.

(25) Buschmann, H.-J.; Mutihac, L. *Anal. Chim. Acta* **2002**, *466*, 101.

(26) Wang, J.; Su, D.; Wang, D.; Ding, S.; Huang, C.; Huang, H.; Hu, X.; Wang, Z.; Li, S. *Inorg. Chem.* **2015**, *54*, 10648.

(27) Soares, R. R. G.; Silva, D. F. C.; Fernandes, P.; Azevedo, A. M.; Chu, V.; Conde, J. P.; Aires-Barros, M. R. *Biotechnol J.* **2016**, *11*, 1.

(28) Tang, S.; Zhang, H.; Lee, H. K. *Anal. Chem.* **2016**, *88*, 228.

(29) Sviben, I.; Galić, N.; Tomišić, V.; Frkanec, L. *New J. Chem.* **2015**, *39*, 6099.

(30) Elçin, S.; Deligöz, H. *J. Incl. Phenom. Macrocycl. Chem.* **2014**, *80*, 337.

(31) Nacham, O.; Clark, K. D.; Anderson, J. L. *Anal. Chem.* **2016**, *88*, 7813.

(32) He, Q.; Zhang, Z.; Brewster, J. T.; Lynch, V. M.; Kim, S. K.; Sessler, J. L. *J. Am. Chem. Soc.* **2016**, *138*, 9779.

(33) Qin, Y.; Mi, Y.; Bakker, E. *Anal. Chim. Acta* **2000**, *421*, 207.

(34) Bakker, E.; Willer, M.; Lerchi, M.; Seiler, K.; Pretsch, E. *Anal. Chem.* **1994**, *66*, 516.

(35) Bakker, E. *Anal. Chim. Acta* **1997**, *350*, 329.

(36) Wang, X.; Qin, Y.; Meyerhoff, M. E. *Chem. Commun.* **2015**, *51*, 15176.

(37) Cantrell, K.; Erenas, M. M.; Orbe-Payá, I. d.; Capitán-Vallvey, L. F. *Anal. Chem.* **2010**, *82*, 531.

Conclusions and Perspective

In this part, we provide a retrospect on the ionophore based titration method by summarizing its merits while consider what is yet insufficient and provide a few future directions for those who will continue to develop this method. We have introduced here the new concept of ionophore based titration reagents with high selectivity and versatility. This platform involves mainly the indicating and chelating nanospheres and the solvent based titration reagents.

For the chelators, the doping of the highly selective ionophores together with the ion exchanger into the nanospheres (made of F127 and plasticizer) or in organic solvent dichloromethane guaranteed the selectivity to the target analytes. Our approach extended the variety of titration reagents which are previously limited to water soluble compounds. Based on the ion exchange principle, the amount of target analytes were determined by the amount of the ion exchanger. One of the drawbacks of the nanospheres based chelators is the limitation to the ionophores with high binding affinity. As demonstrated in Chapter 6, this limitation was overcome by using organic solvent as the matrix instead of nanospheres, which also improved the loading capacity of the sensor components. Using an electrode exhibiting a super-Nernstian slope (inward ion fluxes) as indicator dramatically improved the sensitivity and increased sharpness of the titration curves were obtained.

For the indicators with additional pH indicator (chromoionophore) doped into the chelating nanospheres, the nanospheres can also work as endpoint indicator. As shown in Chapter 3, the endpoints determination of the titrations depended on sample pH. As the sample solution went from more acidic to more basic, the titration curves changed from a sigmoidal response shape to a linear one. Chapter 5 provided a solution to this problem. By replacing the chromoionophore with solvatochromic dye, which is not pH sensitive, the response of the indicator nanospheres also no longer depended on sample pH. However, the lipophilicity of the solvatochromic dyes in this case had to be considered because it would influence the optical response of the indicating nanospheres. It should be noted that, since the matrix of indicating nanospheres are also made with the same

material as chelating nanospheres, it still confronts the same limitations in the choices of ionophores and loading.

Solvent based titration reagents combined both the function of the chelator and the indicator, thereby dramatically simplifying the analytical procedure. However, the titration response time of solvent based reagents is relatively long, especially in the case of titration of human serum samples. It is currently not clear what causes this longer response time, but it may be related to a limited mass transport rate during the titration caused by the serum lipids.

The ionophore doped titration reagents have been successfully used to determine the concentrations of ions including Ca^{2+}, Pb^{2+}, K^{+}, Na^{+}, Li^{+}, NO_3^{-}, and ClO_4^{-}. To enable this general titration method for more applications in the areas of clinical and environmental chemistry, biochemistry, food industry, future research directions may include:

1. Extending the palette of titratable species. Although we have demonstrated the success in the titrations of several ions as listed above, still a large amount of ions of biomedical or environmental relevance have not been covered. Some of these ions in principle could be titrated with our methods. For example, polyions including heparin and protamine could probably be titrated with DNNS doped nanospheres or solvents. Other small inorganic ions could also be titrated given that appropriate ionophores exist.
2. Related to the first point, novel ionophore development becomes very important if we want to titrate an analyte where highly selective ionophores do not exist yet. This is especially important for the titration of anions. So far, we've only demonstrated the anion titration based on their lipophilicity difference (the Hofmeister series). The titration of a very hydrophilic anion, such as sulfate or phosphate, can only be achieved when a good ionophore is available. However, more detailed discussion on the ionophore design and synthesis is beyond the scope and knowledge of this thesis.
3. Searching for nanomaterials compatible with this titration scheme. Keeping the titration reagents at the nanoscale can make the titration ultrafast. Materials forming a more hydrophobic core than the nanospheres made of F127 and plasticizer may extend the choice of the ionophores. There are various materials to be screened, such

as lipid based vesicles, mesoporous silicon, cross linked polymers, and magnetic nanoparticles.

4. Building up a new device with improved mixing for the solvent based titration. In Chapter 6, we demonstrated a homemade device for automatic titration based on a syringe pump and a vortex. The mixing of the titrant and sample is not fast enough. This may be improved with other methods such as mechanical stirring or sonication.
5. Methods to reuse the titration reagents in order to reduce the economic and environmental cost. So far, our titration reagents are for disposable use. Magnetic recycling could serve to collect the titration nanospheres, which then may be washed and reused. Further, electrochemical modulation on the effective ion exchanger in the reagent could force the analyte to be expelled out of the chelating reagents and speed up the regeneration of the chelating reagents.
6. Multi-analyte titration. In fact this possibility was already demonstrated for the titration of perchlorate and nitrate in Chapter 4. However, it is not limited to the titration of these ions. In principle, by doping different ionophores (with different binding affinity) together in one reagent (solvent or nanopheres), consecutive titration could be realized.
7. Automatic titration by using miniaturized devise (lab on chip). Our approach is in principle compatible with microfluidic devices. This direction could also help to establish collaboration with other labs and lead to a higher impact of the new titration method to the scientific community.

Acknowledgements

This thesis was carried out during my PhD study at the University of Geneva, thanks to the help from a number of people, including my supervisor, my colleagues and friends. I would like to sincerely acknowledge those who supported me very generously.

Firstly, I would like to express my sincere gratitude to my advisor Prof. Eric Bakker. I really enjoyed the chance to do research in his group and this overseas experience unique and precious. Eric brought me into this exciting project and always provided me the most support in this research area. I extremely appreciate his patience, his lovely smiling and continuous encouragement during the years of my PhD study. I feel so lucky to be one of his students and his broad knowledge and enthusiasm in science will continue to inspire me in my life.

I thank Prof. Daniel Citterio from Keio University and Prof. Thomas Bürgi from University of Geneva for accepting to be the jury for my PhD defense, for reviewing my thesis and for attending my defense.

I would like to thank my colleagues for kind and helpful support inside and outside the lab. These people include Xiaojiang Xie, Magali Cissokho, Thomas Cherubini, Serge Rodak, Stéphane Jeaneret, Guy Lecoultre, Marylou Tercier, Abra Penezic, Justyna Kowal, Elena Zdrachek, Zdenka Jarolimova, Nadja Pankratova, María Cuartero, Lu Wang, Sutida Jansod, Bastien Néel, Romain Touilloux, Miquel Coll Crespi, Dajing Yuan, Gaston Crespo, Majid Ghahraman Afshar, Istvan Szilágyi, Christoph Bauer, Sandrine Mongin, Jiawang Ding. If I accidentally forgot someone's name, please excuse me.

I also thank Prof. Yu Qin who was my advisor during my master's study in Nanjing University. I would like to thank her for her support at her group during my master's study and thank her for the help with the application of the scholarship to come to Switzerland and the kind recommendation to Prof. Eric Bakker.

I would like to acknowledge China Scholarship Council (CSC) for the financial support during my PhD study in Switzerland.

Last but not least, I thank my friends and family members for their unconditional support.